Distribution Agreement

In presenting this thesis or dissertation as a partial fulfillment of the requirements for an advanced degree from Emory University, I hereby grant to Emory University and its agents the non-exclusive license to archive, make accessible, and display my thesis or dissertation in whole or in part in all forms of media, now or hereafter known, including display on the world wide web. I understand that I may select some access restrictions as part of the online submission of this thesis or dissertation. I retain all ownership rights to the copy right of the thesis or dissertation. I also retain the right to use in future works (such as articles or books) all or part of this thesis or dissertation.

Signature:

_____ _____

Bridgette F. Peake Date

The Role of Growth Differentiation Factor 15 in Breast Cancer

By

Bridgette F. Peake

Doctor of Philosophy
Graduate Division of Biological and Biomedical Sciences
Molecular and Systems Pharmacology

_____

Rita Nahta, PhD
Advisor

_____

Lily Yang, PhD, MD
Co-Advisor

_____

Mala Shanmugam, PhD
Committee Member

_____

Khalid Salaita, PhD
Committee Member

_____

Roy Sutliff, PhD
Committee Member
Accepted:

_____

Lisa A. Tedesco, PhD
Dean of the Graduate School

_____

Date

The Role of Growth Differentiation Factor 15 in Breast Cancer

By

Bridgette Franshar Peake

B.S. Michigan State University, 2006

M.S., Western Illinois University, 2010

Advisor: Rita Nahta, PhD

An abstract of

A dissertation submitted to the Faculty of the Graduate School of Emory University in partial fulfillment of the requirements for the degree of

Doctor of Philosophy

in Molecular and Systems Pharmacology

Graduate Division of Biological and Biomedical Sciences

2017

Abstract

The Role of Growth Differentiation Factor 15 in Breast Cancer

By Bridgette F. Peake

This dissertation seeks to uncover the mechanism by which the inflammatory cytokine growth differentiation factor 15 (GDF15) drives tumorigenesis in breast cancer. GDF15 has been implicated as a biomarker of poor prognosis and decreased survival in several malignancies. However, few studies have examined GDF15 expression, signaling, or function in breast cancer. GDF15 is significantly elevated in many tumor types in association with epithelial mesenchymal transition (EMT), drug resistance, and progressive disease. Our studies demonstrate that GDF15 overexpression is associated with upregulation of mitogenic signaling pathways (TGF-ß, MAPK, and FOXM1). GDF15 expression is further associated with high tumor grade, ER-negativity, and HER2 overexpression in patients with breast cancer. Stable overexpression of GDF15 resulted in upregulation of mesenchymal markers and transcription factors, including FOXM1, and increased cellular invasion. GDF15 stable clones and breast cancer cells stimulated with recombinant human GDF15 demonstrated activation of insulin-like growth factor-1 receptor (IGF-1R). Pharmacologic inhibition of IGF-1R blocked GDF15-mediated FoxM1 up-regulation, EMT, and invasion. Knockdown of FOXM1 dramatically reduced GDF15-mediated invasion and suppressed expression of matrix metalloproteinases MMP2 and MMP9. Finally, knockdown of GDF15 significantly inhibited invasion of HER2-overexpressing and triple-negative breast cancers. Preliminary optimization studies using DZGDF15NPs for targeted GF15 mRNA neutralization show therapeutic promise in the future. The collective findings presented herein provide further insight into the mechanism by which GDF15 drives cancer progression, and suggest potential therapeutic strategies that could benefit patients with breast cancer.

The Role of Growth Differentiation Factor 15 in Breast Cancer

By

Bridgette Franshar Peake

B.S. Michigan State University, 2006

M.S., Western Illinois University, 2010

Advisor: Rita Nahta, PhD

A dissertation submitted to the Faculty of the Graduate School of Emory University in partial fulfillment of the requirements for the degree of

Doctor of Philosophy

in Molecular and Systems Pharmacology

Graduate Division of Biological and Biomedical Sciences

2017

Acknowledgements

I would like to thank my dissertation adviser, Rita Nahta, for her support, guidance, and time. I would also like to thank the members of the Nahta lab, who taught me many scientific techniques and were wonderful colleagues. I would like to extend my appreciation to my dissertation committee who has provided me with excellent guidance. I am also thankful for my parents Sharon, Dennis and Joseph who have given endless support and love, and have always been a source of encouragement. Also I'd like to express deep gratitude to my husband Avery Peake who is an incredible father to our daughter Kyleigh Peake, an amazing spouse and my greatest source of support and encouragement. Finally, I would like to dedicate this dissertation to my family members who I've lost along this journey. They always encouraged me even when I didn't believe in myself, Uncle Willy and Aunt Sarah you faithfully provided unending love, support, understanding, and encouragement. I will forever be grateful.

Index of figures

Index of Tables

List of Abbreviations

BRCA2-breast cancer-associated gene 2

CDK2-cyclin dependent kinase 2

DAG -diacyl glycerol

DMSO-dimethyl sulfoxide

DPBS- Dulbecco's phosphate buffered saline

EGF-epidermal growth factor

EGFR-epidermal growth factor receptor

EMT-epithelial mesenchymal transition

ER-estrogen receptor

FAK-focal adhesion kinase

FISH- fluorescent in situ hybridization

FOXM1-Forkhead box M1 protein

GDF15-growth differentiation factor 15

HER2-human epidermal growth factor receptor 2

HER3- human epidermal growth factor receptor 3

HER4- human epidermal growth factor receptor 4

HRG-heregulin

IGF-1R- insulin-like growth factor-I receptor

IGFBP-IGF binding proteins

IGF-insulin-like growth factor

IGF-IR- insulin like growth factor receptor

IHC- immunohistochemical

IHC-immunohistochemistry

IP3-inositol 1,4,5-triphophate

JAK-Janus kinas

JNK1-c-Jun-N-terminal kinases

LABC-locally advance breast cancer

mAb-monoclonal antibody

MAPK-mitogen activated protein kinase pathway

MBC-metastatic breast cancer

MTOR- mammalian target of rapamycin

PARP-poly-(ADP-ribose) polymerase

PCR-polymerase Chain Reaction

PI3K-phosphatidylinositol 3-kinases

PIP2-phosphatidylinositol 4,5-biphosphate

PIP3-phosphatidylinositol 3,4,5-triphosphate

PI-propidium iodide

PLC- phosphoinositide-specific phospholipase C

PLC-phosphoinositide-specific phospholipase C

PR-progesterone receptor

PTB-protein binding domain

PTEN-phosphatase and tensin homolog

rhGDF15-recombinant GDF15

RTK-receptor tyrosine kinase

SERM-selective estrogen receptor modulator

SGLT- sodium glucose co-transporters

SH2-src homology 2

SH2-src homology 2

STAT- signal transducer and activator of transcription

STAT-signal transducer and activator of transcription

TGFa-transforming growth factor alpha

TGFß-R- Transforming growth factor beta receptor

TNBC-triple negative breast cancer

VEGF-vascular endothelial growth factor

Page

TABLE OF CONTENTS

Chapter 1

Introduction and Background

Portions of this chapter were previously published.
Bridgette F. Peake and Rita Nahta. Resistance to HER2-targeted therapies: a potential role for FOXM1. Published in final edited form as: Breast Cancer Manag. 2014; 3(5): 423–431. doi: 10.2217/bmt.14.33. Available from: https://www.ncbi.nlm.nih.gov/pmc/articles/PMC4294221

1. Breast cancer

Essentially all cancers, including breast cancer, originate due to alterations in gene function (1; 2). Mutations associated with breast cancer can be inherited or sporadic (3). Sporadic breast cancer forms as a result of mutated oncogenes, resulting in oncogene activation, and is characterized by uncontrolled cell proliferation. In inherited breast cancer, there is a combination of allele inactivation and germline mutation in a tumor suppressor gene (4; 5). The process of malignant transformation in breast cancer has yet to be fully elucidated. However, breast cancer progression is characterized by an increase in cell proliferation rates and abnormal cell growth. This process promotes the acquisition of mesenchymal characteristics, a process by which cells lose polarity and cell-cell adhesion (6). Recently, the migratory phenomenon known to drive embryonic development under normal conditions called epithelial to mesenchymal transition (EMT) has been shown to play a pivotal role in breast cancer invasion and metastasis (7) Metastases cause the vast majority of cancer-related deaths (8), and are the most poorly understood hallmark of cancer (9).

Breast cancer remains one of the most common cancers worldwide and is a major cause of cancer-related deaths among adult females in the United States. Approximately 12.4 percent of women born in the US will develop breast cancer (10). Breast cancer is a complex heterogeneous disease, having several pathological subtypes, each distinguished by its own pathological and clinical characteristics (11). Breast cancer diagnosis comprises a combination of clinical examination, mammography, histopathological analysis, and molecular techniques, including immunohistochemistry (IHC) and

fluorescence in situ hybridization (12). Diagnosis, allows individual assessment of patient prognosis based on staging characteristics (i.e. tumor grade and receptor status) (13). Stage 0 is the earliest stage, represents localized disease and stage IV represents metastatic breast cancer (MBC), the most advanced stage of disease (13). Noninvasive, or stage 0, includes the earliest stage of disease. Patients that fall into this category typically have good prognosis and a 5-year relative survival rate of 99% (14). Early stage invasive breast cancers (stages I and II) have a relative survival rate of approximately 85%. Locally advanced breast cancer (LABC or stage III) has spread beyond the breast to the chest wall and/or lymph [http://www.nccn.org/]. Stage III is characterized by poor prognosis and has a long-term survival of approximately 72% [http://www.nccn.org/].Patients having breast cancer progression to distant sites beyond the breast (organ metastasis) are categorized as stage IV or advanced breast cancer (15). The 5-year relative survival after stage IV diagnosis is roughly 22%, however prognosis is dependent on the location of organ metastasis (10). Although there is no cure for stage IV breast cancer, symptoms of disease can be alleviated with palliative treatment.

Within the past two decades, the advances in early detection and treatment options have caused a steady decline in breast cancer mortality rates (16). Yet, MBC remains an incurable disease, as 5–10% of those patients survive more than 5 years, and 2–5% survives more than 10 years (17). Recent, advancements in tumor grading and comprehension of disease heterogeneity have allowed for the progression of targeted therapy and personalized medicine. However, understanding the mechanisms that drive resistance and metastasis remains a major therapeutic challenge.

2. Subtypes of breast Cancer

Gene expression profiling has identified at least five major subtypes of breast cancer- luminal type A (estrogen receptor (ER)+ and/or progesterone receptor positive (PR)+, human epidermal growth factor receptor 2 (HER2)−, low Ki67), luminal B (ER+ and/or PR+, HER2+ or HER2− with high Ki67), ER− and HER2+, triple negative (TNBC) and basal-like (ER−, PR−, HER2−) (18-23) . Histopathological and molecular classifications improve the abilities to predict outcomes and direct appropriate targeted treatment options to patients.

i. Luminal type breast cancer

The most common subtype of breast cancer, luminal tumors express hormone receptors, reminiscent with luminal epithelial cells originating from the inner layer of the mammary duct lining (18). Both Luminal type A and Luminal type B breast cancers are characterized as being ER+ and PR+. Luminal type A cancers are (HER2-negative and account for 54.3% of all patients (24-26). Luminal type A patients respond well to hormone therapy and have the most favorable outcome of all subtypes. Tamoxifen, a selective estrogen receptor modulator (SERM), is a competitive inhibitor of estrogen binding to ER in breast tissue. Contrarily, luminal type B breast cancer is more complex. Luminal type B breast cancer can be either HER2- or HER2+, have lower expression of ER as compared to luminal type A, as well as low expression of PR and higher expression of proliferation cluster genes (e.g., *MKI67*) and cell cycle–associated genes (e.g., *CCNB1* and *MYBL2*) Thus, luminal type B breast cancer has a worse prognosis compared with luminal A, and is most effectively treated with a combination of therapeutic strategies, such as hormonal treatment plus chemotherapy (27).

ii. Basal-like and triple-negative breast cancer (TNBC)

Accounting for approximately 15% of all breast cancer patients, basal-like breast cancer is more prevalent in pre-menopausal African-American women (28). Basal-like breast cancer is the most genetically complex subtype of breast cancer, and is defined by (1) lack of ER, PR, and HER2 expression ('triple-negative' immunophenotype), (2) expression of one or more high molecular weight basal cytokeratins (CK5/6, CK14, and CK17), (3) lack of expression of ER and HER2 in conjunction with expression of CK5/6 and/or epidermal growth factor receptor (EGFR), and (4) lack of expression of ER, PR, and HER2 in conjunction with expression of CK5/6 and/or EGFR (19). Basal-like breast cancer poses a significant treatment challenge given its aggressive phenotype and lack of available targeted therapy options. Treatment with chemotherapy is limited by nonspecific cytotoxicity, significant side effects and the high potential for residual disease progression. Recently, there have been developments of promising targets (eg, FGFR2, TRAIL, antiangiogenic agents) for subgroups of basal-like breast cancers (28).

Oftentimes used synonymously, TNBC and basal-like breast cancer are not the same. Both basal-like and TNBCs lack ER, PR, and HER2 expression, and are associated with aggressive pathologic features, high occurrence in younger African-American women and poor clinical outcomes. Gene expression profiling studies (29); (30) identified approximately 70% of TNBCs as belonging to the basal-like subtype, whereas 8-29% were classified as having extensive heterogeneity (31-34). Given the complexity of this disease, the therapeutic strategies for treating TNBC include targeting DNA repair complexes (platinum compounds and taxanes), P53 (taxanes), cell proliferation

(anthracycline containing regimen) and Poly-(ADP-ribose) polymerase (PARP1) repair. These targeted strategies, when combined with cisplatin, have shown promise in terms of improved progression-free survival (35; 36) .

iii. HER2 and breast cancer

Discovered by Shih et al., in the 1980s, HER2-*neu* (c-ERBB-2) is a proto-oncogene that encodes HER2, a 185-kilodalton type 1 glycoprotein with tyrosine kinase activity (37). The epidermal growth factor receptor (EGFR) family is a group of 4 transmembrane glycoproteins (Figure 1-1) EGFR (ErbB1), HER2 (ErbB2), HER3 (ErbB3), and HER4 (ErbB4) comprised of an extracellular binding domain, an α-helical transmembrane domain and an intracellular receptor tyrosine kinase (RTK) domain (38). HER3 is a pseudokinase having a unique intracellular kinase domain that binds ATP with high affinity, but possesses weak kinase ability to promote autophosphorylation. Ligands bind to the extracellular domain of these receptors causing a conformational change resulting in homo- or-heterodimerization followed by phosphorylation of tyrosine residues within the intracellular region. There is no known ligand for HER2, yet it is the preferred dimerization partner for all erbB receptors (39; 40) . Interestingly, HER2 has the strongest catalytic kinase activity and HER2-containing heterodimers cause potent mitogenic signaling, particularly HER2:HER3 heterodimers (39; 41). The phosphorylated tyrosine residues then become docking sites for src homology 2 (SH2) and phosphotyrosine binding domain (PTB) containing proteins. This process results in the recruitment and activation of downstream second messenger (42) signaling pathways. Activation of intracellular signaling pathways is dependent on phosphorylation of specific receptor residues.

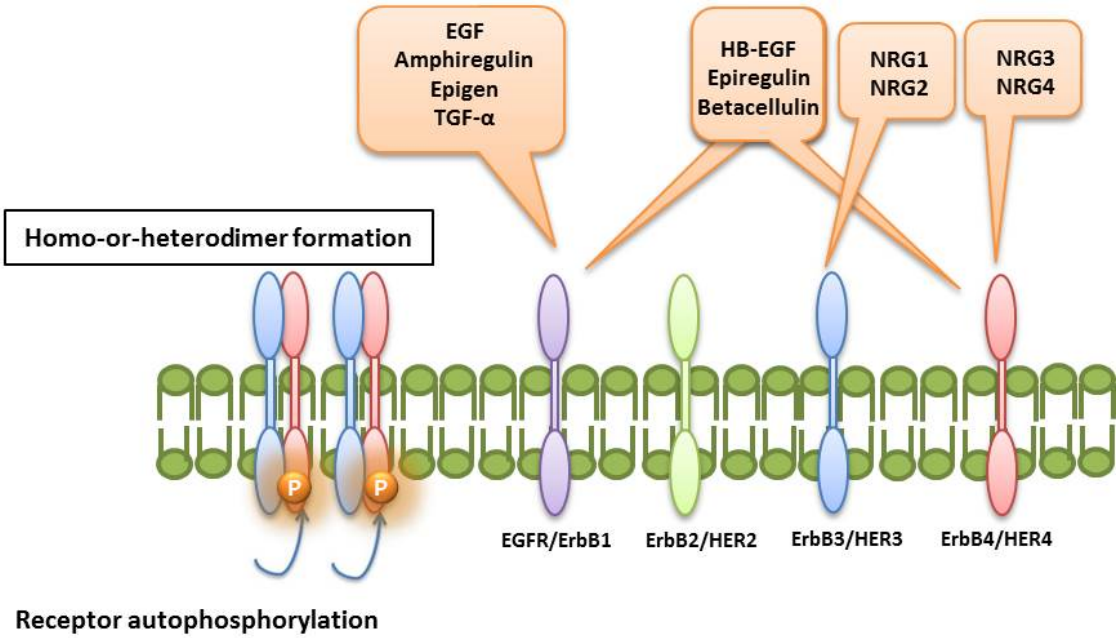

Figure revised from (43)

Figure. 1-1. EGFR/HER family tyrosine kinase receptors.

EGFR/HER receptors and their respective ligands. Each receptor shows an extracellular domain, a helical transmembrane segment, and an intracellular protein tyrosine kinase domain. Once the ligand is bound, these receptors can homodimerize or heterodimerize with each other to form several receptor combinations, which leads to activation of a variety of downstream signaling pathways.

These pathways include the 1) mitogen-activated protein kinase (MAPK) cascade responsible for growth, differentiation and apoptosis, 2) phosphatidylinositol-3 kinase (PI3K/AKT), which regulates anti-apoptotic signaling, 3) other pathways like the mammalian target of rapamycin (mTOR), and the signal transducer and activator of transcription (STAT) pathways (39; 40; 44). Currently, there are 11 known ligands for this family: epidermal growth factor (EGF), transforming growth factor alpha (TGF-α), epiregulin, herparin-binding epidermal growth factor (HBEGF), betacellulin, amphiregulin, epigen, neuregulin-1 (NRG-1)/Heregulin (HRG), NRG-2, NRG-3 and NRG-4 (Fig 1.1) (43).

Under normal physiological conditions, HER2 is expressed in pulmonary bronchial epithelial cells and is involved in multiple physiologic processes, including cell proliferation, wound repair, neuregulin signaling and nervous system development (45). Interestingly, in 1989, studies by Margolis and colleagues determined that HER2 authophosphorylation tyrosine sites are located within the C-terminus, and are identical to EGFR phosphorylation sites (46). In 1990, the HER2 phosphorylation sites were identified as follows: Y1248, Y1023, Y1112, Y1127, Y1139, Y1196, Y1221, and Y1222 (46). Further studies determined that, even in the absence of its intracellular domains, HER2 is capable of dimerization (47; 48). The robust signaling mediated by HER2-containing dimers has been attributed in part to the extracellular domain of HER2, which constitutively exists in an activated conformation (49; 50) with kinase function unnecessary for homodimerization (39; 51).

Among newly diagnosed breast cancer patients, an estimated 15–20% of breast tumors have amplification of the *HER2* gene (25-50 copies) and up to 40- to 100– fold

increase in HER2 protein expression (52-54). *HER2* amplification is associated with a more aggressive tumor biology (55) and an increased incidence of metastasis (56) due to the constitutive activation of numerous downstream signaling networks involved in migration, cell-cycle regulation, proliferation, inhibition of apoptosis, and angiogenesis (57; 58). The increased expression of this cell-surface molecule specifically in tumor cells and its association with unfavorable outcomes in patients with breast cancer provide rationale for selectively inhibiting this molecular target.

3. HER2-targeted therapies

Given the dynamic role of HER2 in the oncogenesis and progression of breast cancer, a significant amount of research has focused on developing HER2-targeted therapies. The first anti-HER2 antibody to be translated to clinical use was trastuzumab (59), which is currently the main first-line therapy for patients with HER2-overexpressing breast cancer. Other methods of treatment include second-generation humanized monoclonal antibodies, as well as both reversible and irreversible small molecule tyrosine kinase inhibitors, which can bind to ATP and prevent phosphorylation of target proteins. Each inhibitor has demonstrated significant clinical response in certain patients; however, the development of resistance remains a major challenge (60).

i. Trastuzumab

Trastuzumab is a humanized monoclonal antibody (mAb), that binds to domain IV of the HER2 extracellular domain and disrupts downstream PI3K signaling (61)and Ras-MAPK signaling (62). Trastuzumab-mediated tumor regression appears to be

partially dependent on the abilities to block angiogenesis (63; 64), induce antibody-dependent cellular cytotoxicity (65; 66) and suppress invasion and metastasis (67; 68), which may be related to the ability to target a HER2-positive stem cell population (69)(Figure 1-2) (70). In addition, the combination of trastuzumab with chemotherapy has been shown to improve both survival and response rate, in comparison to trastuzumab alone (71). As of 2017, there were over 150 active interventional studies incorporating trastuzumab (https://clinicaltrials.gov). Currently, there are several studies investigating the benefits of novel agents, including Hsp90 inhibitors, P13K/AKT/mTOR inhibitors, vascular endothelial growth factor (VEGF) inhibitors, insulin-like growth factor-I receptor (IGF-IR) inhibitors and aromatase inhibitors in combination with trastuzumab.

ii. Lapatinib

Lapatinib (Tykerb ®, GlaxoSmithKline) is a potent, orally active, dual tyrosine kinase inhibitor that blocks both EGFR and HER2. Lapatinib binds to the ATP-binding site of both receptors and prevents signal transduction through MAPK and PI3K/AKT pathways. Lapatinib is commonly used in patients with HER2-positive metastatic breast cancer who have progressed on treatment regimens that included trastuzumab with taxane or anthracycline treatment (72). Clinical trials using trastuzumab and lapatinib in combination with chemotherapy or endocrine therapy have shown a significant improvement in outcome, as compared to single-agent chemotherapy treatment regimens (40; 73; 74). In addition, lapatinib monotherapy induces apoptosis and increases sensitivity to radiation in trastuzumab-resistant cells (75).

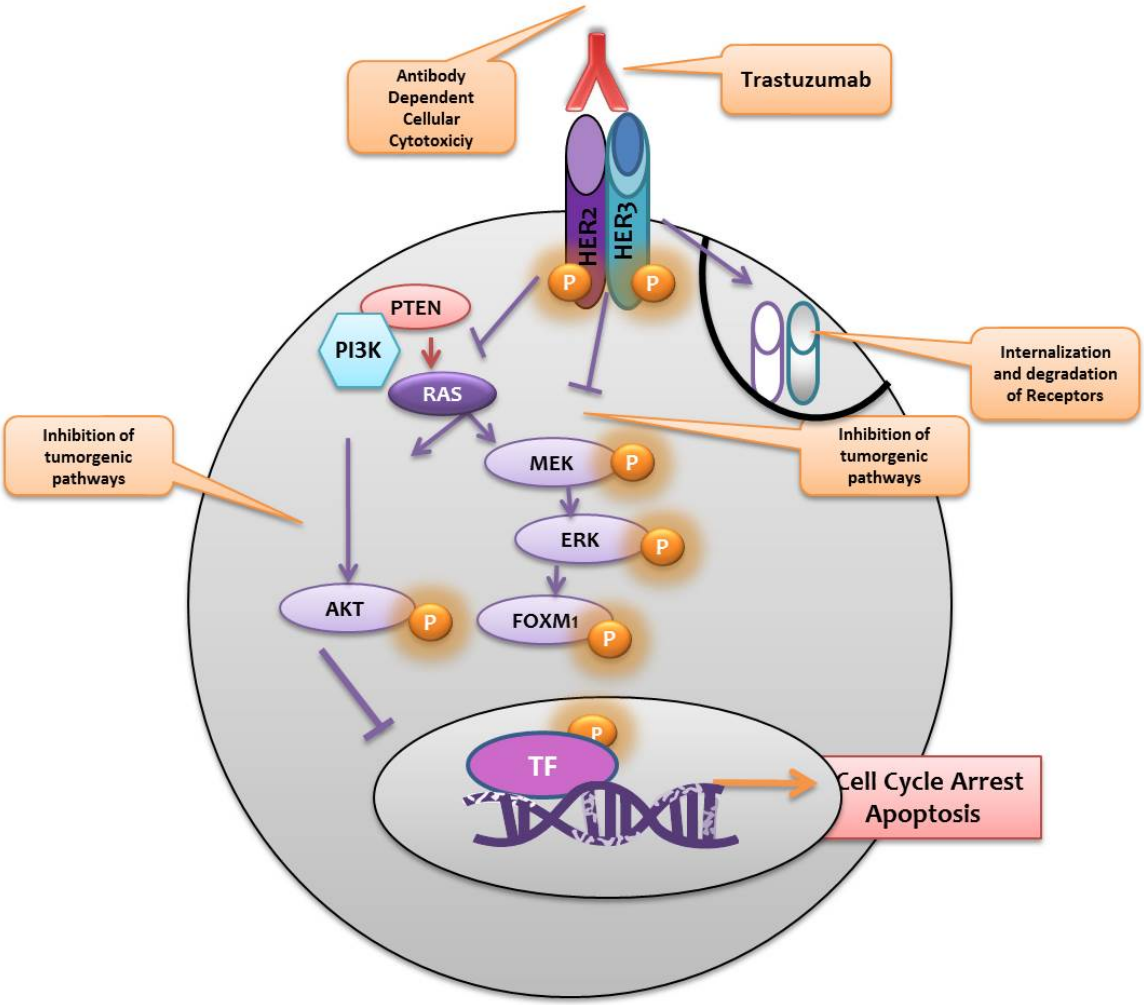
Antibody Dependent Cellular Cytotoxiciy
Trastuzumab
HER2
HER3
P
P
PTEN
PI3K
RAS
Internalization and degradation of Receptors
Inhibition of tumorgenic pathways
Inhibition of tumorgenic pathways
MEK
P
ERK
P
AKT
P
FOXM1
P
P
TF
Cell Cycle Arrest
Apoptosis

Figure 1-2. Mechanism of action for trastuzumab in HER2-expressing breast cancer

In breast cancer, constitutively active HER2 receptors dimerize with other EGFR/HER receptors, activating downstream signaling pathways that promote tumorigenesis. Trastuzumab prevents constitutive activation of HER2, induces internalization and degradation of the protein, and stimulates the immune system to recognize HER2-overexpressing cells.

Lapatinib is also being examined in clinical trials with inhibitors of angiogenesis, P13K/mTOR and cytotoxic agents (76). Lapatinib is currently approved as a second-line therapy in combination with chemotherapy for trastuzumab-refractory metastatic breast cancer.

However, a majority of patients who received prior trastuzumab therapy demonstrate resistance to lapatinib. Thus, improved understanding of the molecular mechanisms contributing to resistance to both trastuzumab and lapatinib is critical for developing new therapies and for identifying those who are most likely to respond to currently available agents.

iii. Other HER2-targeting agents

In addition to the HER2-targeting agents detailed above, there are other agents in use which target HER2 signaling. Pertuzumab is a second-generation humanized mAb that targets the HER2 domain involved in HER2/HER3 dimerization, preventing tumor development (50; 77; 78). In 2012, Keating and colleagues reported that the addition of pertuzumab to trastuzumab and docetaxel for the first-line treatment of HER2-positive metastatic breast cancer prolonged progression-free survival in the randomized, double-blind, multinational, phase III CLEOPATRA trial (79). The antibody-drug conjugate T-DM1, Ado-trastuzumab emtansine, consists of trastuzumab and the chemotherapeutic agent emtansine. Emtansine is a cytotoxic microtubule-depolymerizing agent (80). T-DM1 is specifically approved for patients who have previously been treated with trastuzumab and taxane, separately or in combination, and have metastatic breast cancer

or tumor recurrence within six months of completing adjuvant therapy (Kadcyla (ado-trastuzumab emtansine [T-DM1]) Genentech/Roche; May, 2013.)

iv. Resistance to HER2-targeted therapy

Despite the tremendous efficacy of trastuzumab against HER2-overexpressing metastatic breast cancers, a significant fraction of women demonstrate progressive disease during treatment. There are many proposed mechanisms of resistance (Figure 1-3) (81). One potential mechanism is masking of the HER2 epitope to which trastuzumab binds, which has been described as a result of overexpression of the mucin cell-surface protein MUC4 (82). Compensatory signaling and receptor cross-talk have also been proposed as mechanisms through which HER2 signaling is sustained in resistant cells; for example, the IGF-1R (83; 84) and the hepatocyte growth factor receptor MET (85) have been shown to cluster and crosstalk with HER2. Previous studies have shown that, crosstalk from IGF-1R to HER2 results in sustained HER2 phosphorylation in the presence of trastuzumab resistance (86-89). Moreover, the inhibition of IGF-1R signaling blocks HER2 phosphorylation and restores sensitivity to trastuzumab (83). Moreover, activation of IGF-1R using IGF-1 stimulation results in the phosphorylation of HER2 and activation of PI3K (87; 90).

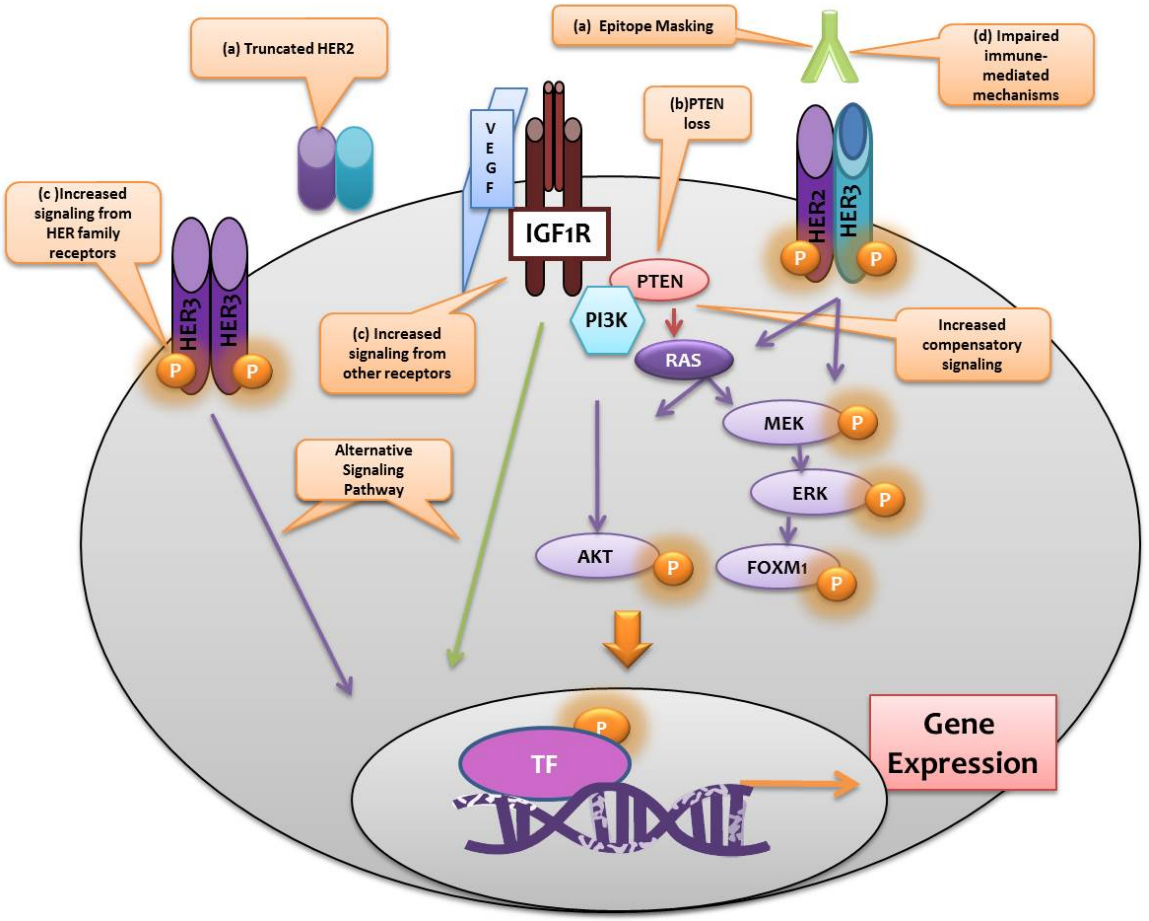
(a) Truncated HER2
(a) Epitope Masking
(d) Impaired immune-mediated mechanisms
(b)PTEN loss
(c)Increased signaling from HER family receptors
VEGF
IGF1R
HER2
HER3
HER3
PTEN
PI3K
RAS
(c) Increased signaling from other receptors
Increased compensatory signaling
MEK
ERK
FOXM1
Alternative Signaling Pathway
AKT
TF
Gene Expression

Figure 1-3. Mechanisms of Trastuzumab Resistance

Relevant mechanisms of trastuzumab resistance in breast cancer include: **(a)** impaired trastuzumab binding to HER2 (i.e. truncated HER2 and epitope masking). **(b)** upregulation of HER2 downstream signaling pathways: PTEN loss, increased PI3K/Akt activity and PDK1 changes. **(c)** alternative signaling pathways: Increased signaling from HER family and other receptors. **(d)** impaired immune-mediated mechanisms.

Increased signaling through the PI3K pathway is recognized as one of the most clinically relevant mechanisms of resistance and may occur due to down-regulation of PTEN (91), hyperactivating mutations in the catalytic subunit of PI3K (92) or subsequent to increased upstream growth factor receptor signaling. Further downstream, reduced expression or cellular relocalization of the p27 protein (19; 71; 93) or increased expression of anti-apoptotic regulators, including Bcl-2 (94), have been described in models of trastuzumab resistance. Another potential mechanism is up-regulation of ligands that increase phosphorylation of HER2, such as the EGFR ligand TGF-alpha (95), HER3 ligand heregulin (95), and the cytokine growth differentiation factor 15 (96).

Lastly, aberrant HER2 signaling constitutively activates multiple downstream signaling pathways, including; those which enhance Forkhead box MI (FOXM1) transcription factor signaling (97). FOXM1 regulates proliferation, mitosis, metastasis, tumor development, and progression in breast cancer (58; 59; 61-63). Thus, FOXM1-mediated trastuzumab resistance may occur through a variety of molecular mechanisms.

4. FOXM1 and breast cancer

i. FOXM1, a downstream target of HER2 signaling

Forkhead box MI (FoxM1) is a member of the forkhead family of transcription factors (98). There are more than 100 proteins in the forkhead family, which represents a subgroup of the helix-turn-helix class of transcription factors; this name refers to the winged nature of the DNA-binding domain, which is flanked by two side loops (98).

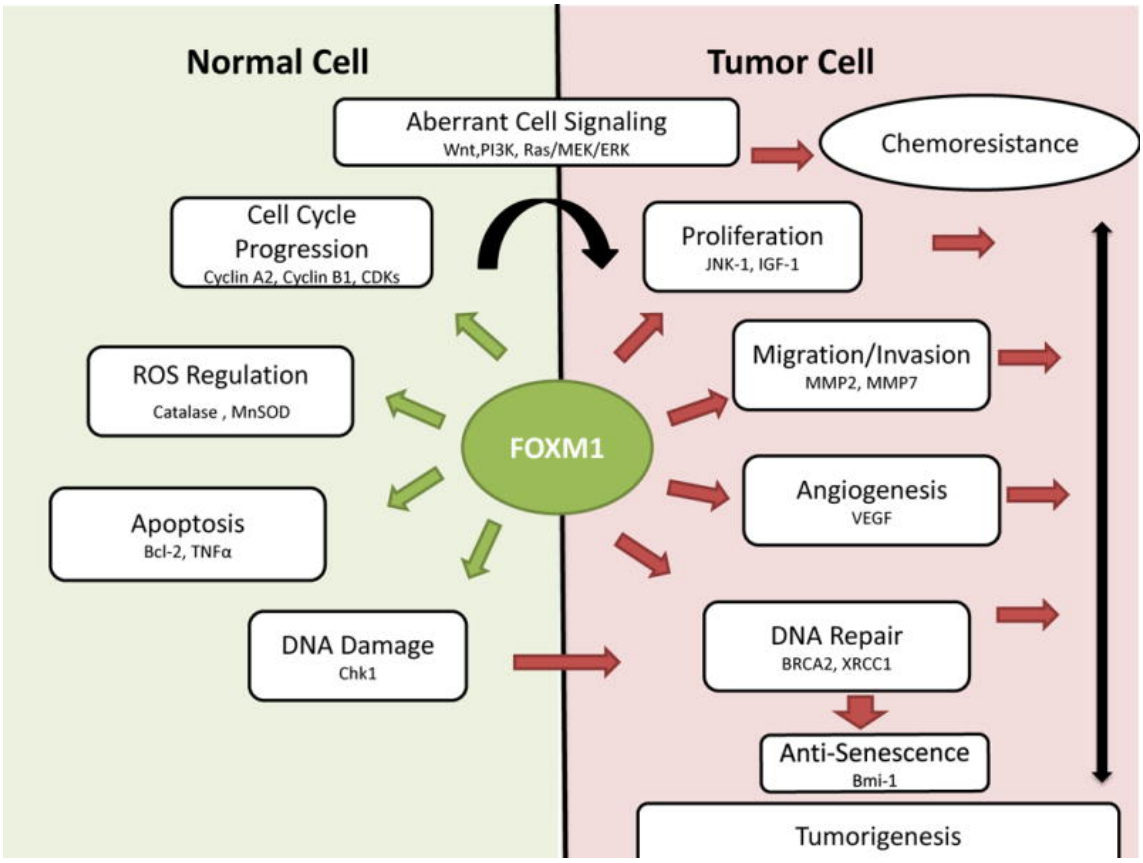
Normal Cell
Tumor Cell
Aberrant Cell Signaling
Wnt,PI3K, Ras/MEK/ERK
Chemoresistance
Cell Cycle Progression
Cyclin A2, Cyclin B1, CDKs
Proliferation
JNK-1, IGF-1
ROS Regulation
Catalase , MnSOD
Migration/Invasion
MMP2, MMP7
FOXM1
Apoptosis
Bcl-2, TNFα
Angiogenesis
VEGF
DNA Damage
Chk1
DNA Repair
BRCA2, XRCC1
Anti-Senescence
Bmi-1
Tumorigenesis

Figure 1-4. The role of FOXM1 in normal cells and the effects of its deregulation in tumor cell chemoresistance.

FoxM1 has several mechanisms of activation. Under normal conditions FOXM1 transcriptional activity and expression are tightly regulated. FOXM1 controls a variety of biological processes by driving the transcription of target genes that regulate cell cycle progression/arrest, cellular responses to oxidative stress, DNA damage and cell death. In tumor cells, FOXM1 homeostatic regulation is compromised due to dysregulation of cell signaling pathways. For example, upregulation of Wnt, PI3K, and/or Ras/MEK/ERK signaling has been shown to increase FOXM1 expression and activation. Sustained FOXM1 signaling promotes increased expression of FOXM1 target genes and evasion of cell death in tumor cells, resulting in chemoresistance and tumorigenesis. Thus, FOXM1 antagonizes the effects of chemotherapy by upregulating DNA repair, self-renewal, proliferation, and migration.

There are three known isoforms of human FOXM1, which are referred to as FOXM1a, FOXM1b, and FOXM1c; these isoforms result from alternative splicing of the transcript of the 25-kb *foxm1* gene, which contains 10 exons and is found at chromosomal location 12p13.33 (98). The FOXM1 isoforms are characterized by a highly-conserved DNA-binding domain, an N-terminal repressor domain, and a strong transactivation domain. FOXM1b and FOXM1c recognize and activate transcription from consensus sequence 5′-A-C/T-AAA-C/T-AA-3′ (98). Both are regulated by MEK signaling, but FOXM1c has two Erk1/2 phosphorylation sites, S330 and S703 (98); thus, FOXM1c may be more dependent upon MEK signaling. The functions of FOXM1 are related to the functions of its target genes, of which there are more than 200; these targets regulate the majority of cancer-related processes, including proliferation, invasion, angiogenesis, senescence, stem cell function, and DNA repair (Figure. 1-4) (98). Normal physiological functions include regulation of replication, mitosis, and repair.

FOXM1 upregulation is associated with poor prognosis in breast cancer (99). FOXM1 transcript levels are significantly elevated in multiple breast cancer tissue data sets (Figure 1-5). FOXM1 plays a role in most subtypes of breast cancer, not just HER2-overexpressing forms. In triple negative breast cancer (TNBC), FOXM1 overexpression protects cancer cells from DNA double-strand breaks, by interacting with NFκB to promote doxorubicin chemoresistance (100). Accordingly, it has been shown that FOXM1 inhibition decreases transcription of DNA repair genes and restores Doxorubicin sensitivity in TNBC (100).

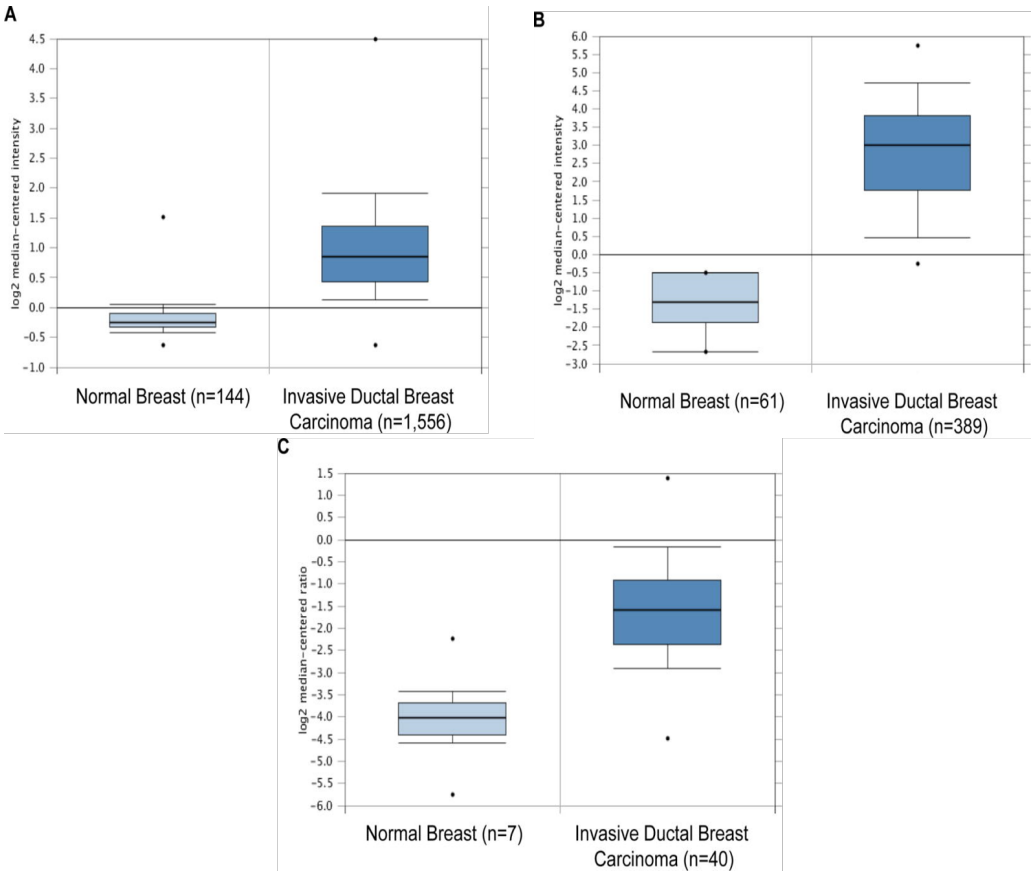
A
log2 median-centered intensity
4.5
4.0
3.5
3.0
2.5
2.0
1.5
1.0
0.5
0.0
-0.5
-1.0
Normal Breast (n=144)
Invasive Ductal Breast Carcinoma (n=1,556)
B
log2 median-centered intensity
6.0
5.5
5.0
4.5
4.0
3.5
3.0
2.5
2.0
1.5
1.0
0.5
0.0
-0.5
-1.0
-1.5
-2.0
-2.5
-3.0
Normal Breast (n=61)
Invasive Ductal Breast Carcinoma (n=389)
C
log2 median-centered ratio
1.5
1.0
0.5
0.0
-0.5
-1.0
-1.5
-2.0
-2.5
-3.0
-3.5
-4.0
-4.5
-5.0
-5.5
-6.0
Normal Breast (n=7)
Invasive Ductal Breast Carcinoma (n=40)

Figure 1-5. Increased FOXM1 transcript levels in breast cancer tissues

(a) FoxM1 transcript levels in breast cancer tissues versus normal breast tissues are shown for the Curtis breast data set retrieved from Oncomine; this data set included 2,136 samples examined on the Illumina Human HT-12 V3.0 R2 Array consisting of 19,273 measured genes. Fold change = 2.21, **p<0.005 **(b)** FoxM1 transcript levels in breast cancer tissues versus normal breast tissues are shown for the TCGA breast data set retrieved from Oncomine; This data set included 593 samples; the array measured 20,423 genes, but the name of the array platform was not provided in the Oncomine database. Fold change = 5.213, **p<0.005 **(c)** FoxM1 transcript levels in breast cancer tissues versus normal breast tissues are shown for the Richardson breast 2 data set retrieved from Oncomine; This data set included 47 samples examined on the Human Genome U133 Plus 2.0 Array consisting of 19,574 measured genes. Fold change = 17.629, **p<0.005; [www.oncomine.org]

Constitutive overexpression of FOXM1 in MCF-7 breast cancer cells promotes acquired cisplatin resistance, by enhancing the expression of the DNA damage response genes; breast cancer-associated gene 2 (BRCA2) and X-ray cross complementing group 1 (XRCC1). Furthermore, in ERα positive and negative breast cancer cells, FOXM1 has been shown to interact with the coactivator CARM1 to regulate ERα transcription (101). Increased FOXM1 levels amplify estrogen-mediated mitogenic actions and promote endocrine therapy resistance in ERα positive breast cancer (102). FOXM1 inhibition has been demonstrated to decrease expression of ERα-regulated genes, suppress estrogen-induced breast cancer cell proliferation, and restore tamoxifen sensitivity (102; 103).

Studies investigating FOXM1 as a downstream target of HER2 signaling have demonstrated a direct correlation between HER2 and FOXM1 expression levels *in vivo* and *in vitro* (104; 105). Stable overexpression of FOXM1 in HER2-overexpressing cell lines effectively diminished trastuzumab sensitivity, increased colony formation, and inhibited lapatinib-induced cytotoxicity (104; 106). Interestingly, inhibition of EGFR/HER2 with lapatinib had no observable effect on FOXM1 protein levels in lapatinib-resistant lines. In contrast, combined inhibition of MEK signaling plus lapatinib diminished nuclear FOXM1 levels (105). Consistent with these findings, inhibition of Raf/MEK/ERK signaling delays G2/M transition and inhibits expression of FOXM1 target genes (107). Additionally, treatment of sensitive and resistant breast carcinoma lines with the anti-EGFR tyrosine kinase inhibitor gefitinib reduces FOXM1 and HER2 phosphorylation only in sensitive cell lines (108). Moreover, FOXM1 blocks paclitaxel-induced apoptosis due to reduced levels of the microtubule-destabilizing protein stathmin in HER2-positive breast cancer cells (104). Aberrant FOXM1 signaling can promote a

drug-resistant phenotype, characterized by activation of anti-apoptotic proteins Bcl-2, up-regulation of genes important for homologous recombination, and promotion of epithelial to mesenchymal transition (EMT) (102; 109). Furthermore, FOXM1 has been shown to sustain TGFβ-induced formation of a SMAD3/SMAD4 nuclear transcription complex that up-regulates the downstream EMT target SLUG to promote breast cancer metastasis (110; 111). This process may also be mediated by growth differentiation factor 15 (GDF15), a divergent member of the TGFβ superfamily, which promotes invasion, EMT, and is increased in the setting of acquired trastuzumab resistance (96). Collectively, these studies provide rationale for further investigation into the mechanisms of FOXM1-mediated chemoresistance in HER2-positive breast cancer.

ii. Targeting FOXM1 in resistant breast cancer

FOXM1 deregulation is a potential diagnostic and prognostic biomarker of oncogenic potential in several malignancies (112). Aberrant HER2 signaling constitutively activates multiple downstream signaling pathways, including PI3K/Akt, and ERK, which enhance FOXM1 signaling (97). FOXM1 regulates proliferation, mitosis, metastasis, tumor development, and progression in breast cancer (58; 59; 61-63). Thus, FOXM1mediated trastuzumab resistance may occur through a variety of molecular mechanisms. Treatment of HER2-positive breast cancer cells with thiostrepton, a selective inhibitor of FOXM1 mRNA, causes increased sensitivity to lapatinib. Furthermore, thiostrepton diminishes proliferation, invasiveness, and transformation, and induces apoptosis in breast cancer cells that express FOXM1, regardless of HER2 overexpression status, indicating that FOXM1-targeting is a relevant approach for

multiple subtypes of breast cancer (101; 106). Knockdown of FOXM1 with thiostrepton in micelle nanoparticles administered to MDA-MB-231 breast cancer xenografts reduced tumor growth rates and increased apoptosis (113). Additionally, co-administration of thiostrepton and lapatinib reduces the survival of HER2-positive breast cancer cells. The natural nontoxic agent 3, 3′-diidolylmethane (DIM) combined with trastuzumab causes down-regulation of Akt, NFκB, and FOXM1 in breast cancer cells (114). DIM enhances trastuzumab efficacy by selectively reducing FOXM1 expression and inhibiting tumor growth without toxicity (115). Injection of FOXM1-specific siRNA into tumor xenografts suppresses tumor growth and reduces expression of FOXM1 transcriptional targets (6). Similarly, treatment of resistant and sensitive breast cancer cells with the ARF-derived peptide, which is a FOXM1 inhibitor, decreases proliferation and restores sensitization to trastuzumab (104). Knockdown of FOXM1 with shRNA diminishes proliferation, anchorage independence, and tumorigenesis of breast cancer cells *in vitro* and *in vivo* (111). These studies demonstrate the therapeutic potential of co-targeting FOXM1 in drug-refractory breast cancer.

5. Scope of Dissertation

This dissertation aims to further understand the mechanisms that drive resistance and metastasis in breast cancer. We have previously shown upregulation of GDF15 in the presence of acquired trastuzumab resistance, and investigated the implications of IGF-1R signaling as a mechanism of compensatory signaling and sustained resistance in HER2 positive breast cancer. In this study, I hypothesize that overexpression of GDF15 is driving activation of IGF-1R/FOXM1 signaling, which drives resistance and cancer

progression. My preliminary studies reveal increased proliferation, invasion, migratory potential and EMT in the presence of GDF15 overexpression. By characterizing the acquired phenotype in the presence of constitutively expressed GDF15, I was able to identify several signaling pathways activated in this setting. The data revealed that GDF15 overexpression promotes increased activation of multiple pathways downstream of HER2 and IGF-1R, such as MEK/ERK, FAK/SRC, PI3K/AKT, and SMAD2/3. Moreover, I determined that GDF15 overexpression promotes activation of receptors that play a key role in mitogenic signaling and tumorigenesis (IGF-1R and TGFβ-R). Lastly, activation of these receptors displayed an increase in protein levels of the proliferation associated transcription factor FOXM1. I proposed targeting these signaling pathways and receptors both individually and in combination to identify the mechanisms by which GDF15 drives resistance and cancer progression. An investigation of TGFβ-R signaling revealed that GDF15 stimulation activates the SMAD2/3 signaling pathway, resulting in increased invasion and mesenchymal markers. However, studies investigating the knockdown of TGFβ-R signaling demonstrated modest restoration of epithelial markers and partial regulation of IGF-1R activation. Inhibition of TGFβ-R signaling was able to partially attenuate invasive potential, but did not restore the epithelial phenotype. These findings suggest that TGFβ-R signaling plays a partial role in GDF15-mediated cancer progression. Moreover, targeting downstream signaling pathways, such as MEK/ERK, SRC/FAK and P13K/AKT, either individually or in combination, does not decrease invasive potential, migration, or EMT status in the presence of GDF15 overexpression. Studies investigating the role of IGF-1R show that stimulation with recombinant GDF15 (rhGDF15) activates IGF-1R with subsequent upregulation of FOXM1 protein levels in

breast cancer cells that express normal levels of GDF15. Further, inhibition and or knockdown of IGF-1R attenuates invasive potential, restores epithelial markers and decreases FOXM1 levels, suggesting that IGF-1R/FOXM1 signaling plays a vital role in GDF15-mediated cancer progression. This dissertation provides insights into the role of GDF15 as a potential biomarker and mediator of invasive potential in breast cancer. Lastly, the data revealed here strongly supports future studies investigating the potential role of targeting IGF-1R/FOXM1 signaling in the presence of GDF15 overexpression and the possibility of further investigation into the signaling pathways activated by GDF15 in breast cancer.

Chapter 2. Materials and Methods

1. General Methods

i. Reagents

Trastuzumab (Herceptin™, Genentech, South San Francisco, CA) was purchased from the Winship Cancer Institute pharmacy and dissolved in sterile water at a stock concentration of 20 mg/mL. HER2 kinase inhibitor AG879 (Sigma-Aldrich, St. Louis, MO) was dissolved in DMSO at a stock concentration of 10 mM. Lapatinib (Santa Cruz, Biotech, Santa Cruz, CA) was dissolved in DMSO at a stock concentration of 10 mM. SB431542 (Sigma-Aldrich, St. Louis, MO) was dissolved in DMSO at a stock concentration of 10 mM. The TGF-beta receptor I kinase inhibitor LY364947 (Cayman Chemical; Ann Arbor, MI) was dissolved in DMSO at a final concentration of 1 mg/mL. The insulin-like growth factor-1 receptor (IGF-1R) antibody alpha IR3 (Calbiochem; San Diego, CA) was provided at a stock concentration of 1 mg/mL. The pan-MMP inhibitor, GM6001 (Millipore; Temecula, Ca) was provided at a stock concentration of 1 mg/mL (2.5mM) in DMSO. In-Solution Src kinase inhibitor PP2 (Calbiochem; San Diego, CA) was provided at a stock concentration of 10 mM in DMSO. IGF-1 ligand (Sigma; St Louis, MO) was dissolved in sterile water to a stock concentration of 1mg/mL. NVP-AEW541 (Cayman Chemical; Ann Arbor, MI) was dissolved in DMSO to a final concentration of 10 mM. Lyophilized recombinant human TGF-βI (rhTGFβI; Sigma Aldrich; St. Louis, MO) was reconstituted in 0.2 μm-filtered distilled water at a final concentration of 50 μg/mL. Lyophilized recombinant human GDF15 (rhGDF15; R&D Systems, 614 McKinley Place NE, Minneapolis, MN 55413) was dissolved in 4 mM HCl containing 0.1% BSA at a final concentration of 100 μg/mL; the solvent (HCl-BSA) was used as vehicle control. The pLKO.1-IGF1R-α/β short hairpin RNA (shRNA) plasmid

and pLKO.1 empty vector plasmid (negative control) were purchased from Open Biosystems (Huntsville, AL, USA). The pGFP-C- FoxM1 B (CTTGCAGCCAATCGTTCTCTGACAGAAGG) and D (CCTTGAATCACCGCAAAGGCTCCTCAGTT) short hairpin (shRNA) and scrambled negative control non-effective pGFP-C-shLenti plasmid were purchased from OriGene (Rockville, MD).

ii. Bacterial transformations

Expression vectors for each gene were used for protein expression in mammalian cells. Transformations were done using MAX Efficiency DH5a cells (Invitrogen; Grand Island, NY), according to the manufacturer's protocol. Briefly, DNA was added to competent cells, incubated on ice for 30 minutes, heat shocked for 45 seconds, followed by incubation on ice for 2 minutes. SOC Medium (Invitrogen) was added, then shaken at 225 rpm 37°C for 1 hour. Reaction containing plasmid DNA was diluted into SOC medium and incubated overnight at 37°C under selective pressure with ampicillin. The following morning, cells were harvested by centrifugation, and purified using a Midi-Prep (Qiagen; Valencia, CA), according to the manufacturer's instructions. Briefly, The bacterial pellet was resuspended in buffer P1(50 mM Tris-HCl pH 8.0, 10 mM EDTA, 100 g/ml RNase A), lysed in buffer P2 (200 mM NaOH, 1% SDS), and neutralized in buffer P3 (3M potassium acetate pH 5.5). The lysate was incubated in a cartridge that allowed the separation and precipitation of genomic DNA, proteins, and detergent. Contaminants were removed by washing with buffer QC (1 M NaCl, 50 mM MOPS pH 7.0, 15% isopropanol), and DNA eluted using buffer QF (1.25 M NaCl, 50 mM Tris-HCl pH 8.5, 15% isopropanol). DNA was precipitated by adding 70% ethanol,

concentrated using a QIA-Precipitator, and washed using 70% ethanol. DNA was eluted with sterile water.

iii. Cell culture

JIMT-1 cells were purchased from DSMZ (Braunschweig, Germany); all other cell lines were purchased from American Type Culture Collection (Manassas, VA). MDA-MB-231, MDA-468, JIMT-1, and BT474 cells were maintained in Dulbecco's Modified Eagle's Medium (DMEM) with 4.5 g/L glucose, glutamine, and sodium pyruvate (Corning; Manassas, VA) with 10% FBS and1% penicillin/streptomycin (P/S). The HCC1954 breast cancer cells were maintained in RPMI with 10% FBS and 1% P/S. All cells were cultured in humidified incubators at 37°C with 5% CO_2.

iv. Creation of trastuzumab-resistant cells

BT474 cells were maintained in 4-μg/ml trastuzumab for three months, at which point surviving pools or clones were selected. All of the acquired resistant cells were maintained on 4 μg/mL trastuzumab, but the drug was removed from culture for 24 hours prior to performing experiments.

v. Creation of stable GDF15-over-expressing clones

GDF15 stable clones were created by transfecting BT474 cells with 3 μg of pCMV empty vector or pCMV-myc-GDF15, both from Origene (Rockville, MD), using Lipofectamine (Invitrogen, Carlsbad, CA) combined with DMSO shock and selecting

cells in 200 μg/mL G418. After approximately 2–3 weeks, surviving clones were isolated and tested by real-time PCR for GDF15 expression.

vi. Creation of stable GDF15-knockdown clones

Lentiviral shRNA constructs for GDF15, or control shRNA in pLKO1 vector were purchased from Open Biosystems (RHS4078) (Huntsville, AL). Lentiviral helper plasmids (pCMV-dR8.2 dvpr and pCMV-VSV-G) were obtained from Addgene (8455 and 8454) (Cambridge, MA). Transient lentivirus stocks were prepared following the manufacturer's protocol. Briefly, 2.5×10^6 293T cells were plated in 10-cm dishes. Cells were co-transfected with shRNA construct (3 μg) together with 3 μg pCMV-dR8.2 dvpr and 0.3 μg pCMV-VSV-G helper constructs. Culture medium containing virus was harvested, and breast cancer cells were infected with shGDF15 or control shRNA for 72 h. Virus-containing cells were selected for 1 week in media containing puromycin (2 μg/ml).

vii. Creation of stable IGF-1R-knockdown clones

HEK-293T cells (1.5×10^6) were seeded in 100-mm dishes for 24 h and co-transfected with 3 μg shRNA construct (pLKO.1-IGF1R-α/β shRNA (KD) or pLKO.1 empty vector control plasmids), 3 μg pCMV-dR8.2, and 0.3 μg pCMV-VSV-G helper constructs using TransIT-LT-1 transfection according to the manufacturer's instructions (Mirus Bio LLC, Madison, WI, USA). Viral stocks were harvested from culture media by centrifugation 48 h after transfection and were syringe-filtered. JIMT-1 cells were seeded at sub-confluent densities and infected with lentiviral vectors (1:20 dilution) in fresh

culture media. Culture media was replaced with media containing 5 μg/ml puromycin 48 h after lentiviral infection to select for cells stably expressing the shRNAs (IGF1R-KD or EV control plasmid). Stable knockdown was confirmed by western blotting for IGF-1R. The IGF1R-KD cells or EV control cells are routinely maintained on 5 μg/ml puromycin in DMEM.

viii. DNA/siRNA Transfection

Cells were plated in antibiotic-free media at a concentration of 2×10^5 cells/mL in antibiotic-free media. The next day, cells were transfected using Lipofectamine 2000 (Invitrogen; Carlsbad, CA) with 10 μg/mL of one of the following plasmids: constitutively active (CA) Src or pcDNA3 empty vector control (kind gifts from Dr. Sumin Kang, Emory); or 100 nM FOXM1 siRNA (Cell Signaling; Danvers, MA), 100 nM GDF15 siRNA (sc-39798), 100 nM control siRNA (sc-37007) (Santa Cruz Biotechnology; Santa Cruz, CA), 100 nM MEK1 siRNA plus 100 nM MEK2 siRNA), according to the manufacturer's protocol. Media was changed after 6 h of transfection and replaced with complete media; cells were harvested after 24 h or 48 h.

ix. Cell cycle analysis.

For cell cycle analysis, cells were harvested, washed twice with DPBS+10% FBS, fixed in ice-cold 80% ethanol, and stored at -20°C for at least 24 hours. Fixed cells were incubated in 50 μL of propidium iodide buffer (20 μg/mL PI (Sigma), 0.1% Triton-X 100, 200 μg/mL RNaseA (Promega) in DPBS) for 30 minutes in the dark. The cells were then resuspended in 400 μL DPBS for flow cytometric analysis. Samples were analyzed

using a BD FACS Canto II cytometer (BD Biosciences; San Jose, CA) and BD FACS Diva software; experiments were performed in triplicate and repeated twice with reproducible results.

x. Immunofluorescence.

Cells were plated on no. 1.5 coverslips placed in tissue culture plates and were allowed to adhere overnight. Cells were fixed in pre-warmed 37°C PHEMO buffer, (3.7% formaldehyde, 0.05% glutaraldehyde, 60 mM PIPES, 25 mM HEPES, 10 mM EGTA, and 4 mM $MgCl_2$ for 10 minutes). Cells were then washed in PBS 3 times and blocked with 10% BSA for 10 minutes. The coverslips were incubated with a combination of rabbit anti-GDF15 (Santa Cruz Biotechnology, sc66904; 1:100) or rabbit-anti TGFβI (Santa Cruz Biotechnology, sc146; 1:250) and mouse anti-TGFβRII (Santa Cruz Biotechnology, sc17791; 1:250) overnight at 4°C with gentle shaking. After 3 washes with PBS, cells were incubated with appropriate Alexa Fluor-conjugated secondary antibody 488 and 555 (Invitrogen) at 1:500 dilution for 1h at room temperature. Nuclear staining was performed by incubating cells with DAPI (350nM) prior to mounting slides with Prolong Gold (Life Technologies) on microscope slides. Slides were then imaged using Zeiss LSM_{510} META confocal microscope with a 40× oil objective lens. Z-stacks were taken from 4 different areas per sample and an average of the overlap coefficient was used to determine co-localization. Experiments were repeated at least twice with reproducible results.

xi. Immunohistochemistry (IHC)

Paraffin-embedded breast tumor tissues from 605 patients were spotted in triplicate per patient to create tumor microarrays (TMAs). TMAs were kindly provided by Dr. Fabrice Andre (Gustave Roussy Cancer Center, Villejuif, France). IHC staining was performed using a standard immunoperoxidase procedure as previously described. Tissues were deparaffinized by heating at 60 °C, passaging through xylene and alcohol grades, and ultimately to water. Antigen retrieval was performed by boiling in 10 mM citrate buffer, pH 6.0 for 10 minutes (min), and cooling in the same buffer for 30 min. Endogenous peroxidase was quenched by incubating with 0.3% H_2O_2 in methanol for 15 min. After washing with water and PBS/TBS, TMA slides were incubated in 10% swine serum (Dako North America, Inc., 6392 Via Real, Carpinteria, CA 93013) for 1 hour to block nonspecific background staining. TMAs were then stained with rabbit polyclonal anti-human GDF15 (also known as Mic-1; Cell Signaling 3249; dilution 1:100; Cell Signaling Technology, Inc., 3 Trask Lane, Danvers, MA 01923) overnight at 4 °C. Secondary antibody staining was then performed with biotinylated anti-rabbit antibody (Dako), followed by visualization with 3,3-diaminobenzidine solution (DAB+ chromogen; Dako North America, Inc.) and hematoxylin as a counterstain. Slides were washed in water, dehydrated by passing through alcohol grades and xylene, and mounted with Permount (Fisher Scientific, 300 Industry Dr., Pittsburgh, PA 15275). GDF15 staining intensity was viewed under a light microscope, and scored on a 0 to 3 scale by a breast pathologist in a blinded manner; the pathologist had no knowledge of any of the molecular or clinical characteristics of the tumor samples. Correlations between GDF15 score and clinical characteristics were determined by two-tailed Fisher's exact test, with

P<0.05 considered statistically significant. Univariate survival analyses were performed by the Kaplan-Meier method and log-rank test, comparing negative staining with positive staining.

xii. Spheroid migration assays.

Stable BT474 pCMV empty vector control or BT474 GDF15 stable overexpressing clones 2, were seeded (5×10^4) in 1% agar-coated 96-well plates and cultured for 48 h in a humidified atmosphere containing 5% CO_2 at 37ºC. Intact tumor spheroids were carefully transferred to a 96-well plate and cultured in complete media for 24 h. Spheroids and migrated cells were fixed with 100% methanol, stained with 0.05% crystal violet, and observed using a normal light microscope (20×) and Olympus DP-30BW digital camera. Experiments were repeated three times with eight replicates per group; representative images are shown for all groups.

xiii. Invasion chamber assays.

Cells were plated in serum-free media in BD BioCoat Matrigel Invasion Chambers (BD Biosciences; Franklin Lakes, NJ) (1 x 10^5 cells/mL) with 0.75 mL of chemoattractant (culture media containing 10% FBS) in the wells. Depending on the experiment, cells were pre-treated with control mouse IgG or alpha IR3 (0.25 μg/mL) or were transfected with control siRNA, GDF15 siRNA or FoxM1 siRNA overnight prior to placing cells in invasion chambers. Treatments were added directly to chambers in non-transfection experiments. Non-invading cells were removed from the interior surface of the membrane by scrubbing gently with dry cotton tipped swab. Each insert was then transferred into 100% methanol for 10 minutes followed by Crystal Violet staining for 20

minutes. Membranes were then washed in water and allowed to air dry completely before being separated from the chamber. Membranes were mounted on slides with permanent mounting medium Permount (Fisher Scientific). Multiple photographs of each sample were taken at 20x magnification, with triplicates performed per treatment group. The number of cells was counted in each field; the sum total of the fields was calculated for each sample. Experiments were performed twice with reproducible results.

xiv. Stimulation experiments

Cells were plated and serum starved for at least 24 hours. Cells were then stimulated with vehicle control, 100 ng/mL IGF-1, 2 or 20 ng/mL recombinant human TGF-βI (rhTGFβI; Sigma Aldrich; St. Louis, MO), or 2 or 20 ng/mL of rhGDF15 for varying time points. Experiments were repeated at least twice with reproducible results.

xv. Quantitative RT-PCR analyses.

Total RNA was extracted using the RNeasy purification kit (Qiagen; Valencia, CA) and treated with DNase (Invitrogen; Carlsbad, CA). Total RNA was used to prepare cDNA using random primers and the Superscript III first strand synthesis Kit (Invitrogen; Carlsbad, CA). Relative levels of mRNA were determined by real-time quantitative PCR using an Applied Biosystems cycler and the TaqMan Universal PCR master mix (4304437; Applied Biosystems; Carlsbad, CA). Primers for RPLPO (Hs99999902_M1), FOXM1 (Hs01073586_M1), GDF15 (Hs00171132_m1), MMP2 (Hs01548733_m1), MMP9 (Hs00234579_m1), SNAIL (Hs00195591_m1), SLUG (Hs00950344_m1), and E-Cadherin (Hs01023894_m1), were obtained from Applied Biosystems (Taq-Man Gene

Expression Assays; Carlsbad, CA). After amplification, the data was normalized with RPLPO levels and analyzed by delta Ct method. Samples were run in triplicate, and experiments were repeated twice to ensure reproducibility.

xvi. Western blot analyses.

Cells were lysed in RIPA buffer (Cell Signaling; Danvers, MA) supplemented with protease and phosphatase inhibitors (Sigma-Aldrich). Total protein extracts were run on SDS-PAGE and blotted onto nitrocellulose. Blots were probed overnight using the following antibodies from Cell Signaling: rabbit anti-phospho-IGF-1 receptor β (Tyr1131) (#3021, 1:200); rabbit anti-IGF-1 receptor β (#3018, 1:250); p-Thr202/Tyr204 p42/p44 ERK1/2 (1:1000), total p42/p44 ERK1/2 (1:1000); rabbit-anti-N-Cadherin (#4061, 1:1000); rabbit anti-phospho-FAK (Tyr397) (#8556, 1:250); rabbit anti-FAK (#3285, 1:500); rabbit anti-phospho-Src (Tyr416) (#2101, 1:1000); rabbit anti-Src (#2123, 1:1000). The following antibodies were purchased from AbCam (Cambridge, MA): rabbit anti-GDF15 (#8479, 1:200); rabbit anti-phospho-ErbB2 (Y877) (ab108371, 1:200); and mouse anti-ErbB2 (ab16901, 1:200). Rabbit anti-TGF-βRII (Santa Cruz Biotechnology, sc-400) was used at 1:200; rabbit anti-phospho-SMAD2 (Ser245/250/255) (#3104, 1:200); rabbit anti-SMAD2 (#5339, 1:200); rabbit anti-FoxM1 (#5436, 1:200). Rabbit anti-TGF-beta receptor II (Santa Cruz Biotechnology, sc-400) was used at 1:200. Mouse anti-E-Cadherin was purchased from BD Biosciences (#610181, 1:1000). Mouse anti-vimentin (Sigma-Aldrich; V6630) was used at 1:1000. Mouse anti-β-actin monoclonal AC-15 (Sigma-Aldrich) was used at 1:10,000 to control for variations in gel loading. All primary antibodies were diluted in 5% BSA/TBS-T. Goat anti-mouse

secondary IRDye 800 antibody (#926-32210, 1:10,000) was purchased from Li-Cor Biosciences (Lincoln, NE). Goat anti-rabbit alexa-fluor 680 secondary antibody (#1027681, 1:10,000) was purchased from Invitrogen (Grand Island, NY). Protein bands were detected using the Odyssey Imaging System (Li-Cor Biosciences, Lincoln, NE). All blots were repeated at least 3 times with reproducible results.

xvii. ELISA

To quantify the amount of GDF15 and TGF-βI released into the media from cells, human GDF15 or human TGF-βI immunoassay (R&D Systems; Minneapolis, MN) were used according to the manufacturer's directions. Media from cells was briefly incubated in GDF15 or TGF-βI antibody-coated microplate for 2 hours. The plate was then washed 4 times and incubated with GDF15 or TGF-βI antibody conjugated to horseradish peroxidase for 1 hour. After washing the wells 4 times, the plate was incubated with hydrogen peroxide-chromagen mix (a color reagent) for 30 minutes, at which point the stop solution was added. Optical density of each well was determined using a microplate reader set to 450nm. The concentrations were calculated according to the standards supplied with the kits by creating four parameter logistic curve-fit.

xviii. Statistics

Relative quantities of mRNAs were calculated using the $\Delta\Delta C_t$ method and normalized using human Ribosomal Protein, Large, P0 (RPLP0) as an endogenous control. Error bars for data are shown as ± SEM or as mean ± SD (RT-PCR only). Significant differences were determined by two-tailed student's t-test. P value was shown as: ns ($p>0.05$, not significant), * ($0.05>P>0.01$, significant), ** ($0.01>P>0.001$, very

significant), *** (P<0.001, extremely significant). Experiments were performed at least three times independently with similar results. IHC staining correlations were determined by two-tailed Fisher's exact test.

2. GDF15 DNAzyme assays

i. Synthesis of gold nanoparticles

Modified from (116)

A 500 mL solution of 1 mM hydrogen tetrachloroaurate (III) trihydrate solution was brought to a vigorous boil, and once boiling, 50 mL of a 38.8 mM sodium citrate tribasic dihydrate solution was added and allowed to reflux for 15 minutes. The reaction mixture was filtered using a 0.45-μm acetate filter, producing monodisperse AuNPs. The resonance wavelength of the gold nanoparticles was determined using UV-vis spectrometry and particle size was determined using transmission electron microscopy (TEM).

ii. Preparation of deoxyribozyme-functionalized gold nanoparticles

Modified from (116)

Disulfide-modified oligonucleotides at either the 5′ or 3′ end were purchased from Integrated DNA Technologies (IDT). The disulfide was reduced to a free thiol by incubating 35 nmols of lyophilized oligonucleotide with 700 μL of disulfide cleavage buffer (0.1 M dithiothreitol (DTT), 170 mM phosphate buffer at pH = 8.0) for 3 hours at room temperature. The reduced oligonucleotides were purified using a NAP™-25 column (GE Healthcare, Piscataway, NJ) with Nanopure water as the eluent. Subsequently, 30 nmols of DNA were added to 7.5 mL of 14 nm gold nanoparticles (10 nM) bringing the

final concentration of oligonucleotide, and gold nanoparticles to ~3.2 μM, and ~7.3 nM, respectively. The pH of the solution was adjusted to pH = 7.4 by adding 93.8 μL of 100 mM phosphate buffer, thus bringing the phosphate buffer concentration to 9 mM. The particles were stabilized by adding sodium dodecyl sulfate (SDS) to the solution and bringing its final concentration to 0.1% (g/ml) by using a stock solution of 10% SDS. The particles were successively salted with eight NaCl additions that were spaced 20 minutes apart using a stock solution of 2.0 M NaCl and 10 mM phosphate buffer. The final NaCl concentration of the DNA-AuNP solution was increased to 0.7 M. The first two NaCl additions increased the concentration by 0.05 M increments while the remaining six NaCl additions increased the NaCl concentration by 0.1 M increments. The particles were immediately sonicated for 10 seconds after each salt addition to maximize DNA packing. The fully salted particles were then incubated overnight, in the dark and at room temperature. We found that the 10–23 active catalytic core of the DNAzyme had a tendency to drive the formation of nanoparticle aggregates at 0.7 M NaCl due to partial self-complementarity of sequences. The following day, the particles were centrifuged four times, reconstituted in Nanopure water each time, and stored at 4 °C for future use for a maximum duration of 1 month.

iii. *Confirmation of DNAzyme (DZNP) catalytic activity*

Modified from (116)

In a typical DzNP synthesis, we reduced 3′thiol-modified oligonucleotides (50 μM), then mixed with gold nanoparticles suspended in phosphate buffered saline (pH 7.4) at a final DNA, and particle concentration of 3 μM, and 6 nM, respectively. The solution

was then stabilized with sodium dodecyl sulfate and salted to 0.7 M NaCl over a period of 3 hours with intermittent sonication. The oligonucleotide density of the purified $DzT_{10}NPs$, where T_{10} refers to the thiolated poly T spacer linking the DNAzyme to the nanoparticle, was 160 ±10 oligonucleotides/particle based on a fluorescence DNA quantification kit (Invitrogen). To verify particle integrity, TEM and UV-Vis analysis were performed before and after particle functionalization, and indicated that the particles remained dispersed following modification with DNAzymes. The catalytic activity of these particles was determined by measuring the rate of hydrolysis of a diribonucleotide within a DNA substrate that was functionalized with a 5′ 6-fluorescein (FAM6) and a 3′ black hole quencher™ (BHQ™) hydrolysis.

iv. Cell culture and DzNP-mediated gene knockdown

Modified from (116)

HCC1954 were maintained in RPMI supplemented with 10% FBS and 1% penicillin-streptomycin in standard culture conditions (37 °C, 5% CO_2). Cells were seeded in a 12-well plate at a concentration of 30,000 cells/well and were allowed to adhere overnight under standard cell culture conditions. Nanoparticles were sterilized by filtering through a 0.2-μm filter prior to addition to the cell media. To achieve the desired nanoparticle concentration, the filtered particles were centrifuged at high speed (13,200 rpm) for 40 min and then resuspended in a known volume of complete RPMI medium. Cells were incubated with 5 nM Dz-gold nanoparticle solution for 48 hours. The medium containing particles was subsequently removed and the cells were gently washed with PBS. This procedure was repeated twice to remove any potential remaining residual

traces of nanoparticles. Total RNA was then isolated using an RNA isolation kit (Sigma, Cat. # RTN-70) and used following the manufacturer's instructions. RNA (48 ng) was used to synthesize cDNA using the Qiagen Sensiscript cDNA synthesis kit (Cat #205213). Real-time PCR was performed using Taqman gene expression primers for GDF15and housekeeping gene, RPLPO. The data was analyzed using the ΔC_T method and reported as such.

Chapter 3

The Characterization of Growth Differentiation Factor 15 in Breast Cancer

1. Introduction

Growth differentiation factor 15 (GDF15; also referred to as macrophage inhibitory cytokine-1, MIC-1, and nonsteroidal anti-inflammatory drug activated gene-1, NAG-1) is a stress-induced cytokine that shares structural features with members of the transforming growth factor-beta (TGF-β) superfamily and bone morphogenic proteins (BMP) (117; 118). All members of the TGF-β superfamily function as ligands to regulate cellular response signaling, including differentiation, adhesion, growth, apoptosis and migration (119). TGF-β ligands bind to type II receptors and regulate cell response by causing heterodimerization with type I receptors, resulting in activation of serine/threonine kinases, which then activate intracellular proteins, such as Smad proteins (Figure 3-1) (120; 121). Recent studies suggest that alternate regulatory mechanisms can be induced by TGF-β ligands via non-Smad signaling pathways activated directly by ligand-occupied receptors that regulate downstream cellular responses. Non-Smad signaling pathways can be regulated by inhibitory Smads, including Smad6 and Smad7. Inhibitory Smads play a critical role in the regulation of TGF-β/BMP signaling by regulating negative feedback loops (122). For example, TGF-β has been shown to recruit intracellular kinase signaling via activation of MAPK, TGF-β-activated kinase 1 (MAPK-TAK1), (123; 124). Activation of TAK1 has also been implicated in regulation of the NFκB pathway (125).

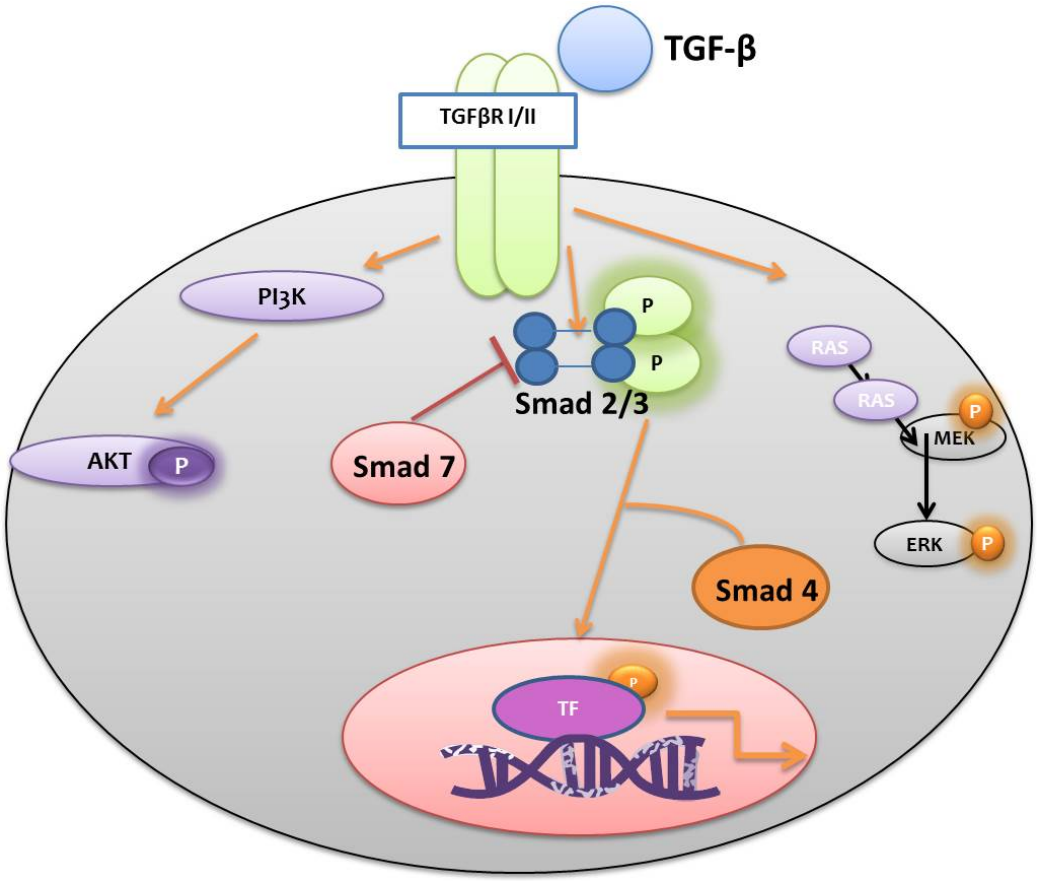
TGF-β
TGFβR I/II
PI3K
P
P
Smad 2/3
RAS
RAS
P
MEK
AKT
P
Smad 7
ERK
P
Smad 4
P
TF

Figure 3-1. TGF-β signaling pathway. TGFβ dimers induce heteromeric formation between type II and type I receptors (such as TGFβ receptor type II (TβRII) and TβRI, respectively). Type II receptors then transphosphorylate type I, resulting in phosphorylation of TGFβ receptor-specific SMADs, which can then form complexes and translocate to the nucleus to drive transcription. Inhibitory SMADS (SMAD6 or SMAD7) inhibit the TGFβ pathway through multiple mechanisms, driving non-SMAD-dependent cellular responses.

Additionally, other non-Smad pathways have been shown to promote activation of the phosphatidylinositol 3-kinase (PI3K)-Akt signaling pathway and Rho-like GTPase signaling pathways (126).

Thus, the TGF-β superfamily plays a diverse role in cytokine-activated regulation of intracellular signaling mechanisms that can be influenced by either a classical Smad pathway or by a growing number of non-Smad pathways. Similar to TGF-β, GDF15 has been shown to induce phosphorylation of Smad2/3 and drive transcriptional activity (127). Further studies have also demonstrated that GDF15 can activate or transactivate HER2, AKT, ERK1/2 (128) and steroid receptor coactivator (Src) signaling via non-Smad-dependent signaling pathways (129). Although, GDF15 has structural similarity to TGF-β, particularly sharing the conserved cysteine-rich domain, it is unique in that it shares less than 30% amino acid homology with members of the TGF-β superfamily (117; 130; 131).

The GDF15 gene is localized on chromosome 19p12–13.1; it is 2,746 base pairs and is comprised of two exons separated by an intron (Figure 3-2) (132). Several regulatory sites have been identified upstream of the open reading frame (ORF) region, comprised of multiple Ap-1 and SP-1 sites, in addition to WT-1, NF-κB, AP-2, PUR factor, HiNF-c and MIG-1 binding sites (131). Furthermore, the SP-1C site plays a crucial role in recruiting transcription factors downstream of the AKT signaling pathway (133).

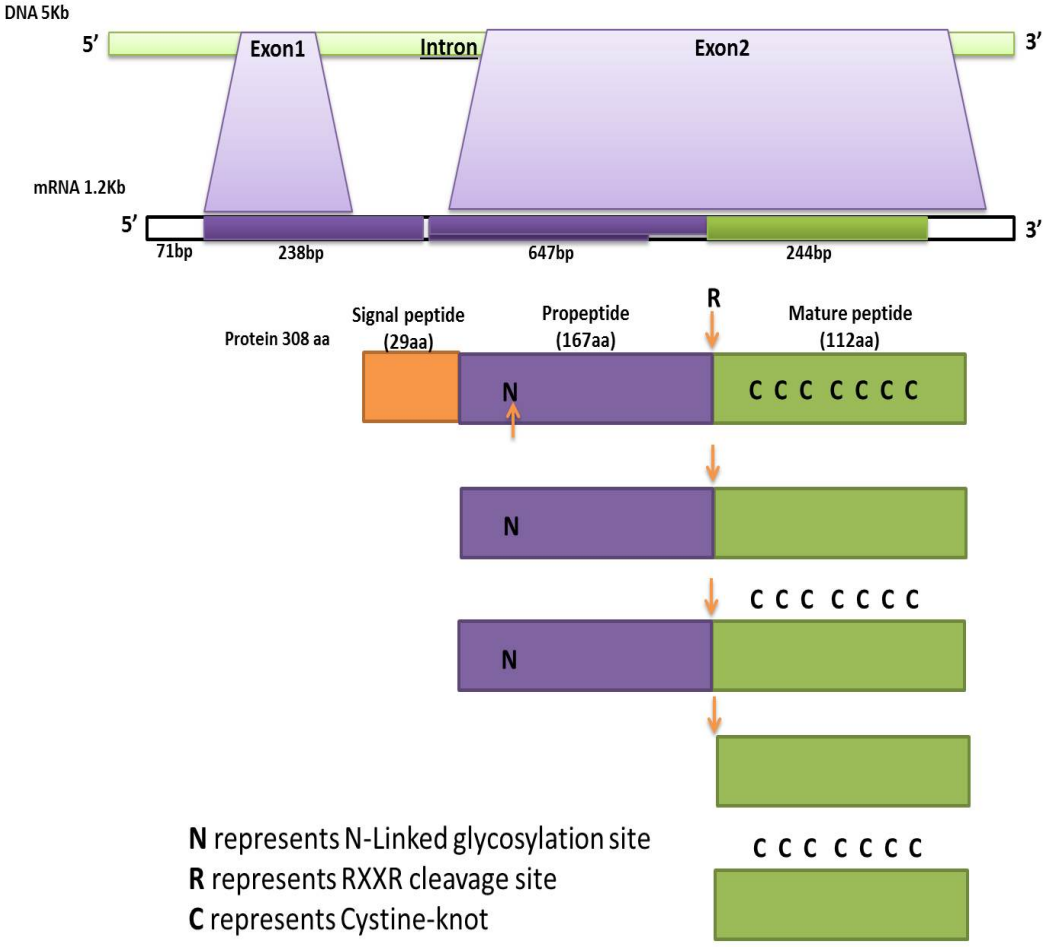

Modified from (132)

Figure 3-2. Genomic and proteomic schematics of GDF15. Gene described in above text. The precursor GDF protein consists of 308 amino acids that contain a 29 amino acid signal peptide, a 167-amino acid pro-peptide, and a 112-amino acid mature protein. The mature protein is secreted as a disulfide-linked homodimer and is released from the following intracellular cleavage at RXXR furine-like cleavage site. The mature peptide of GDF-15 contains the seven conserved cysteines necessary for the cysteine knot, a structural hallmark of the TGF-β superfamily.

Current evidence suggests that *GDF15* is a target gene of p53 (134) and early growth response-1 (Egr-1) (135). Although these transcription factors have been shown to induce expression of GDF15, the exact conditions that determine the regulation of GDF15 are still being explored.

GDF15 is expressed in the cytoplasm anchored to the endoplasmic reticulum as a 40-kDa propeptide, that is proteolytically cleaved by a furin-like proconvertase at the conserved RXXR site (amino acid 196) and undergoes disulfide-linked dimerization to circulate as a 25-kDa protein (136-138) . It has been shown that the unprocessed (pro-peptide) form can be secreted and bind to the extracellular matrix (ECM) (139) and act as a regulator of GDF15 distribution between the circulation and stroma. The mature protein contains two cysteine residues and the typical seven cysteines required to form the cysteine knot, a conserved feature throughout the entire TGF-β superfamily (120; 140). An interesting study by Fairlie and colleagues found that a single nucleotide polymorphism in the GDF15 coding region of histidine (H) to aspartic acid (D) called H5D can significantly impact susceptibility for cancer and patient survival (138; 141).

In normal physiologic conditions, GDF15 expression is restricted primarily to placenta, prostate and colon (142). Elevated serum concentrations of GDF-15 can be detected in pregnant women (143; 144), although the mechanism driving this elevated GDF15 expression in the placenta has yet to be extensively studied. Contrarily, the expression and regulation of GDF15 under pathological conditions has received far more attention. Elevated serum concentrations of GDF15 *have been implicated in* tumor progression, and associated with development and resistance to chemotherapy in breast, prostate, ovarian, and colorectal cancer (145-150) . Similar to other members of the TGF-

β superfamily, GDF15 plays a pleiotropic role in cytoprotection, tumorigenesis (Figure 3-3) (132; 147; 151-153). In advanced-stage disease, GDF15 expression levels are significantly increased in the presence of malignancy, inflammation and injury (118; 154-157). In 2003, Liu and colleagues (158) reported GDF15-mediated morphological and pro-apoptotic regulation in prostate cancer cell lines *in vitro*. This pro-tumorigenic, pro-apoptotic phenomenon has also been recorded in colorectal cancer (159), colon carcinoma (70) and endometrial cancer (160). Thus, GDF15 can induce positive or negative cellular responses depending on the cellular context, microenvironment and disease stage. Moreover, the receptor for GDF15 is unknown, so identifying the signaling pathways and mechanisms by which these responses are regulated is difficult.

There is a substantial amount of clinical evidence linking GDF15 expression with disease progression and resistance to chemotherapy in breast, prostate, ovarian, and colorectal cancers (25; 147-150), suggesting that GDF15 may serve as a diagnostic biomarker of advanced disease or predictor of therapeutic resistance.

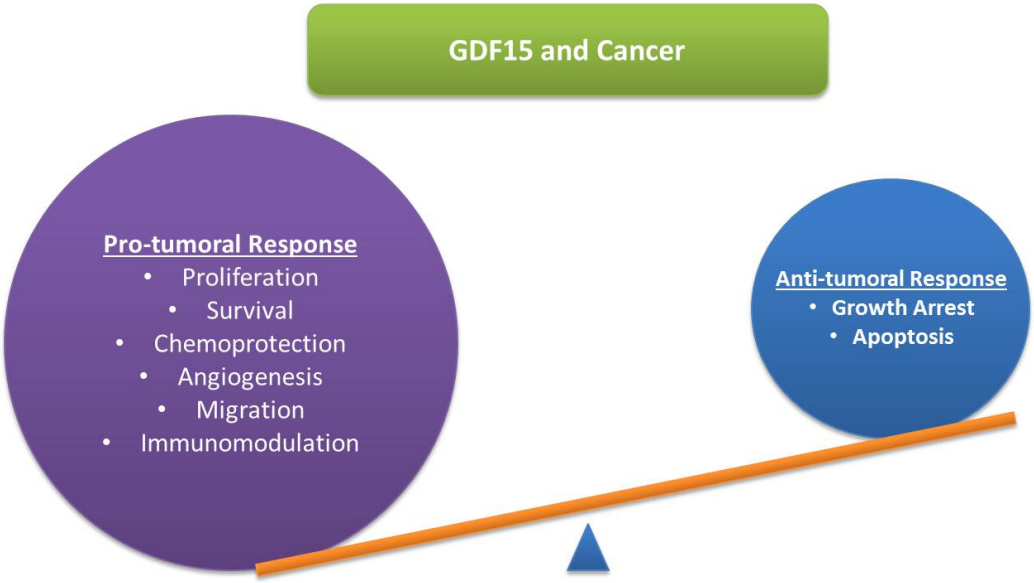
GDF15 and Cancer
Pro-tumoral Response
• Proliferation
• Survival
• Chemoprotection
• Angiogenesis
• Migration
• Immunomodulation
Anti-tumoral Response
• Growth Arrest
• Apoptosis

Figure 3-3. The role of GDF15 in tumorigenesis. GDF15 plays a divergent role in cellular response to stimuli. Opposite effects have been recorded in response to cellular environment, disease stage, or microenvironment (e.g., protumoral or antitumoral). However, the protumoral effects seem to be more prevalent when GDF15 is expressed. Abbreviation: GDF15, growth differentiation factor 15.

Furthermore, GDF15 expression levels are significantly increased in patients with advanced-stage (161) breast, prostate, ovarian, and colorectal cancers (147-150; 158). Studies have reported increased expression of GDF15 transcript, endogenous and secreted forms, in HER2-overexpressing breast cancer cell lines having either acquired or intrinsic trastuzumab resistance (96). Additionally, studies report that stable overexpression of GDF15 promotes an EMT in ovarian cancer cells, which is associated with increased cellular invasiveness (48). Exogenous stimulation with rhGDF15 promotes increased survival of stroma-dependent myeloma cells (162), thus supporting the role of GDF15 in tumorigenesis.

The MAPK signaling pathway plays a critical role in response to extracellular stimuli and drives pathways that regulate gene expression, morphology, cell division and survival (163; 164). There are 3 members of the MAPK family: MAPK (ERK), C-Jun N terminal kinase/stress-activated protein kinase (JNK/SAPK), and p38 kinase. Boyle and colleagues reported in 2009 that expression of GDF15 is partially dependent on mitogen-activated protein kinase (MAPK) signaling (70). In addition, it has been reported that there is a high correlation between GDF15, MAPK 1/2, urokinase-type plasminogen activator (uPA), and invasive potential in gastric cancer cells. It has been previously reported that GDF15 activates p38-MAPK in HER2-positive cells and promotes invasiveness (88). In addition, immunohistochemical analysis of a breast tumor tissue array (TMA) revealed a significant ($p=0.0053$) correlation between HER2 and phosphorylated p38-MAPK in tissues with GDF15-positive staining (88). Functionally, p38-MAPK has been implicated in a plethora of fundamental biological processes, including inflammation, proliferation, differentiation, and cell cycle regulation (165;

166). High levels of p38-MAPK in breast cancer patients are associated with poor prognosis and unfavorable outcome (166). In 2011, Tanizaki and colleagues demonstrated that treatment of HER2-positive breast cancer with lapatinib inhibits MEK/ERK signaling. (167). It was previously reported that stimulation of Tov21 ovarian cancer cell lines with GDF15 promotes activation of ERK1/2 (48). Several reports demonstrate that GDF15 induces downstream signaling through both PI3K and MAPK pathways (168-170). For example, in human gastric and breast cancer cells, GDF15 has been shown to activate Akt and ERK-1/2 (128). This co-activation has been attributed to GDF15-mediated induction of HER2 in SK-BR-3 breast cancer and SNU-216 gastric cancer cells (128). It has been suggested that GDF15 drives breast cancer progression by activating several signaling pathways simultaneously, including those that upregulate estrogen receptor alpha (ERα) (133). ERα is a transcription factor that drives expression of many target genes by directly binding to estrogen-response elements in the target gene promoter.

The Forkhead box transcription factor M1 (FoxM1) is an ERα target gene and proliferation-associated transcription factor downstream of MEK/ERK signaling pathway. The FoxM1 transcription factor regulates the expression of proteins that induce proliferation, cell survival, EMT, and invasion (171). MEK inhibition causes diminished FoxM1 levels and restores sensitivity to the dual EGFR/HER2 kinase inhibitor lapatinib (106). However, the exact regulator(s) of MEK/ERK/FoxM1 signaling in breast cancer have yet to be determined.

Interestingly, studies in myeloma have demonstrated that GDF15 bioactivity can be attributed to an Akt-dependent mechanism independent of ERK1/2 and Src signaling

(162). The PI3K family is a lipid kinase family that phosphorylates inositol phospholipids, which then interact with Akt to drive second messenger signaling within the cell (172). Under normal and pathological (e.g., cancer) conditions, the PI3K/AKT signaling pathway participates in aspects of cell growth and survival (173). Crosstalk between the PI3K and the TGF-β/BMP signaling pathways is crucial for the regulation of numerous responses, including proliferation, apoptosis, and migration (174). In 2005, Wollmann and colleagues discovered an AKT response element located on the GDF15 promoter, and that AKT directly increases GDF15 expression in breast cancer cells (133). Moreover, in breast cancer, the pharmacologic inhibition of HER2 kinase has been shown to prevent GDF15-mediated Akt signaling (96). Thus, although some studies suggest that GDF15 contributes to malignant progression in cancer and promotes chemoresistance, more experiments are required to elucidate this complex paradigm. Here we investigated the effect of stable GDF15 overexpression in HER2-positive breast cancer cell lines having acquired trastuzumab resistance. First, we performed baseline western blots comparing receptor and signaling pathway activation between pCMV empty vector control and the GDF15 stable transfectants. Transfection of BT474 parental cells with GDF15 caused a noticeable increase in total protein levels of multiple signaling pathways (Figure 3-4). Based on these findings, we chose to investigate roles of MEK/ERK, FoxM1 and TGF-βR in GDF-15 signaling.

2. Results

i. Receptors and signaling pathways associated with overexpression of GDF15 in BT474 breast cancer cells.

To further elucidate the potential signaling pathways activated in the presence of GDF15 overexpression (Figure 3-4B), RT-PCR was performed to confirm stable transfection in BT474 breast cancer cells. Previous studies have implicated GDF15 in the activation of several signaling cascades including Smad2/3, PI3K/Akt, and MAPK/ERK (161; 169). Since GDF15 shares structural similarity to TGF-β, we probed for TGF-βRII and Smad2 phosphorylation. Both TGF-βRII and Smad2 phosphorylation have a noticeable increase in protein expression when GDF15 is overexpressed (Figure 3-4B). It has been shown that HER2-positive breast cancer cells having both acquired and intrinsic resistance display hyperactive IGF-1R signaling and subsequent up-regulation of the transcription factor FoxM1 (87) Consistent with these findings, our results indicate increased activation of the IGF-1R receptor (Figure 3-4C). FoxM1, is located downstream of IGF-1R signaling and plays a major role in drug resistance and EMT. Moreover, ER-α binds directly to the promoter for FoxM1 and contributes to mitogenic function in cancer (102). Here we show upregulation of both FoxM1 and ER-α in stable GDF15 transfectants (Figure 3-4D). These preliminary findings support further investigation into the mechanisms by which GDF15 drives carcinogenesis in breast cancer.

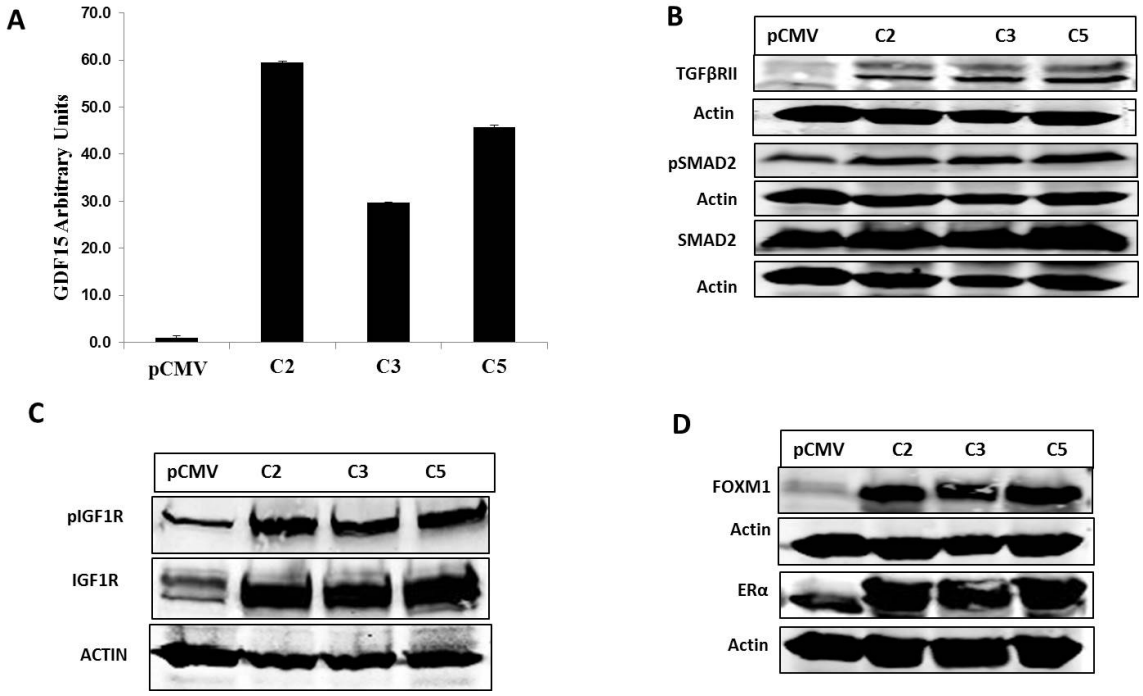
A
70.0
60.0
50.0
40.0
30.0
20.0
10.0
0.0
GDF15 Arbitrary Units
pCMV
C2
C3
C5
B
pCMV
C2
C3
C5
TGFβRII
Actin
pSMAD2
Actin
SMAD2
Actin
C
pCMV
C2
C3
C5
pIGF1R
IGF1R
ACTIN
D
pCMV
C2
C3
C5
FOXM1
Actin
ERα
Actin

Figure 3-4. Receptors and signaling pathways associated with overexpression of GDF15 in BT474 breast cancer cells. **(A)** Real-time PCR was performed for GDF15 in BT474 PCMV control clone and three GDF15 stable clones (C2, C3 and C5). Total protein lysates were collected from the BT474 pCMV empty vector control clone (pCMV) and GDF15 stable clones 2, 3, and 5 (C2, C3, and C5). Western blots were performed for **(B)** TGF-βRII and Smad2, **(C)** pIGF-1R/IGF-1R and **(D)** FoxM1 and ER-α. Blots were repeated at least three times, and representative blots are shown.

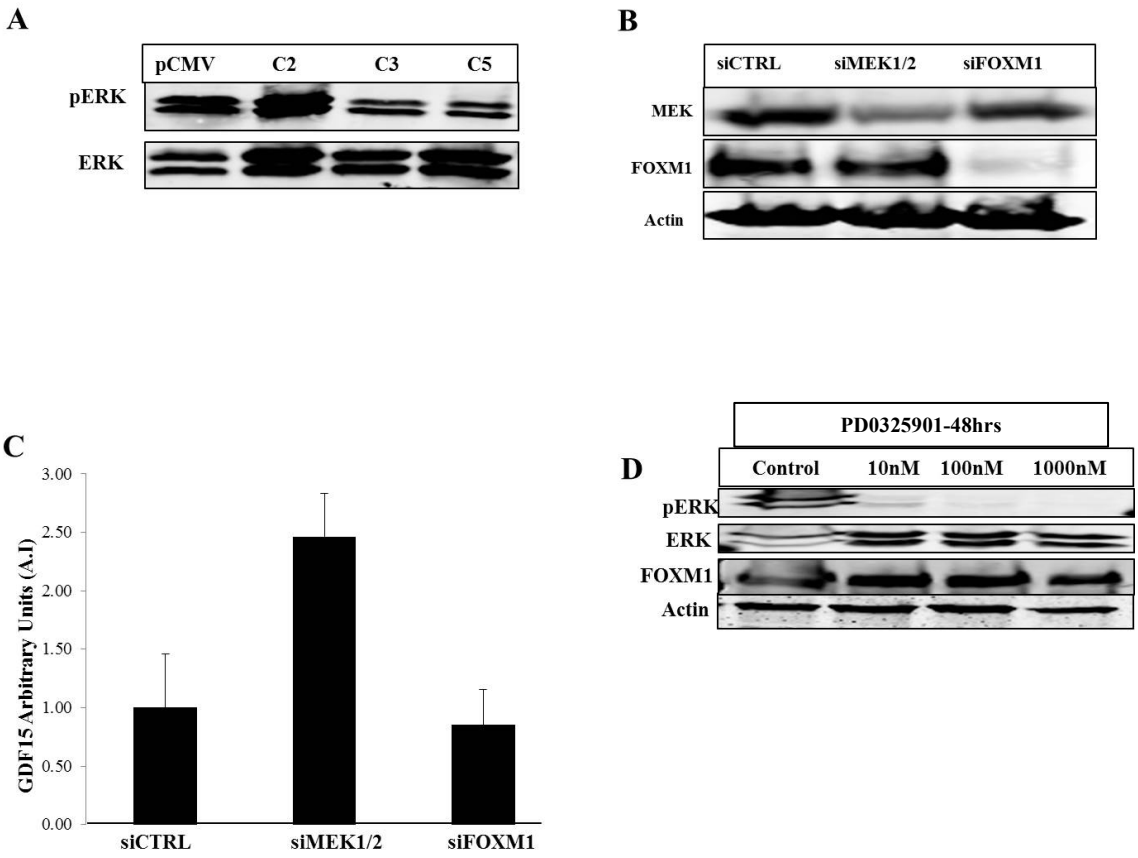
A
pCMV
C2
C3
C5
pERK
ERK
B
siCTRL
siMEK1/2
siFOXM1
MEK
FOXM1
Actin
C
GDF15 Arbitrary Units (A.U)
3.00
2.50
2.00
1.50
1.00
0.50
0.00
siCTRL
siMEK1/2
siFOXM1
D
PD0325901-48hrs
Control
10nM
100nM
1000nM
pERK
ERK
FOXM1
Actin

Figure 3-5. Sustained MEK signaling is associated with GDF15 overexpression. . **(A)** Whole cell protein lysates were isolated from BT474 PCMV empty vector control clone and three GDF15 stable clones (C2, C3 and C5) and immunoblotted for p-ERK, total ERK or actin loading control. Blots were repeated at least three times with reproducible results. A noticeable increase in total ERK was observed in the presence of GDF15 overexpression . **(B)** BT474-myc-GDF15 clone 2 cells were transfected with 100 nM control siRNA (si-CTRL), in combination with 100 nM siRNA MEK1 and siRNA MEK2 or 100 nM siRNA FOXM1. Whole cell protein lysates were isolated and probed for MEK, FOXM1 and actin loading control to confirm successful siRNA knockdown. **(C)** Real-time PCR was performed for GDF15 in the presence of siMEK and siFOXM1. There was no observable difference in GDF15 expression during transient FOXM1 knockdown, however transient knockdown of MEK caused a 1.5 fold increase in GDF15 mRNA expression.**(D)** GDF15 stable clones (C2) were treated with vehicle control, 10 nM, 100 nM or 1000 nM of the MEK kinase inhibitor PD0325901 for 48 h. There was no observable increase in FOXM1 expression in the presence of PD0325901 treatment, suggesting that FOXM1 is regulated via a MEK-independent mechanism in the presence of GDF15 overexpression.

ii. GDF15 overexpression is associated with Sustained MEK/ERK signaling.

Stable GDF15 transfectants derived from BT474 were used to investigate the role of GDF15 overexpression in MEK/ERK signaling. GDF15 promoted increased total ERK; however, there was no observable increase in ERK phosphorylation in the presence of GDF15 overexpression (Figure 3-5A). Next, transfection of siRNA oligonucleotides against MEK1, MEK2 and FOXM1 was used to achieve transient knockdown and confirmed by Western blotting (Figure 3-5B). Knockdown of FOXM1 caused no observable change in GDF15 transcript levels, while knockdown of MEK resulted in approximately a 2-fold increase of GDF15 transcript levels (Figure 3-5C). Interestingly, treatment of stable GDF15 clone 2 with concentrations of the MEK kinase inhibitor PD0325901 up to 1000 nM failed to reduce FOXM1 protein expression (Figure 3-5D). These findings suggest the involvement of a MEK-independent pathway that drives activation of FOXM1 in the presence of GDF15 overexpression. The observed upregulation of GDF15 transcript in response to MEK knockdown could be the result of an unknown oncogenic feedback loop caused by crosstalk between MEK and FOXM1 signaling. For example, increased FOXM1 levels have been observed in the presence of constitutively active MEK/ERK in ovarian cancer cells (175). Thus, inhibiting MEK could be a mechanism by which this system overrides inhibitory signals and drives GDF15 expression. Further studies are required to fully elucidate the role of MEK signaling in the presence of GDF15 overexpression.

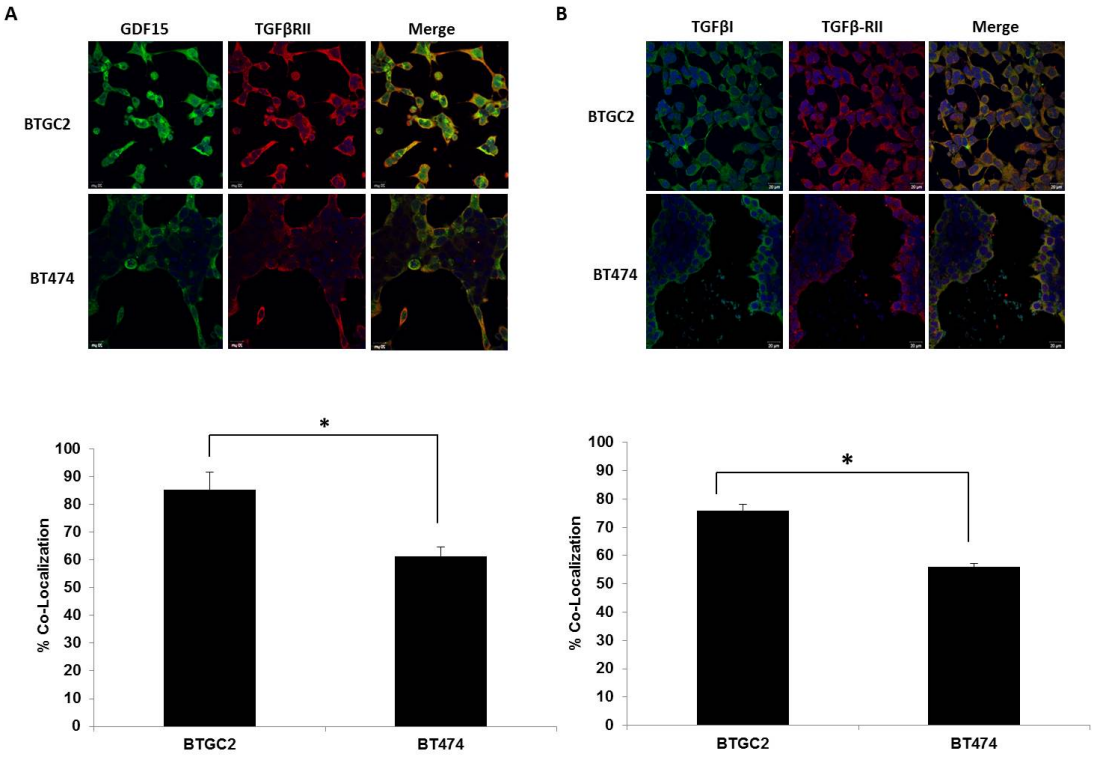
A
GDF15
TGFβRII
Merge
BTGC2
BT474
B
TGFβI
TGFβ-RII
Merge
BTGC2
BT474
% Co-Localization
100
90
80
70
60
50
40
30
20
10
0
*
BTGC2
BT474
% Co-Localization
100
90
80
70
60
50
40
30
20
10
0
*
BTGC2
BT474

Figure 3-6. GDF15 and TGF-beta 1 co-localize with TGF-beta receptor II.

Co-immunofluorescence staining was performed for **(A)** GDF15 and TGF-beta receptor II or **(B)** TGF-beta 1 and TGF-beta receptor II in BT474 GDF15 stable clone 2 (BTGC2) and parental BT474 cells. Representative images are shown at a magnification of 40×. The average of the overlap coefficient percentages was calculated from three different z-stacks. The average percentage of co-localization is shown, with error bars representing standard deviation between replicates. All groups were run in triplicate, and immunofluorescence experiments were performed three times. Significance of differences between GDF15-overexpressing cells and parental cells was determined by student's t-test (*$p<0.05$).

iii. GDF15 and TGF-beta 1 co-localize with TGF-beta receptor II.

Based on structural homology between GDF15 and TGF-beta I, we examined if GDF15 co-localized with TGF-beta receptor II (Figure 3-6A). We also examined co-localization of TGF-beta I with TGF-beta receptor II as a positive control (Figure 3-6B). Immunofluorescence staining for GDF15 or TGF-beta 1 showed a high degree of overlap with staining for TGF-beta receptor II, which is reported as percentage of co-localization. GDF15-overexpressing cells showed a higher percentage of GDF15/TGF-beta receptor II co-localization compared to that of the parental cell line. A similar pattern of co-localization was observed for TGF-beta 1 and TGF-beta receptor II in GDF15-overexpressing cells.

iv. TGF-beta receptor kinase inhibition blocks IGF-1R signaling in stable GDF15-overexpressing cells.

We previously showed that GDF15 stimulates phosphorylation of the TGF-beta receptor substrate Smad2 (96). This is consistent with our current data demonstrating that GDF15 and TGF-beta receptor co-localize. We examined if TGF-beta receptor signaling was required for the induction of IGF-1R phosphorylation and FoxM1 expression in stable GDF15-overexpressing cells. Treatment with the pharmacological TGF-beta receptor II kinase inhibitor LY364947 decreased IGF-1R phosphorylation and FoxM1 expression in GDF15-overexpressing cells (Figure 3-7A).

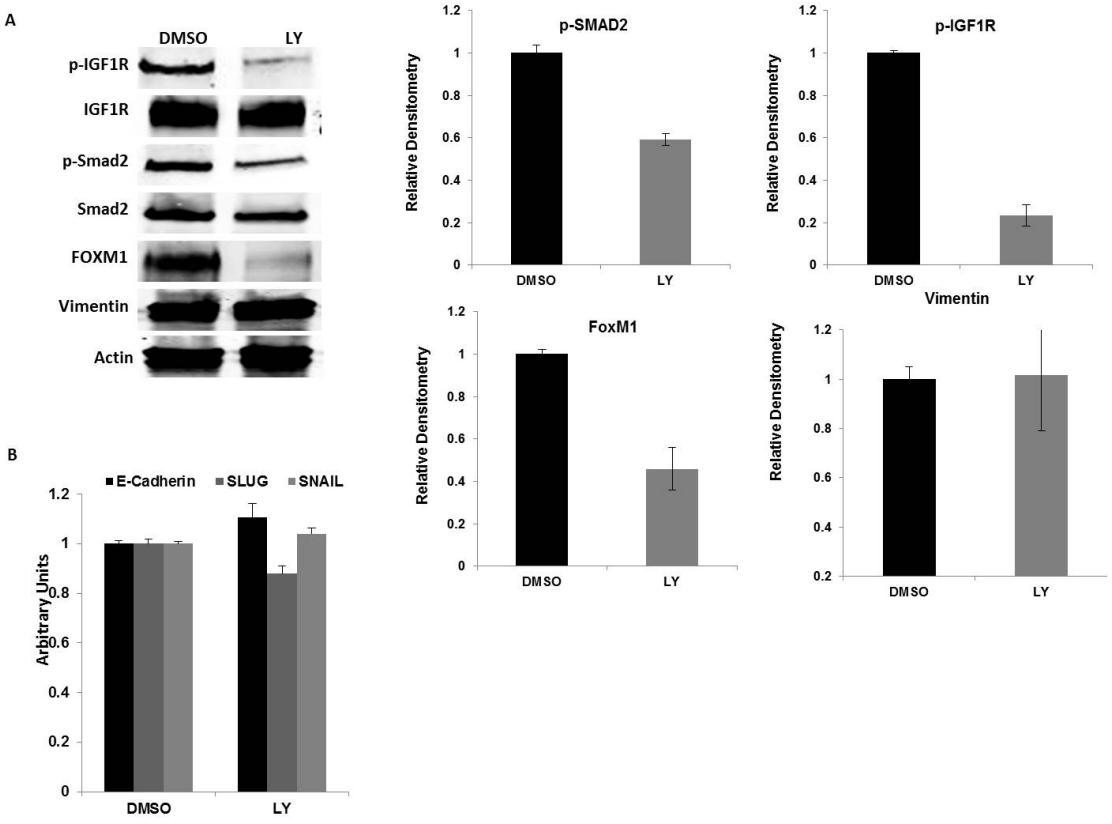
A
DMSO
LY
p-IGF1R
IGF1R
p-Smad2
Smad2
FOXM1
Vimentin
Actin
p-SMAD2
Relative Densitometry
DMSO
LY
p-IGF1R
FoxM1
Vimentin
B
E-Cadherin
SLUG
SNAIL
Arbitrary Units

Figure 3-7. TGF-β receptor inhibition reduces IGF-1R phosphorylation and FoxM1 expression in GDF15-overexpressing cells. BT474 GDF15 stable clone 2 cells were treated with vehicle control (DMSO) or 500 nM LY364947 (LY) for 48 h. **(A)**Western blots of total protein lysates were performed for p-Tyr1131 IGF-1R, total IGF-1R, p-Ser245/250/255 Smad2, total Smad2, FoxM1, vimentin, or actin. Blots were repeated at least three times; representative blots are shown. Densitometry was performed, and the averages of at least two replicates of each blot were calculated. The ratios of phosphorylated to total protein are shown for IGF-1R and Smad2, and the ratio of total protein to actin is shown for FoxM1 and vimentin. **(B)** Real-time PCR was performed for E-cadherin, SLUG, and SNAIL. Values were normalized to the RPLPO housekeeping gene and reflect the fold change in each transcript in the LY-treated group relative to control group.

However, despite the well-documented role of TGF-beta receptor signaling in EMT, inhibition of TGF-beta receptor kinase II did not reduce expression of the mesenchymal markers vimentin (Figure 3-7A), Snail, or Slug (Figure 3-7B) and did not induce expression of the epithelial marker E-cadherin (Figure 3-7B). Thus, TGF-beta receptor signaling regulates IGF-1R phosphorylation and FoxM1 expression in GDF15-overexpressing cells. However, other mechanisms seem to drive EMT in the presence of GDF15 overexpression.

3. Discussion

GDF15 overexpression has been reported in multiple tumor types in association with advanced-stage and/or metastatic disease. Many reports demonstrate that GDF15 induces downstream signaling through the PI3K, mTOR, and/or MAPK pathways (43; 48; 176; 177). Inhibition of these signaling pathways can partially rescue the proliferative and invasive effects of GDF15. In addition, GDF15 shares a high degree of structural similarity with TGF-beta 1 (178) and induces phosphorylation of the TGF-beta receptor substrates Smad2/3 (96; 130). However, other than studies that have reported activation of EGFR/HER2 (88; 96; 129; 179), few studies have directly examined the upstream signaling events activated by GDF15. The findings here provide mechanistic insights into the upstream signaling pathways regulated by GDF15.

Co-immunofluorescence demonstrated a high degree of overlap (80-90%) between GDF15 and TGF-beta receptor II fluorescence in GDF15-overexpressing cells. Control BT474 cells also showed co-localization of GDF15 and TGF-beta receptor II, although to a lesser degree, most likely due to the relatively low level of endogenous GDF15

expression in this line. Pharmacological inhibition of TGF-beta receptor I kinase with LY364947 did not restore E-cadherin expression or reduce expression of mesenchymal markers in GDF15 stable cells. However, TGF-beta receptor inhibition did partially overcome the increased IGF-1R phosphorylation and FoxM1 expression in these cells. These data suggest that TGF-beta receptor signaling contributes to IGF-1R-FoxM1 signaling in breast cancer cells that express high levels of GDF15, but TGF-beta receptor inhibition alone is not sufficient for restoring the epithelial phenotype.

We are the first to report that GDF15 induces IGF-1R phosphorylation. Our data suggest that TGF-beta receptor signaling contributes to IGF-1R phosphorylation and FoxM1 up-regulation. Crosstalk between TGF-beta receptor signaling and IGF-1R has previously been reported (180) and directly supports a potential connection between GDF15 and IGF-1R signaling. Elevated FoxM1 levels promote invasiveness and correlate with poor prognosis (181; 182). Other studies have demonstrated that elevated FoxM1 levels are associated with HER2 overexpression (105; 183) and TGF-beta 1-induced EMT (184). Moreover, it has been shown that IGF-1R and HER2 co-regulate FoxM1 expression and drive invasiveness in the presence of trastuzumab resistance (87). Here, we show that FoxM1 levels are elevated in the presence of stable GDF15 overexpression. However, the mechanisms by which GDF15 overexpression activates TGF-βR/IGF-1R signaling and increases FoxM1 expression remain to be determined.

In summary, we have identified a novel TGF-beta receptor-IGF-1R-FoxM1 signaling mechanism. These findings provide information regarding the cellular effects of GDF15 overexpression and indicate a previously unknown link between GDF15 and

IGF-1R-FoxM1 activation. Future studies should examine co-targeting of TGF-beta receptor signaling and IGF-1R in models of GDF15-overexpressing breast cancer.

Chapter 4

Correlative Analyses of Growth Differentiation Factor 15 in Breast Cancer

1. Introduction

The stress-induced cytokine growth differentiation factor 15 (GDF15) is a distant member of the transforming growth factor-beta (TGF-beta) superfamily and bone morphogenic proteins (117; 145) . These cytokines are ubiquitous, versatile in regulation of cellular response, and essential for survival. In normal physiologic conditions, GDF15 expression is restricted primarily to placenta, prostate, and colon (145). The placenta is the only tissue that normally expresses GDF15 in large amounts (149). Given that GDF15 promotes viability within the maternal-fetal interface, a causal link has been shown between low GDF15 levels and likelihood of miscarriage (144; 149).

Serum levels of GDF15 have been stratified into three categories, normal (<1200 pg/mL), moderately elevated (1200-1800 pg/mL), and highly elevated (>1800 pg/mL) (185). The vast majority of data available investigating the role of GDF15 serum levels has been associated with cardiovascular function. In patients with acute heart failure, circulating levels of GDF15 are increased (186). Moreover, gradual increases in GDF15 serum levels can be used as a sign of adverse outcome in heart failure (187). High expression levels of circulating GDF15 are also an indicator of myocardial infarction and the presence of atherosclerotic lesions (186; 188; 189). Interestingly, induction of GDF15 upon injury is thought to be a protective response, to prevent further apoptosis or tissue injury (186). For example, GDF-15 has been shown to prevent hypertrophy and loss of ventricular function (130). Thus, in cardiovascular disease, increased circulating GDF15 levels act as an indicator of cardiometabolic risk.

GDF15 is an independent predictor of prostate cancer and high-grade tumors (146). GDF15 serum levels have been implicated in prostate tumor progression and bone

metastases (190). In patients with dysplastic colonic polyps and colorectal cancer, GDF-15 serum levels are elevated and associated with decreased overall survival (146). GDF15 plasma levels have been shown to correlate with poor prognosis in endometrial cancer (149). Increased serum levels of GDF15 also influence tumor-associated "cachexia syndrome", via hypothalamic appetite suppression, as a result of downregulation in neuropeptide Y and an increase in pro-opiomelanocortin (POMC) (191). Fascinatingly, the GDF15 propeptide can interact with the latent stromal stores to regulate diffusion of GDF15 into the bloodstream after secretion (139). Taken together, elevation of GDF15 serum levels are closely associated with various pathologic conditions, including diabetes, cardiovascular disease, neurodegeneration and malignancies.

Although few studies have measured GDF15 in breast cancer, two studies indicated that serum (170) and tumor tissue (133) levels of GDF15 were elevated in patients with breast cancer when compared with normal controls. The current study aims to investigate potential correlations between GDF15 expression and clinical characteristics, including molecular subtype and patient survival. Moreover, the purpose of the current study is to evaluate expression of GDF15 in breast tumors (Figure 4-1) and an *in vitro* model of elevated levels of secreted GDF15.

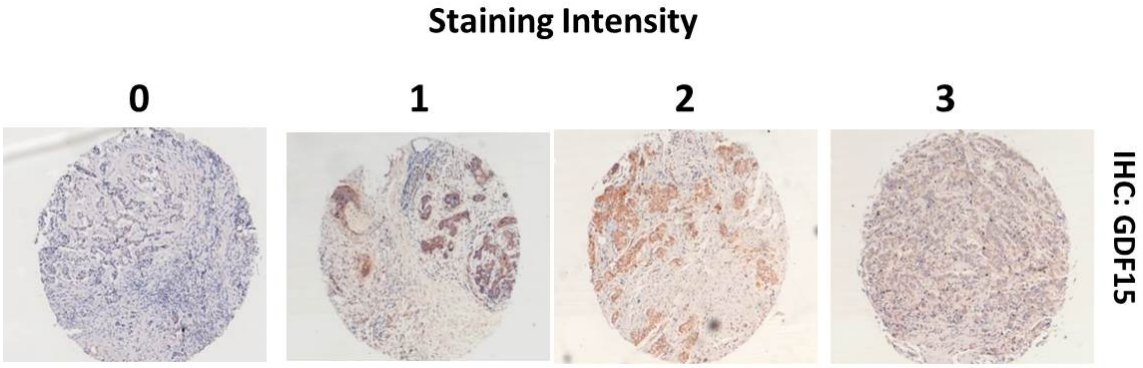
Staining Intensity
0
1
2
3
IHC: GDF15

Figure 4-1. IHC of tumor tissue microarray (TMA) of breast tumors. TMAs consisting of tumor tissue samples representing 605 patients were stained for GDF15. Staining intensity was scored blindly by a breast pathologist, Dr. Amy Adams, Emory University School of Medicine. Photos (left to right) represent staining intensity of negative (0), intermediate, (1-2) and positive (3). Photos were taken at 10x magnification under the microscope, and representative photos of GDF15 staining are shown.

2. Results

i. GDF15 expression correlates with ER-negative and HER2-positive status

Among 605 patients represented on the TMAs, 592 had recorded information for all of the following characteristics available: age, grade, lymph node number (≤ 3 vs > 3), ER and HER2 status. Clinical characteristics and correlations with GDF15 expression are presented for the cohort (N=592) in Table 4-1. The majority (75%) of patients was older than 50 years and had low-grade tumors. GDF15 expression (staining score > 1) was observed in approximately two-thirds (66%) of patients. GDF15 positivity correlated with high tumor grade (P=0.002), with approximately 75% of patients with high-grade tumors exhibiting GDF15 score of 1+ versus 61% with low-grade tumors. Most (87%) patients in the cohort had fewer than four lymph node metastases. Stratification of patients based on ≤ 3 lymph node metastases versus > 3 lymph node metastases did not show significant correlation with GDF15 staining. The molecular subtypes of breast cancers represented in the cohort were consistent with published literature with ~70% estrogen receptor (ER)-positive disease and ~15% human epidermal growth factor receptor 2 (HER2)-positive. Statistically significant correlations were observed between GDF15 expression and ER-negative (P=0.03) or HER2-positive (P=0.03) status.

Table 4-1. Correlations between GDF15 IHC score and clinical characteristics in subgroup with all clinical data available

Characteristic, n (%)	**N=592**	**GDF15 IHC score**		**P value**
		0 (n=204)	**1+** (n=388)	
Age (years)				
< 50	147 (24.8)	48 (32.7)	99 (67.3)	0.7
≥ 50	445 (75.2)	156 (35.1)	289 (64.9)	
Grade				
1-2	402 (67.9)	156 (38.8)	246 (61.2)	**0.002**
3	190 (32.1)	48 (25.3)	142 (74.7)	
Lymph node (#)				
≤ 3	515 (87.0)	173 (33.6)	342 (66.4)	0.3
> 3	77 (13.0)	31 (40.3)	46 (59.7)	
ER				
Negative	192 (32.4)	54 (28.1)	138 (71.9)	**0.03**
Positive	400 (67.6)	150 (37.5)	250 (62.5)	
HER2				
Negative	517 (87.3)	187 (36.2)	330 (63.8)	**0.03**
Positive	75 (12.7)	17 (22.7)	58 (77.3)	

Abbreviations: ER, estrogen receptor; GDF15, growth differentiation factor 15; HER2, human epidermal growth factor receptor 2; IHC, immunohistochemistry

Table 4- 1. Correlations between GDF15 IHC score and clinical characteristics in subgroup with all clinical data available. IHC for GDF15 (Cell Signaling antibody 3249) was performed on arrays consisting of breast tumor tissues from a subgroup of 592 patients. Staining intensity was scored blindly by collaborating breast pathologist, Dr. Amy Adams, as negative (no staining) or positive (scored as intensity levels of 1, 2, or 3). The number (and percentage) of GDF15-positive tissues is shown based on HER2-overexpression (positive) or non-overexpression (negative) status, ER-negative or ER-positive status, and tumor grade (grades 1-2 or grade 3). P-values were determined by two-tailed Fisher's exact test.

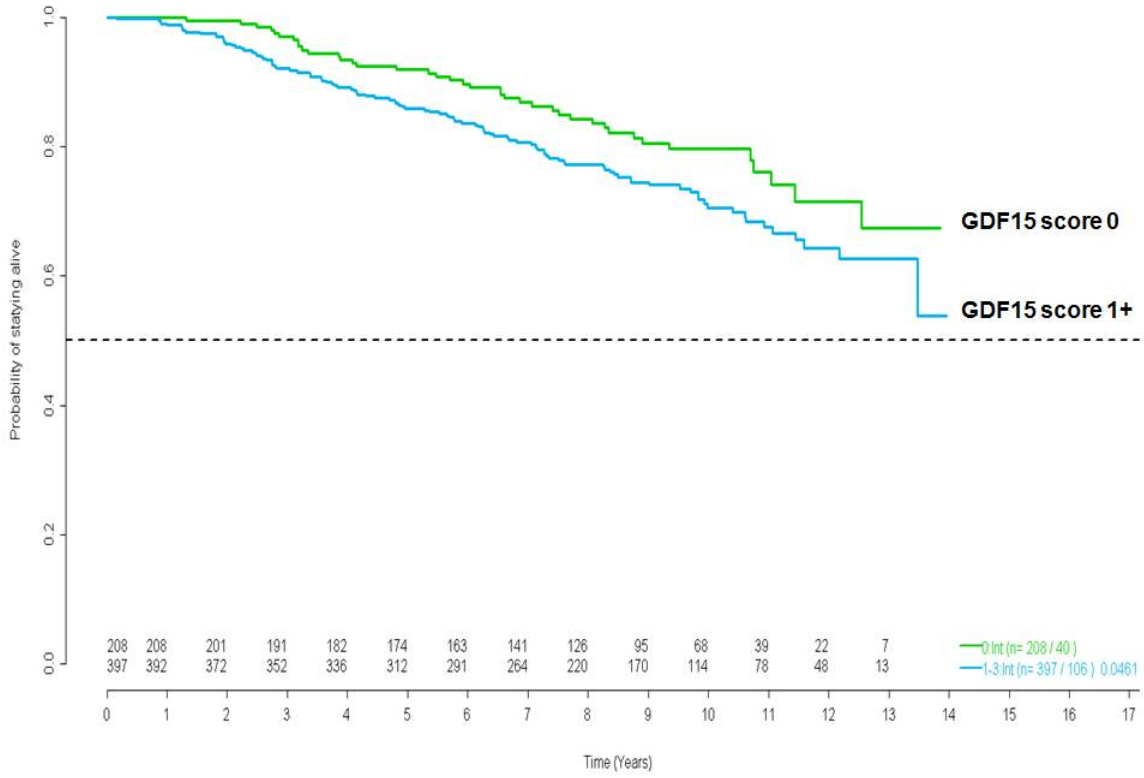
Probability of staying alive
1.0
0.8
0.6
0.4
0.2
0.0
GDF15 score 0
GDF15 score 1+
208 208 201 191 182 174 163 141 126 95 68 39 22 7
397 392 372 352 336 312 291 264 220 170 114 78 48 13
0 Int (n= 208 / 40)
1-3 Int (n= 397 / 106) 0.0461
0 1 2 3 4 5 6 7 8 9 10 11 12 13 14 15 16 17
Time (Years)

Figure 4-2. Kaplan-Meier survival plots stratified by GDF15-positive vs negative staining in patients with breast cancer. Survival analysis was performed to correlate the levels of GDF15 with overall patient survival; GDF15 score 0 and GDF15 score 1^{+}.

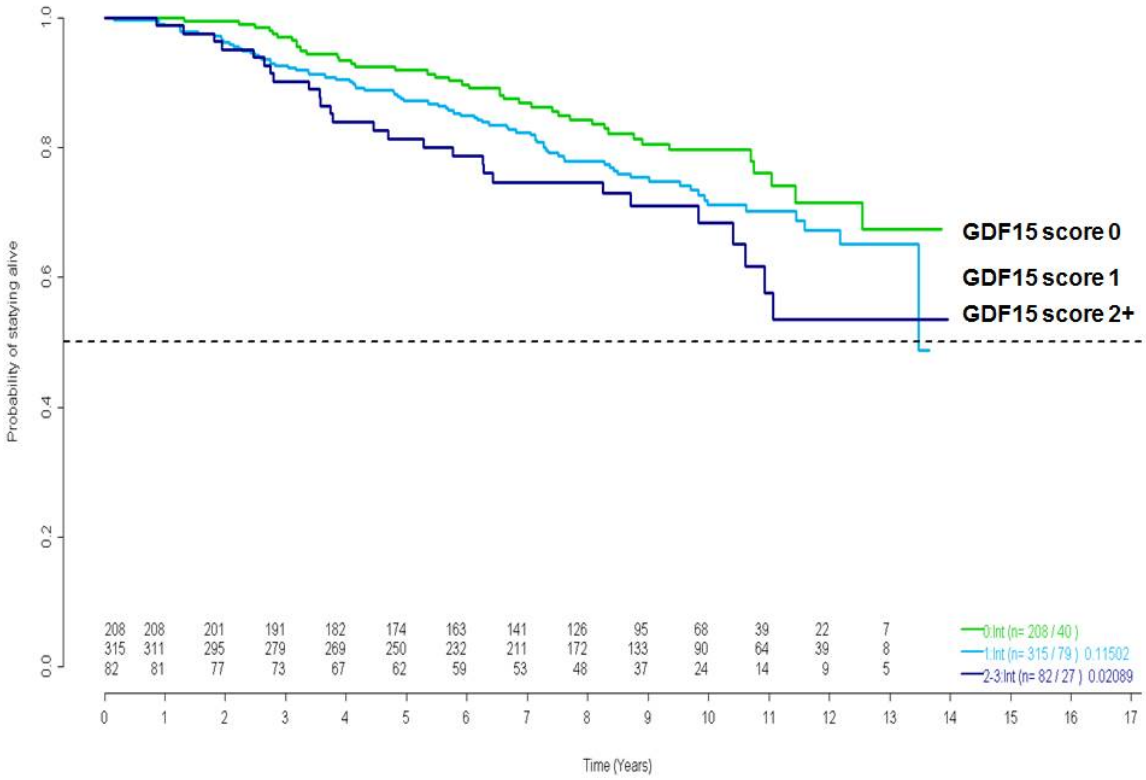
Probability of staying alive
1.0
0.8
0.6
0.4
0.2
0.0
GDF15 score 0
GDF15 score 1
GDF15 score 2+
208 208 201 191 182 174 163 141 126 95 68 39 22 7
315 311 295 279 269 250 232 211 172 133 90 64 39 8
82 81 77 73 67 62 59 53 48 37 24 14 9 5
0 Int (n= 208 / 40)
1 Int (n= 315 / 79) 0.11502
2-3 Int (n= 82 / 27) 0.02089
0 1 2 3 4 5 6 7 8 9 10 11 12 13 14 15 16 17
Time (Years)

Figure 4-3. Kaplan-Meier survival plots stratified by GDF15 IHC score 0, 1, and 2+ in patients with breast cancer. Survival analysis was performed to correlate the levels of GDF15 with overall patient survival; GDF15 score 0, GDF15 score 1 and GDF15 score 2^{+}.

ii. GDF15 expression correlates with reduced overall survival

Among all patients, GDF15 expression (score 1+) demonstrated a modest but significant (P=0.046) correlation with reduced survival versus patients with GDF15-negative staining (84% vs 79% 5-year survival; 33% vs 29% 10-year survival) (Figure 4-2). Stratification of GDF15-positive subgroups demonstrated a significant (P=0.021) correlation between GDF15 score 2+ and reduced survival versus patients with GDF15-negative staining (84% vs 76% 5-year survival) (Figure4- 2). Although survival was also slightly lower in patients with GDF15 score 1 versus GDF15 score 0 (84% vs 79% 5-year survival), the correlation did not reach statistical significance (P=0.115). Therefore, the highest expression levels of GDF15 may predict for reduced survival among patients with breast cancer.

iii. GDF15 transcript and secretion are increased in an in vitro model of HER2-positive/ER-negative breast cancer.

HCC1954 is an *ER-negative*/ *HER2-positive* epithelial breast cancer cell line that displays primary resistance to trastuzumab. We examined HCC1954 for expression levels of GDF15 transcript and observed a noticeable increase compared with the ER-positive/HER2-positive BT474 breast cancer cell line, which is sensitive to trastuzumab. As expected, the stable BT474 GDF15 transfectant C2 displayed noticeably higher transcript levels compared with HCC1954 (Figure 4-4A).

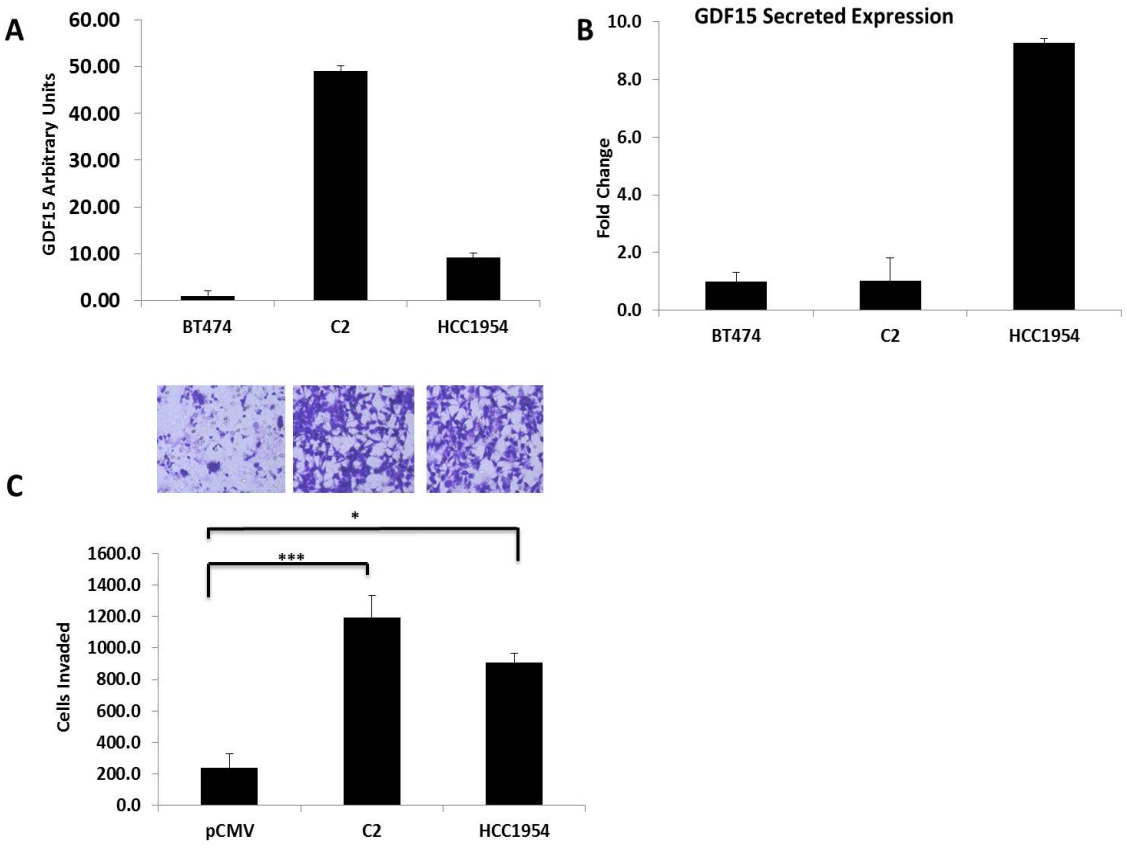
A
GDF15 Arbitrary Units
60.00
50.00
40.00
30.00
20.00
10.00
0.00
BT474
C2
HCC1954
B
GDF15 Secreted Expression
Fold Change
10.0
8.0
6.0
4.0
2.0
0.0
BT474
C2
HCC1954
C
*
***
Cells Invaded
1600.0
1400.0
1200.0
1000.0
800.0
600.0
400.0
200.0
0.0
pCMV
C2
HCC1954

Figure 4-4. HCC1954 breast cancer cells express increased levels of GDF15.

(A) Total RNA was extracted from BT474 parental (BT474), BT474 stable GDF15 transfectant clone 2 (C2), and HCC1954. RNA was converted to cDNA and analyzed by real-time PCR for GDF15 transcript level. Results are reported as fold increase in GDF15 transcript level versus parental counterpart. Values were normalized to RPLPO housekeeping ribosomal gene transcript levels as internal control. **(B)** ELISA using cell culture media only from BT474 parental (BT474), BT474 stable GDF15 transfectant clone 2 (C2), and HCC1954. Error bars represent standard deviation between triplicates. P-values were calculated by student's t-test for each resistant line versus the parental line; *p<0.05, **p<0.005. Results were confirmed on three separate occasions. **(C)** BT474 stable empty vector control clone (pCMV) or BT474 stable GDF15 clone 2 (C2) were plated in BD Matrigel-coated Boyden chambers. After 48 hours, cells were stained, and images were taken at 10x magnification. The total number of invading cells was counted in ten random fields, and the average from triplicate cultures is shown for each group. The experiment was performed twice; Gc2 versus control was compared by student's t-test, ***p<0.005*.

Since GDF15 is believed to become bioactive as a secreted cytokine, we performed ELISAs for secreted GDF15 protein in BT474, HCC1954 and GDF15 stable transfectant C2 (Figure 4-4B). GDF15-specific ELISA was performed on media collected from cells and showed that concentration of secreted GDF15 was approximately 5-fold higher in HCC1954 vs BT474 and stable GDF15 transfectant C2.

Thus, although stable GDF15 transfectants display high levels of GDF15 transcript, secreted forms of GDF15 are dramatically higher endogenously in HCC1954. Moreover, it has previously been shown that GDF15 stimulates ovarian cancer cell growth and invasion (48). Similarly, we observed a significant increase in cell invasion in both stable GDF15 transfectants ($p<.001$) and HCC1954 ($p<.05$) in comparison to BT474 pCMV empty vector controls (Figure 4-4C). These results suggest that HCC1954 could be used as model of endogenous GDF15 overexpression in future studies. In addition, we observed that GDF15 drives invasive potential in both stable transfectants and HCC1954. Interestingly, the strong increase observed in HCC1954 GDF15 serum levels suggests that variations in protein/transcript or secreted expression could regulate cancer progression and phenotypic changes.

iv. GDF15 and TGFβ1 colocalize with TGFβ-RII in HCC1954 breast cancer cells

Next, we investigated the colocalization of GDF15 with TGFβ-RII in HCC1954 breast cancer cells. Colocalization of GDF15 and TGFβ-RII was significantly lower in control BT474 parental and HCC1954 cells compared with stable GDF15 overexpressing clones (Figure 4-5). GDF15 colocalization may vary based on differential gene expression and sera levels, but the overall mechanisms contributing to potential

colocalization of GDF15 with TGFβ-RII remain unclear. Moreover, there is a possibility that in the presence of stable GDF15 overexpression, there is more robust signaling to latent GDF15 stores on the extracellular membrane, increasing available GDF15 and localization with TGFβ-RII (118). However, the relevant pathways driving the observed changes have yet to be elucidated.

v. GDF15 pharmacologic inhibition has no effect on downstream signaling in HCC1954 breast cancer cells.

To determine the effects of GDF15 neutralization, HCC1954, BT474, pCMV and stable GD15 clone 2 (C2) breast cancer cells were treated with GDF15 monoclonal antibody (mAb). This resulted in the neutralization of secreted GDF15 as compared to control IgG treated cells (Figure 4-6A and D). Based on previous findings that GDF15 drives upregulation of downstream signaling pathways, we performed Western blotting for a multitude of signaling molecules in cells treated with mAb. Neutralization of secreted GDF15 had no effect on protein expression levels (Figure 4-6B and D). Treatment with GDF15 mAb had no effect on transcript expression of invasion markers MMP2 and MMP9 or the proliferation associated transcription factor FoxM1 (Figure 4-6C). Western blots were performed on protein lysates from BT474, pCMV and C2 cells treated with GDF15 mAb, but there were no observable effects on protein expression in response to mAb treatment. The apparent lack of effect of GDF15 neutralization on downstream signaling may be due to sustained regulation by factors other than GDF15. These factors would not be suppressed by the GDF15 mAb, and would thus sustain signaling.

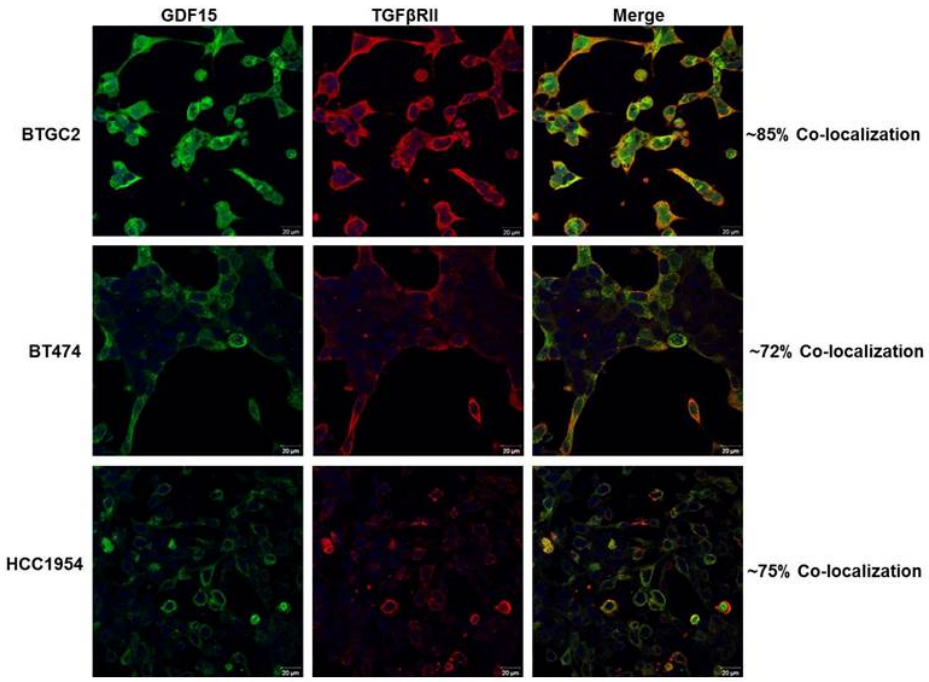
GDF15
TGFβRII
Merge
BTGC2
~85% Co-localization
BT474
~72% Co-localization
HCC1954
~75% Co-localization

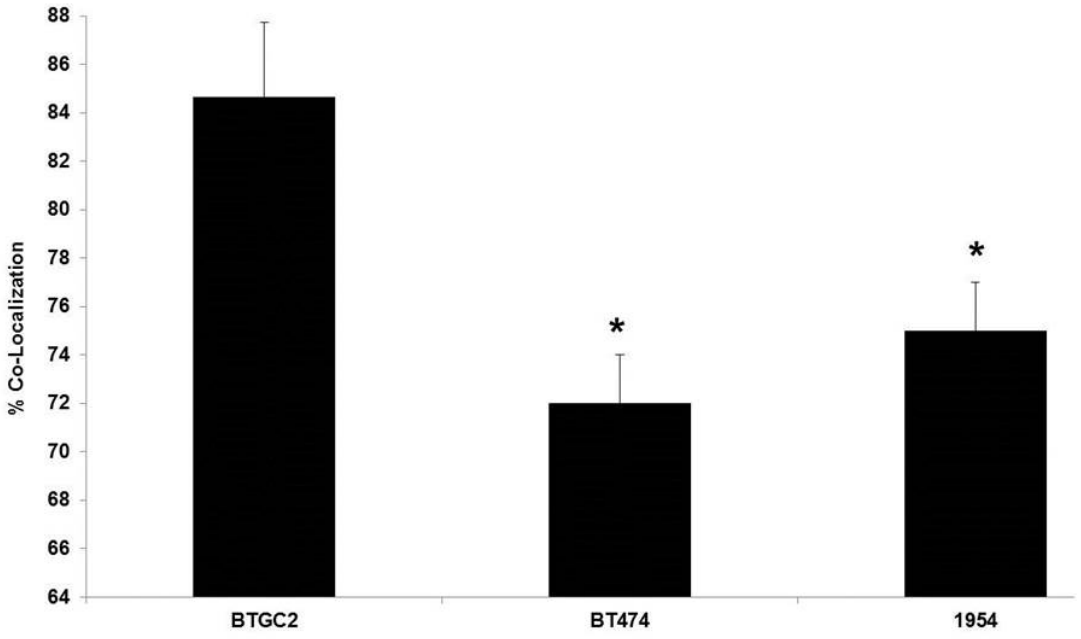
% Co-Localization
88
86
84
82
80
78
76
74
72
70
68
66
64
*
*
BTGC2
BT474
1954

Figure 4-5. GDF15 & TGFβI co-localizes with TGFβRII. BT474 GDF15 stable clone 2 (C2), BT474, and HCC1954 cells were plated on glass coverslips and allowed to recover 24 h prior to being harvested. Immunofluorescence was performed to determine the co-localization of GDF15 and TGFβRII. Cells were observed at a magnification of 40× using z-stack. The average of the overlap coefficient percentages was calculated using 3 different z-stacks. The average percentage of co-localization was graphed.

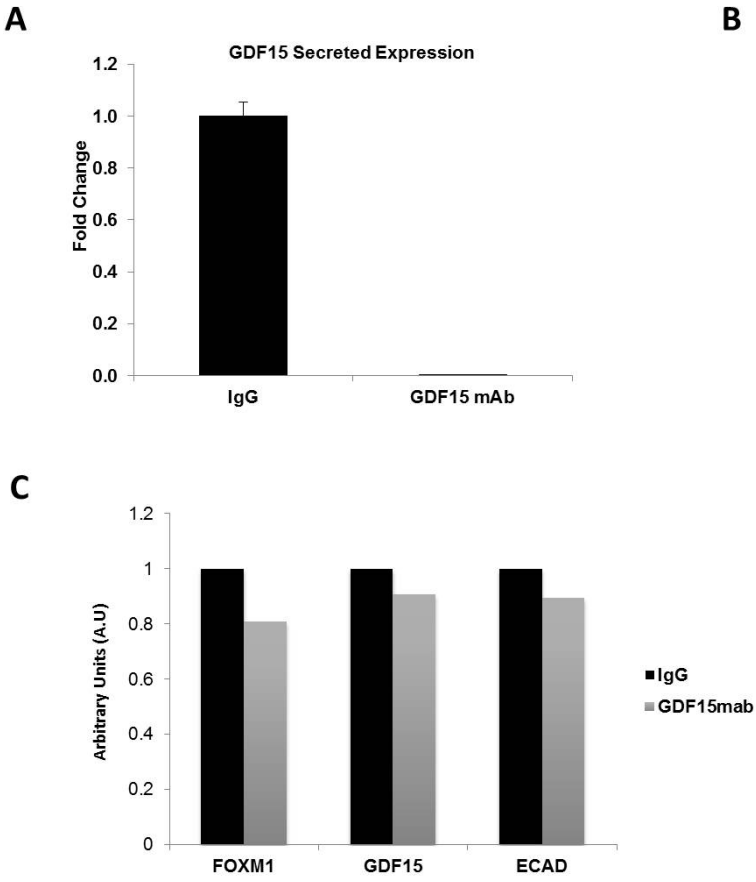
A
GDF15 Secreted Expression
Fold Change
1.2
1.0
0.8
0.6
0.4
0.2
0.0
IgG
GDF15 mAb
B
IgG
GDF15 mAb
p-IGF1R
IGF1R
p-Smad2
Smad2
FOXM1
Vimentin
E-Cadherin
p-Src
Src
p-Fak
Fak
Actin
C
Arbitrary Units (A.U)
1.2
1
0.8
0.6
0.4
0.2
0
FOXM1
GDF15
ECAD
IgG
GDF15mab

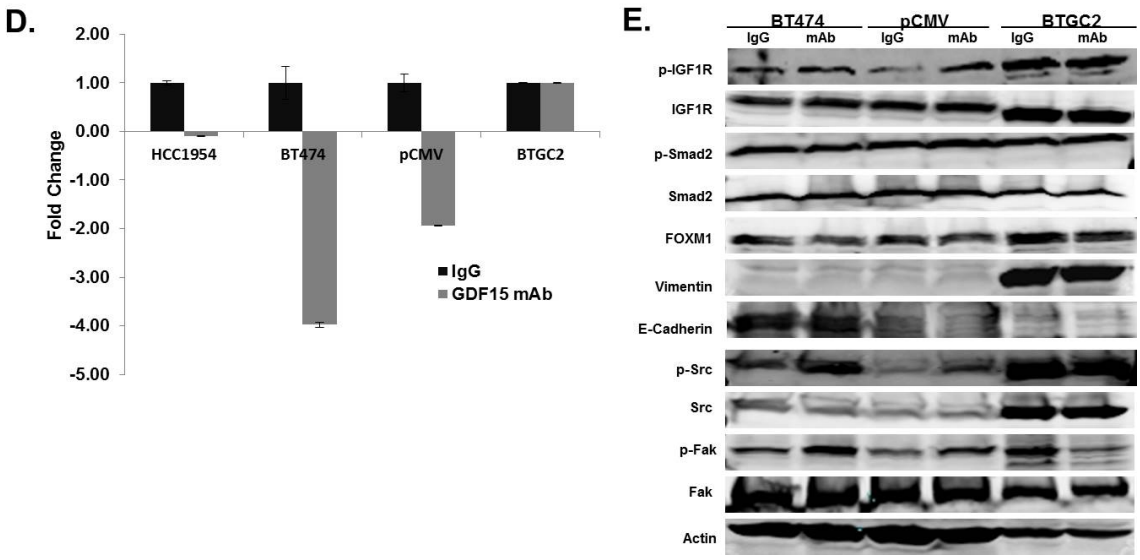
D.
2.00
1.00
0.00
-1.00
-2.00
-3.00
-4.00
-5.00
Fold Change
HCC1954
BT474
pCMV
BTGC2
IgG
GDF15 mAb
E.
BT474
pCMV
BTGC2
IgG
mAb
IgG
mAb
IgG
mAb
p-IGF1R
IGF1R
p-Smad2
Smad2
FOXM1
Vimentin
E-Cadherin
p-Src
Src
p-Fak
Fak
Actin

Figure 4-6. Pharmacologic inhibition of GDF15 in HCC195. (A) HCC1954 cells treated with control IgG or GDF15 mAb for 24 h. The concentration of GDF15 in media was measured by ELISA in triplicates. Values reflect average fold expression. **(B)** HCC1954 cells were treated with control IgG or GDF15 mAb for 24 h. Western blots of total protein lysates were performed for pIGF-1/IGF-1R, pSmad2/Smad2, pSrc/Src, pFak/Fak, E-cadherin, Vimentin and FoxM1. **(C)** Real-time PCR was performed for MMP-2, MMP-9, and FoxM1, and normalized to RPLPO. Values reflect the average fold change in normalized transcript. **(D)** BT474, pCMV and GDF15 stable clone (C2) were treated with control IgG or GDF5 mAb for 24h. The concentration of GDF15 in media was measured by ELISA in triplicates. Values reflect the average fold expression. **(E)** BT474, pCMV and GDF15 stable clone (C2) were treated with control IgG or GDF15 mAb for 24h. Western blots of total protein lysates were performed for pIGF-14/IGF-1R, pSmad2/Smad2, pSrc/Src, pFak/Fak, E-cadherin, Vimentin and FoxM1.

Alternatively, GDF15 mAb treatment may trigger compensatory signaling, which in turn activates and sustains downstream signaling. Finally, it is conceivable that endogenous GDF15 drives signaling, such that neutralization of secreted GDF15 alone would have no effect on these downstream pathways. Further studies are needed to gain insights into the regulation of GDF15-mediated signaling and differential molecular and biological effects of secreted vs endogenous GDF15.

3. Discussion

Although increased expression of GDF15 is associated with advanced disease in patients with multiple types of malignancies, limited data is available regarding the expression levels of GDF15 in breast cancer. (150). Welsh and colleagues examined changes in gene expression of secreted proteins in the sera of cancer patients representing 10 different tumor types. Serum levels of GDF15 were elevated in patients with metastatic colorectal (8/8), prostate (8/9), and breast (6/10) cancers when compared with sera from normal controls (150) (133) compared GDF15 transcript levels in 10 breast tumor samples matched with adjacent normal tissue controls, and found higher GDF15 expression in half of the tumor samples. Thus, according to these studies, which included a relatively small number of patient samples, GDF15 expression was elevated in 50% to 60% of serum or tumor tissue specimens from patients with breast cancer. Consistent with those studies, we demonstrate by IHC staining that GDF15 is expressed in 66% (397/605) of patients with breast cancer.

Sasahara et al. recently reported that GDF15 expression was higher in breast cancer tissues compared with normal controls, with HER2-positive tumors demonstrating the highest expression levels of GDF15(192). We examined potential associations between

GDF15 IHC staining and available clinical data, which included age, tumor size, tumor grade, disease involving >3 lymph nodes, ER and HER2 positivity, and overall survival. GDF15 expression was significantly associated with high tumor grade, and ER-negative or HER2-positive status. A limitation of our IHC study was that most patients in this cohort had low-grade tumors with either non-metastatic disease or fewer than 3 lymph node metastases. Thus, this cohort may represent a relatively low-risk population or subgroup with primarily localized or locally invasive disease. Another potential limitation to our study is that IHC analysis of tumor tissue does not account for contributions from circulating or stroma-derived GDF15. Future analyses should examine cohorts that include a greater percentage of patients with lymph node-positive or metastatic disease to determine if GDF15 overexpression is associated with metastasis, recurrence, or reduced survival rates in patients with advanced-stage disease, as is reported in other tumor types (193; 194). These studies should also evaluate potential subtype-specificity of GDF15 expression in HER2-positive and ER-negative breast cancer, based on results presented here, and associations between GDF15 expression and treatment response or survival.

Our *in vitro* findings support further investigation into the relationship between GDF15 and HER2. These studies may help validate preclinical implications that GDF15 activates HER2, increases signaling through downstream proliferative and mitogenic pathways, and promotes resistance to HER2-targeted agents (96). Previous studies demonstrate that secreted GDF15 derived from stroma or tumor cells can promote metastasis and is a potential biomarker of disease progression in cancers, including prostate and ovarian cancer (145; 149). Given that GDF15 expression can take on a

multitude of forms, future studies should include detailed analyses that measure GDF15 serum concentration and gene expression from breast cancer patients to evaluate potential correlations with metastasis and survival.

Chapter 5

Growth Differentiation Factor 15 Mediates Epithelial Mesenchymal Transition and Invasion of Breast Cancers through IGF-1R-FoxM1 Signaling

1. Introduction

Epithelial-to-mesenchymal transition (EMT) is an essential part of tumor progression. EMT is characterized by a process by which, the cell takes on a plethora of phenotypic changes, including a change in polarity, loss of epithelial cell-cell contact, and acquisition of migratory behavior (195). A critical hallmark in EMT is loss of the epithelial marker E-cadherin, which results in the induction of cytoskeletal reorganization (196). Growth differentiation factors, such as TGF-β, have been shown to induce EMT during cancer progression, embryogenesis and fibrosis (195). Growth differentiation factor 15 (GDF15), a distant member of the TGF-β superfamily, has been shown to enhance the EMT process in colorectal cancer via activation of Smad2 and Smad3 pathways (197). Pathologic conditions, such as insulin resistance, diabetes, cardiovascular diseases, impaired cognitive ability, and malignancies, are associated with elevated levels of circulating GDF15 (170; 191; 198; 199).

Although GDF15 shares structural features with members of the transforming growth factor-beta (TGF-beta) superfamily (117), the receptor for GDF15 remains unidentified, and the signaling and phenotypic effects induced by GDF15 occur through TGF beta receptor/SMAD-independent and -dependent mechanisms (170; 200). GDF15 overexpression stimulates PI3K/Akt/mTOR and MEK/ERK signaling (96; 130; 192; 201) and promotes EMT in ovarian cancer cells (48; 197)(Griner et al., 2013; Li et al., 2016a). We previously demonstrated that GDF15 drives resistance to targeted therapy in breast cancer (96). Furthermore, it has been reported that GDF15 promotes the acquisition of cancer stem cell-like properties in breast cancers (192). In the current study, we demonstrate that GDF15 promotes EMT and invasiveness of breast cancers through a

unique mechanism involving activation of the insulin-like growth factor-1 receptor (IGF-1R) and upregulation of transcription factor FoxM1.

2. Results.

i. GDF15 overexpression alters cell cycle profiles and induces EMT in breast cancer.

BT474 and JIMT1 breast cancer cells express low levels of GDF15, whereas MDA231 breast cancer cells express high levels of GDF15 (Figure 5-1A). Stable overexpression of GDF15 in BT474 (Figure 5-1B) resulted in a 3-fold increase in the percentage of cells in S phase compared with parental and empty vector control cells (Figure 5-1C-D). We previously found that GDF15 induces EMT in ovarian cancer cells (48). To determine if stable GDF15 overexpression also promotes EMT in breast cancer cells, we examined expression of mesenchymal and epithelial markers by western blotting. Stable GDF15-overexpressing clones exhibited dramatic downregulation of the epithelial marker E-cadherin, whereas mesenchymal markers N-cadherin, vimentin, and transcription factor FoxM1 were upregulated (Figure 5-A). Expression levels of mesenchymal transcription factors Snail, Zeb-1, and Slug were also increased (Figure 5-2B), with phenotypic morphological changes consistent with acquisition of a mesenchymal phenotype noted (Figure 5-2C). EMT is associated with increased potential for tumor development and migration. Consistent with this concept, stable overexpression of GDF15 conferred spheroid-forming capabilities compared with parental cells, which did not form spheroids in 3-d culture (Figure 5-2D).

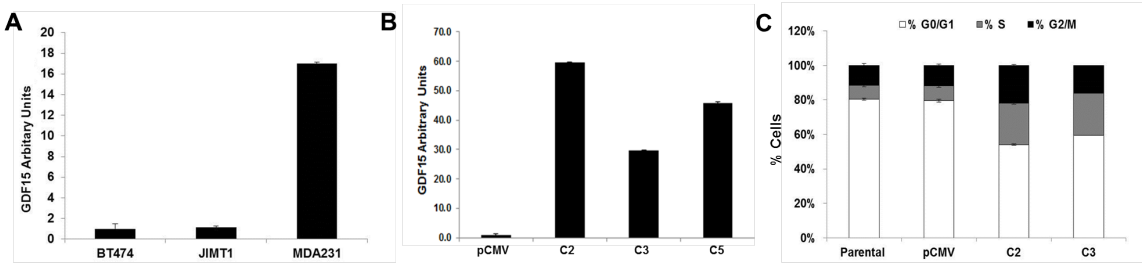
A
GDF15 Arbitary Units
20
18
16
14
12
10
8
6
4
2
0
BT474
JIMT1
MDA231
B
GDF15 Arbitrary Units
70.0
60.0
50.0
40.0
30.0
20.0
10.0
0.0
pCMV
C2
C3
C5
C
% G0/G1
% S
% G2/M
% Cells
120%
100%
80%
60%
40%
20%
0%
Parental
pCMV
C2
C3

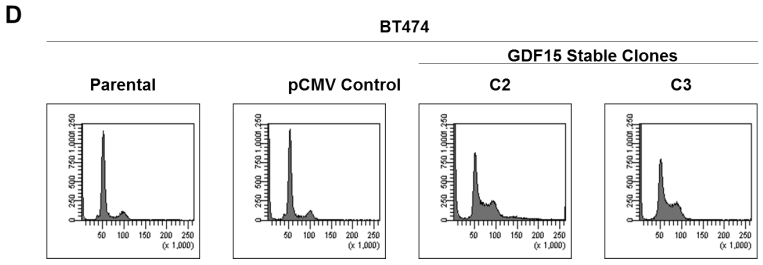
D
BT474
GDF15 Stable Clones
Parental
pCMV Control
C2
C3
50 100 150 200 250
(x 1,000)

Figure 5-1. GDF15 overexpression alters cell cycle profile.

(A) Real-time PCR for parental BT474, JIMT1 and MDA231 breast cancer cell lines. Values reflect fold change in GDF15 transcript level normalized to RPLPO housekeeping gene level. Error bars represent standard deviation between triplicate samples; experiments were repeated at least 3 times. **(B)** Real-time PCR for GDF15 in BT474 pCMV stable empty vector control clone (pCMV) and GDF15 stable clones 2, 3, and 5 (C2, C3, and C5). Values reflect fold change in GDF15 transcript level normalized to RPLPO housekeeping gene level. Error bars represent standard deviation between triplicate samples; experiments were repeated at least 3 times. **(C-D)** BT474 parental, pCMV empty vector control clone (pCMV), and GDF15 stable clones 2 and 3 (C2, C3) were fixed, stained with propidium iodide, and analyzed for DNA content by flow cytometry. The percentage of cells in each cell cycle phase is shown per cell line **(C)** (white bar, G0/G1; gray bar, S; black bar, G2/M). Error bars represent standard deviation between triplicate samples; experiments were repeated at least 3 times. Representative cell cycle histograms are shown per line **(D)**.

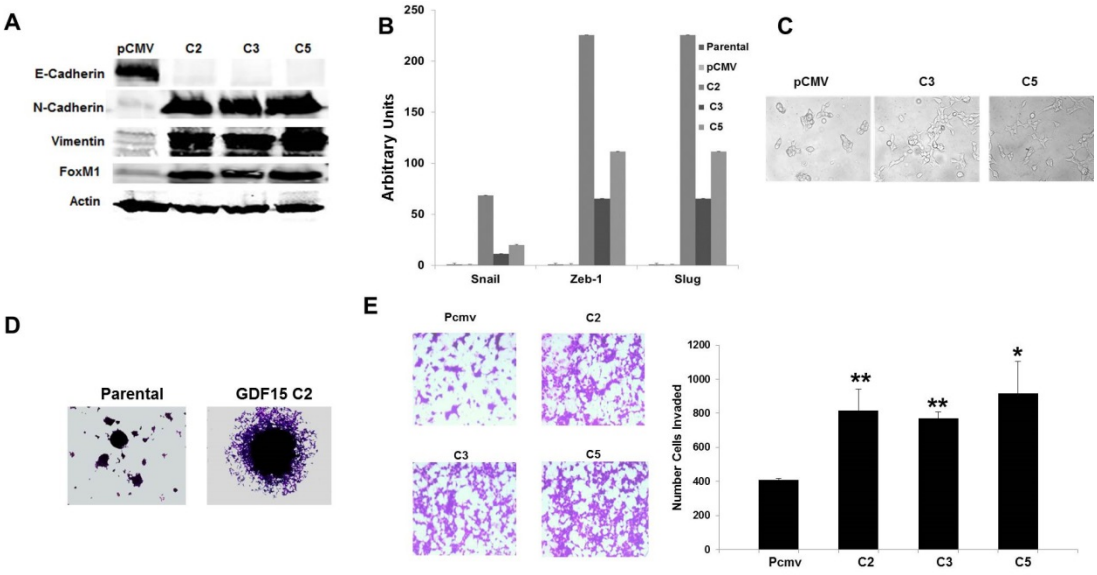
A
pCMV
C2
C3
C5
E-Cadherin
N-Cadherin
Vimentin
FoxM1
Actin
B
Arbitrary Units
250
200
150
100
50
0
Snail
Zeb-1
Slug
Parental
pCMV
C2
C3
C5
C
pCMV
C3
C5
D
Parental
GDF15 C2
E
Pcmv
C2
C3
C5
Number Cells Invaded
1200
1000
800
600
400
200
0
**
**
*
Pcmv
C2
C3
C5

Figure 5-2. GDF15 induces epithelial mesenchymal transition and invasion in breast cancer cells. (A) Total protein whole-cell lysates were collected from BT474 pCMV stable empty vector control clone (pCMV) and GDF15 stable clones 2, 3, and 5 (C2, C3, and C5). Western blots were performed for E-Cadherin, N-Cadherin, Vimentin, and FoxM1; blots were probed for actin as loading control. Blots were repeated at least three times, and representative blots are shown. **(B)** Real-time PCR for Snail, Zeb-1 and Slug in BT474 parental, pCMV stable empty vector control clone (pCMV) and GDF15 stable clones 2, 3, and 5 (C2, C3, and C5). Values reflect fold change in transcript normalized to RPLPO housekeeping gene. Error bars represent standard deviation between triplicate samples; experiments were repeated at least 3 times. **(C)** BT474 pCMV empty vector control clone (pCMV) and GDF15 stable clones 3 and 5 (C3 and C5) were imaged at 10× magnification to evaluate changes in morphology. **(D)** Representative images of spheroids are shown at 4× magnification for BT474 parental and GDF15 stable clone 2 (C2). **(E)** BT474 stable empty vector control clone (pCMV) and GDF15 stable clones 2, 3, and 5 (C2, C3, and C5) were plated in basement membrane matrix (Matrigel)-coated Boyden chambers in serum-free media; 10% FBS was added to the well below each chamber as a chemo-attractant. After 24 hours, chambers were fixed and stained. Representative photos of invading cells are shown at 20× magnification. The total number of invading cells was counted in 10 random fields; the average number of invading cells is shown for triplicate cultures per cell line; student's t-test, $**p<0.005$, $*p<0.05$.

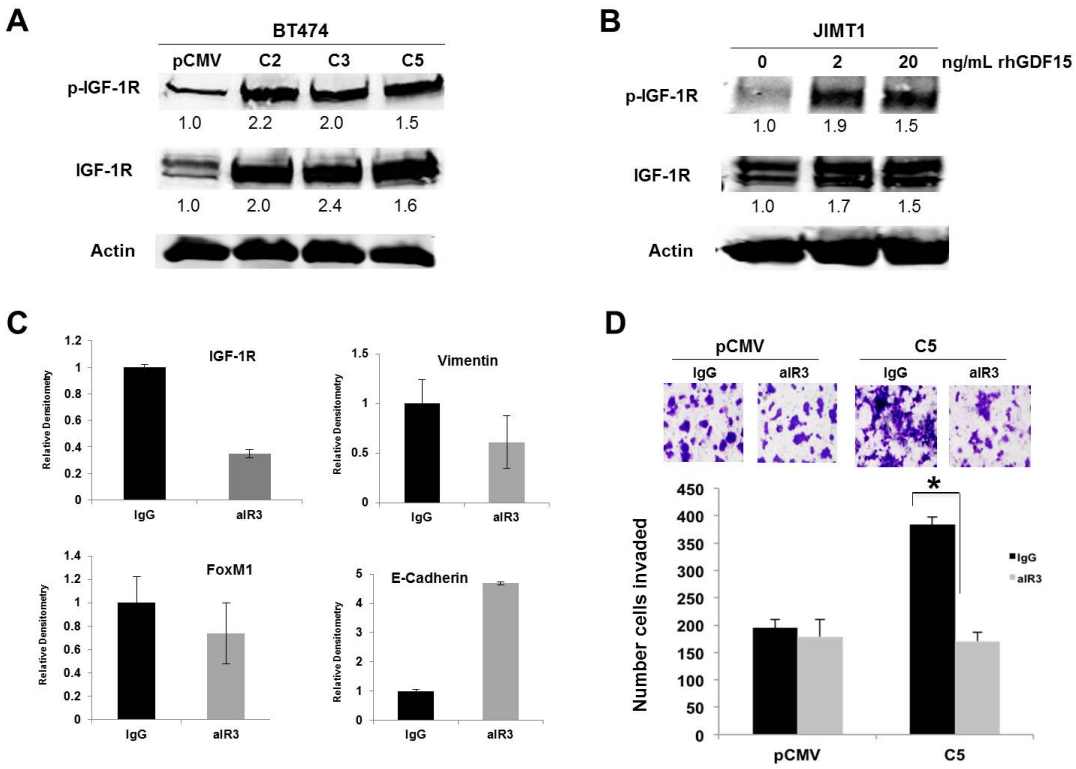
A
BT474
pCMV
C2
C3
C5
p-IGF-1R
1.0
2.2
2.0
1.5
IGF-1R
1.0
2.0
2.4
1.6
Actin
B
JIMT1
0
2
20
ng/mL rhGDF15
p-IGF-1R
1.0
1.9
1.5
IGF-1R
1.0
1.7
1.5
Actin
C
IGF-1R
Vimentin
FoxM1
E-Cadherin
Relative Densitometry
IgG
aIR3
D
pCMV
C5
IgG
aIR3
Number cells invaded
*
IgG
aIR3
pCMV
C5

Figure 5-3. IGF-1R activation mediates EMT and invasion of GDF15-overexpressing breast cancer cells. (A) Total protein lysates were collected from BT474 stable empty vector control clone (pCMV) and GDF15 stable clones 2, 3, and 5 (C2, C3, and C5). Western blots were performed for p-Tyr1131 IGF-1R and total IGF-1R; actin was probed as loading control. Experiments were repeated 3 times; representative blots are shown. Quantification (shown beneath each band) was normalized to actin and performed using Odyssey Li-Cor imaging software. **(B)** JIMT1 cells were serum-starved for 24 hours, and then stimulated with 2 or 20 ng/mL of recombinant human GDF15 (rhGDF15) for another 24 hours. Western blots of total protein lysates are shown for p-Tyr1131 IGF-1R and total IGF-1R; actin was probed as loading control. Experiments were repeated 3 times; representative blots are shown. Quantification (shown beneath each band) was normalized to actin and performed using Odyssey Li-Cor imaging software. **(C)** BT474 GDF15 stable clone 2 (C2) cells were treated with normal mouse IgG control or 0.25 μg/mL alpha IR3 (aIR3) IGF-1R monoclonal antibody for 48 hours. Western blots of total protein lysates were performed for total IGF-1R, Vimentin, FoxM1, and E-Cadherin. Bar graphs show quantification relative to actin loading control, and was performed using Odyssey Li-Cor imaging software. Error bars represent standard deviation between triplicates; experiments were performed at least 3 times. **(D)** BT474 stable empty vector control clone (pCMV) and BT474 GDF15 stable clone 5 (C5) cells were pre-treated with normal mouse IgG or 0.25 μg/mL alpha IR3 (aIR3) IGF-1R monoclonal antibody for 24 hours. Cells were then seeded in Matrigel-coated Boyden chambers in serum-free media plus control IgG or aIR3; 10% FBS was added to the well as a chemo-attractant. After 24 hours of invasion,

cells in chambers were fixed and stained. Representative photos of invading cells are shown at 20× magnification. The total number of invading cells was counted in 10 random fields; the average number of invading cells is shown for triplicate cultures per cell line; student's t-test, *$p<0.05$.

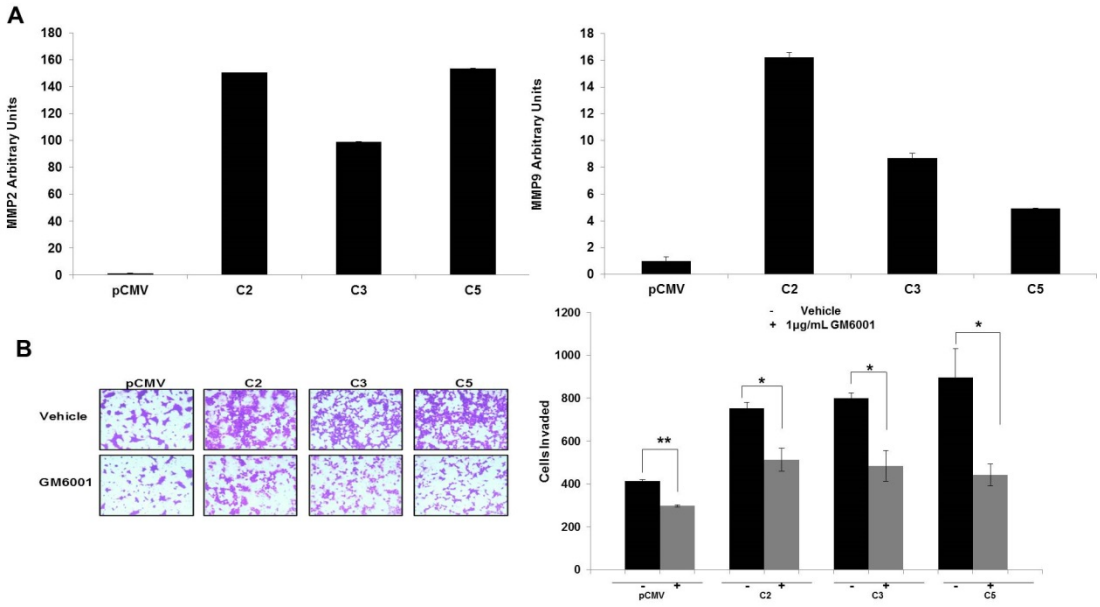
A
MMP2 Arbitrary Units
180
160
140
120
100
80
60
40
20
0
pCMV
C2
C3
C5
MMP9 Arbitrary Units
18
16
14
12
10
8
6
4
2
0
pCMV
C2
C3
C5
B
pCMV
C2
C3
C5
Vehicle
GM6001
- Vehicle
+ 1µg/mL GM6001
Cells Invaded
1200
1000
800
600
400
200
0
**
*
*
*
- +
pCMV
C2
C3
C5

Figure 5-4. Matrix metalloproteinases (MMPs) mediate invasion of GDF15-overexpressing breast cancer cells. (A) Real-time PCR of total RNA from BT474 pCMV empty vector control clone (pCMV) and GDF15 stable clones (C2, C3, and C5) for MMP2 (left graph) and MMP9 (right graph). Values reflect average fold in transcript normalized to internal control RPLPO relative to pCMV group. Error bars represent standard deviation between triplicate samples; experiments were repeated 3 times. **(B)** BT474 pCMV empty vector control clone (pCMV) and GDF15 stable clones (C2, C3 and C5) were plated in serum-free media in Matrigel-coated Boyden chambers and treated with vehicle control or 1 μg/mL pan-MMP inhibitor GM6001 for 24 hours, after which cells were fixed and stained. Representative photos of invading cells are shown at 20× magnification. The total number of invading cells was counted in 10 random fields; the average number of invading cells is shown for triplicate cultures per cell line; student's t-test, $**p<0.005$, $*p<0.05$.

ii. GDF15 activates IGF-1R signaling.

IGF-1R is a major upstream mediator of breast cancer cell invasion (87; 202). Stable overexpression of GDF15 resulted in a 1.5- to 2.5-fold increase in total and phosphorylated IGF-1R relative to empty vector control (Figure 5-3A). Similarly, exogenous stimulation of JIMT1 cells with recombinant human GDF15 (rhGDF15) induced IGF-1R expression and phosphorylation by 1.5- to 2-fold (Figure 5-3B). Treatment of stable GDF15-overexpressing cells with IGF-1R-targeted antibody alpha IR3 reduced expression of IGF-1R and FoxM1 (Figure 5-3C). Pharmacologic inhibition of IGF-1R using alpha IR3 treatment significantly downregulated protein expression of mesenchymal marker vimentin and induced expression of epithelial marker E-cadherin. Consistent with these changes in expression of EMT markers, alpha IR3 inhibited the invasiveness of GDF15-overexpressing cells without significantly affecting control cells (Figure 5-3D). These results suggest that IGF-1R activation contributes to FoxM1 upregulation, EMT, and invasiveness of GDF15-positive breast cancers.

iii. Matrix metalloproteinases MMP2 and MMP9 are upregulated in GDF15-overexpressing breast cancer cells.

To further elucidate the molecular mechanism through which GDF15 enhances breast cancer cell invasion, we measured expression levels of MMP2 and MMP9, which are transcriptional targets of FoxM1 and mediators of cancer cell invasion. Stable GDF15-overexpressing clones demonstrated significant upregulation of MMP2 and MMP9 (Figure 5-4A). Treatment with the broad-spectrum MMP inhibitor GM6001

significantly reduced invasiveness of stable GDF15-overexpressing clones (Figure 5-4B). These data suggest that upregulation of MMP2 and MMP9 contributes to the invasive phenotype of GDF15-overexpressing breast cancer cells.

iv. Knockdown of FoxM1 or GDF15 inhibits invasion of GDF15-overexpressing cells.

Increased FoxM1 expression contributes to cancer cell invasiveness (171). To determine if FoxM1 upregulation contributes to the increased invasiveness of GDF15-overexpressing cells, we transiently *knocked down FoxM1* expression (Figure 5-5A). Downregulation of FoxM1 significantly decreased invasion (Figure 5-5B) and reduced expression of MMP2 and MMP9 (Figure 5-5C).

GDF15 expression was knocked down in HER2-overexpressing BT474 empty vector control, BT474 GDF15 stable clone, and *triple-negative MDA*-MB-231 breast cancer cells (Figure 5-6A). Downregulation of GDF15 significantly reduced invasion through a basement membrane matrix (Figure 5-6B), supporting a functional role for GDF15 in breast cancer cell invasion.

3. DISCUSSION

In the current study, we provide mechanistic insights into the signaling pathways driving GDF15-mediated EMT and invasion in breast cancer. GDF15 overexpression activated IGF-1R signaling with subsequent upregulation of FoxM1 and target MMPs, increased expression of EMT mediators, and increased cellular invasion (Figure 7).

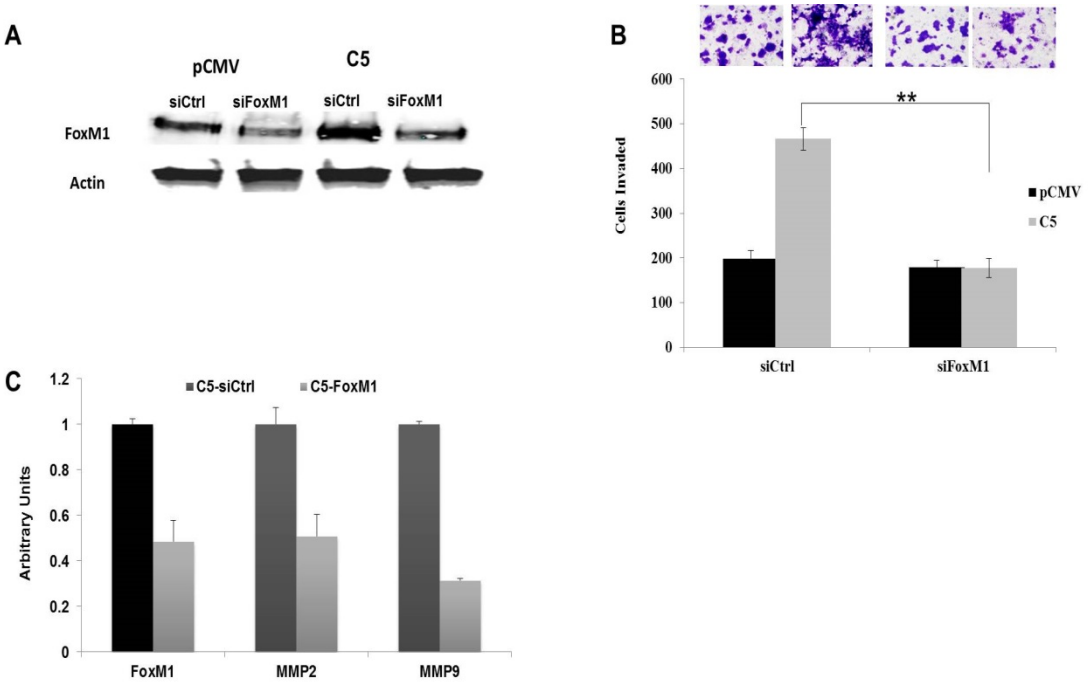
A
pCMV
C5
siCtrl
siFoxM1
siCtrl
siFoxM1
FoxM1
Actin
B
600
500
400
300
200
100
0
Cells Invaded
**
pCMV
C5
siCtrl
siFoxM1
C
1.2
1
0.8
0.6
0.4
0.2
0
Arbitrary Units
C5-siCtrl
C5-FoxM1
FoxM1
MMP2
MMP9

Figure 5-5. FoxM1 promotes invasion and upregulation of MMP2 and MMP9 in GDF15-overexpressing breast cancer cells. (A) BT474 stable empty vector control clone (pCMV) and GDF15 stable clone 5 (C5) was transfected with 100 nM control siRNA (siCtrl) or FoxM1 siRNA (siFoxM1). Representative Western blots of total protein lysates are shown for FoxM1; actin was probed as loading control. **(B)** BT474 stable empty vector control clone (pCMV) and GDF15 stable clone 5 (C5) were transfected with 100 nM control siRNA (siCtrl) or FoxM1 siRNA (siFoxM1) for 48 hours, and then plated in serum-free media in Matrigel-coated Boyden chambers. After 24 hours, cells were fixed and stained. Representative photos of invading cells are shown at 20× magnification. The total number of invading cells was counted in 10 random fields; the average number of invading cells is shown for triplicate cultures per cell line; student's t-test, **$p<0.005$. **(C)** BT474 GDF15 stable clone 5 (C5) cells were transfected with 100 nM control siRNA (siCtrl) or FoxM1 siRNA (FoxM1) for 48 hours. Real-time PCR was performed for FoxM1, MMP2, and MMP9. Values reflect average fold in transcript normalized to internal control RPLPO. Error bars represent standard deviation between triplicate samples; experiments were repeated 3 times.

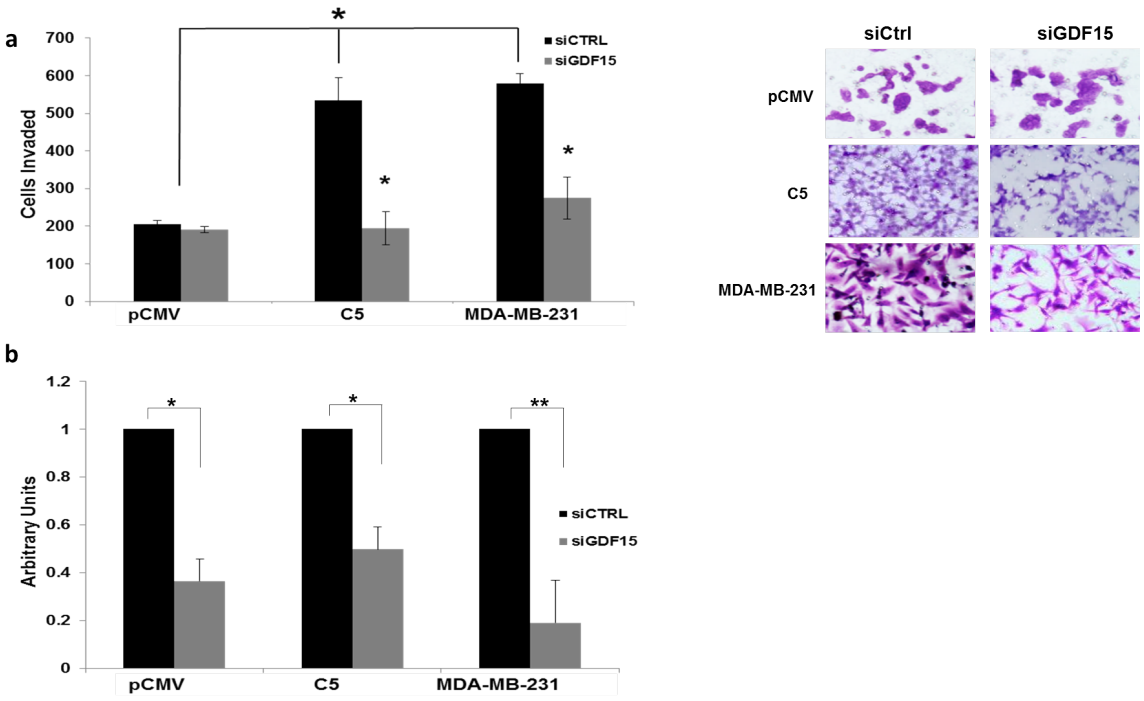
a
Cells Invaded
700
600
500
400
300
200
100
0
siCTRL
siGDF15
*
*
*
pCMV
C5
MDA-MB-231
siCtrl
siGDF15
pCMV
C5
MDA-MB-231
b
Arbitrary Units
1.2
1
0.8
0.6
0.4
0.2
0
*
*
**
siCTRL
siGDF15
pCMV
C5
MDA-MB-231

Figure 5-6. GDF15 knockdown inhibits invasion of breast cancer cells. (A) BT474 stable empty vector control clone (pCMV) and BT474 GDF15 stable clone 5 (C5), and MDA-MB-231 cells were transfected with 100 nM siRNA control (siCtrl) or GDF15 siRNA (siGDF15). After 24 hours, transfected cells were plated in serum-free media in Matrigel-coated Boyden chambers with 10% FBS in the wells as a chemo-attractant. After 24 hours, cells were fixed and stained. Representative photos of invading cells are shown at 20× magnification. The total number of invading cells was counted in 10 random fields; the average number of invading cells is shown for triplicate cultures per cell line; student's t-test, * $p<0.05$. **(B)** BT474 stable empty vector control clone (pCMV) and BT474 GDF15 stable clone 5 (C5), and MDA-MB-231 cells were transfected with 100 nM siRNA control (siCtrl) or GDF15 siRNA (siGDF15) for 48 hours. Real-time PCR was performed to confirm GDF15 knockdown. Values reflect the fold change in transcript normalized to RPLPO housekeeping gene. Error bars represent standard deviation between triplicate samples; experiments were repeated twice.

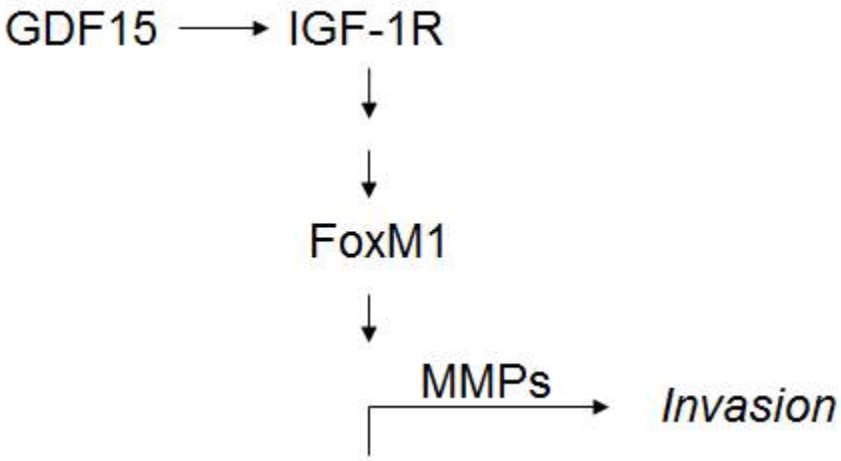
GDF15
IGF-1R
FoxM1
MMPs
Invasion

Figure 5-7. Schematic summarizing model.

GDF15 overexpression activates the IGF-1R signaling pathway, resulting in upregulation of FoxM1 and downstream markers MMP2 and MMP9, which degrade the basement membrane, a vital process in EMT, proliferation and invasion.

These data suggest that the inflammatory cytokine GDF15 contributes to breast cancer progression in part by activating signaling pathways that control EMT and cellular invasion.

IGF-1R activation and overexpression promote EMT in many tumor types. In breast cancer, IGF-1R signaling induces EMT, migration, and invasion in HER2-positive and triple-negative breast cancer (87; 88). Acquisition of a mesenchymal phenotype has been reported to confer stem cell-like and migratory characteristics, resulting in recurrent metastases and drug resistance in multiple tumor models (203; 204). Consistent with the GDF15-driven EMT we observed in our studies, GDF15 was recently shown to maintain stem cell characteristics in breast cancer cell lines (201; 205)

The mechanisms through which IGF-1R promotes a switch to a mesenchymal phenotype are not fully understood. However, IGF-1R activation is known to stimulate MEK-Erk1/2 and PI3K-Akt signaling, which in turn regulate EMT transcription factors. We previously demonstrated that GDF15 induces PI3K and Erk1/2 phosphorylation in HER2-overexpressing breast cancer cells, in association with drug resistance (205). Further, MEK inhibition blocked the ability of GDF15 to induce tumor sphere formation (192), indicating that MEK activation downstream of IGF-1R activation may contribute to GDF15-stimulated EMT. These data provide rationale for evaluating IGF-1R and MEK inhibition as a potential therapeutic strategy in mesenchymal GDF15-positive breast cancers.

In addition to regulating expression of EMT markers, IGF-1R inhibition decreased expression of the transcription factor FoxM1 and blocked invasion of GDF15-overexpressing cells. We previously reported that FoxM1 is a critical mediator of IGF-

1R-stimulated invasion in breast cancer cells (87). The current study further supports FoxM1 as a major mediator of IGF-1R-mediated invasion. FoxM1 knockdown reduced invasion and overcame upregulation of MMP2 and MMP9 in GDF15 stable clones. These data demonstrate that GDF15-IGF-1R-FoxM1 signaling plays an important role in breast cancer invasion, with IGF-1R and FoxM1 representing potential downstream targets for inhibiting GDF15-mediated invasion.

Additional mechanisms are likely to contribute to GDF15-mediated EMT and invasion. GDF15 induces phosphorylation of the TGF-β signaling effectors Smad2 and Smad3 (96; 130). GDF15 also activates focal adhesion kinase (FAK) signaling, driving prostate cancer metastasis (206). We previously reported that IGF-1R regulates FAK signaling and EMT in triple-negative breast cancer. Further, we and others previously have shown that GDF15 activates HER2 kinase activity (88; 96; 129), resulting in acquired and intrinsic resistance to HER2-targeted antibody therapy. These results are consistent with previous reports that IGF-1R/HER2 cross-signaling causes trastuzumab resistance (205), and suggest that GDF15 overexpression may represent one mechanism driving activation of the HER2 and IGF-1R receptor kinase signaling network and drug resistance.

In summary, while GDF15 exhibits pleiotropic effects in cancer cells (147), the majority of studies support a role for GDF15 in disease progression, with overexpression linked to EMT, invasion and metastasis. Our studies are the first to report activation of IGF-1R-FoxM1 as a mechanism of invasion in GDF15-overexpressing breast cancers, providing rationale for preclinical evaluation of treatments that co-target IGF-1R and FoxM1. Further, based on the dramatically reduced invasiveness of HER2-positive and

triple-negative breast cancers in response to GDF15 knockdown, future studies should evaluate GDF15 as a potential molecular target in breast cancer.

Chapter 6

Targeting GDF15 in Breast Cancer Using Catalytic Deoxyribozyme Down-Regulation

1. Introduction

Gene regulation differs between cancer cells and normal cells, but can also differ amongst patients with histologically identical tumors. Improved understanding of variability in gene expression may help predict divergent responses to treatment and aid in the identification of more effective alternatives to targeted therapy. Thus, manipulation of gene regulation has the potential to enhance treatment options and improve patient outcomes.

Several methods are used for gene knockdown, and some have previously been discussed in detail. Here we use RNA interference (RNAi) a process that allows specific and selective knockdown of a target gene. Conceptually, this method uses chemically synthesized double-stranded small interfering RNAs (siRNAs) and recruitment of RNA-induced silencing complex (RISC) to hybridize with the mRNA of interest and target it for cleavage (207). siRNAs are efficient for preliminary studies aimed at determining transient molecular and functional effects of gene inhibition. However, more complementary downstream experiments include the use of bacterial and viral carriers that express short-hairpin RNAs (shRNAs), which are processed into siRNAs by endogenous RNAi machinery and allow continuous (stable) siRNA production. Lentiviral carriers of shRNA are typically delivered to target cell *ex vivo*, and then modified cells are injected into the target (i.e. patient or mouse model) (208). Although, both siRNA and shRNA have been shown to be effective, delivery methods *in vivo* pose a challenge. Because systemic administration can make it difficult to target organs, studies have tried to optimize *in vivo* delivery by conjugating siRNA to aptamers (209; 210), vitamins, antibodies, and other targeting ligands (211).

Deoxyribozymes (also called DNA enzymes or DNAzymes) are catalytic DNA molecules that bind their RNA substrate via Watson-Crick base pairing, forming a DNA: RNA interaction (212). Next, the DNA promotes transesterification and cleavage of its target RNA backbone. The ’10-23’ DNAzyme is the most commonly used catalytic oligonucleotide in animal models, given its ability to inhibit translation of genes that promote tumorigenesis (213-216). Thus DNAzymes provide a relatively stable alterative to selectively target and cleave RNA. However, since DNAzymes are composed of nucleic acids, they are prone to nuclease degradation. Functionalized gold nanoparticles have been shown to be an effective method of delivering DNAzymes for cellular uptake. Here, we investigate the utility of GDF15 DNAzyme-gold nanoparticle (DzNP) conjugates as a tool for effective inhibition of GDF15 in vitro.

2. Results

i. *GDF15 gene silencing in breast cancer*

To examine the effects of GDF15 siRNA gene silencing we transfected 100 nM of GDF15 siRNA into BT474, BT474 stable GDF15 transfectant clone 2 (C2) and HCC1954 breast cancer cells for 48 hours (h). As shown in Figures 6-1A and 6-1B, GDF15 gene silencing by siRNA caused significant inhibition of GDF15 expression, while the control siRNA had no effect on GDF15 gene expression.

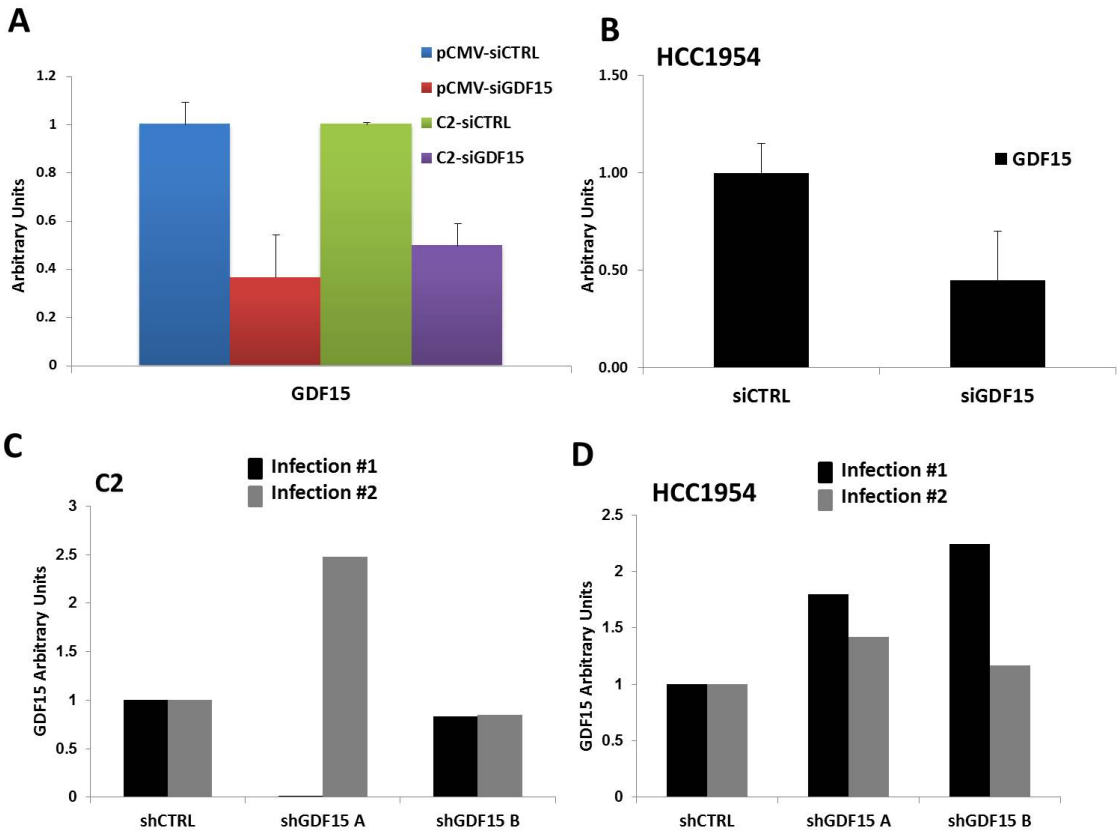
A
pCMV-siCTRL
pCMV-siGDF15
C2-siCTRL
C2-siGDF15
Arbitrary Units
1.2
1
0.8
0.6
0.4
0.2
0
GDF15
B
HCC1954
GDF15
Arbitrary Units
1.50
1.00
0.50
0.00
siCTRL
siGDF15
C
C2
Infection #1
Infection #2
GDF15 Arbitrary Units
3
2.5
2
1.5
1
0.5
0
shCTRL
shGDF15 A
shGDF15 B
D
HCC1954
Infection #1
Infection #2
GDF15 Arbitrary Units
2.5
2
1.5
1
0.5
0
shCTRL
shGDF15 A
shGDF15 B

Figure 6-1. GDF15 gene silencing. (A) BT474, BT474 stable GDF15 clone 2 (C2) and HCC1954 **(B)** were transfected using Lipofectamine and 100 nM GDF15 siRNA for 48 hours. Real-time PCR was performed for GDF15. Values reflect average fold in transcript normalized to internal control RPLPO. **(C and D)** GDF15 clone 2 (C2) and HCC1954 cells were infected with lentiviral control shRNA (shCTRL) or GDF15 shRNA (shGDF15); knockdown of GDF15 was confirmed by real-time PCR. Results are reported as fold change in GDF15 transcript level versus control shRNA. Values were normalized to RPLPO housekeeping ribosomal gene transcript levels as internal control.

We also tested the knockdown of GDF15 expression using GDF15-specific shRNA. BT474 parental, stable GDF15 transfectant clone 2 (C2) and HCC1954 breast cancer cells were infected with GDF15-shRNA in a lentiviral backbone or with corresponding control shRNA in the same lentiviral vector backbone. RT-PCR was performed to confirm GDF15 knockdown. However, there was no observed effect on GDF15 gene expression when stable GDF15 transfectant clone 2 (C2) (Figure 6-1C and D) and HCC1954 were infected with shGDF15. Following these results, we chose to explore several routes of troubleshooting, including: making sure that 12 hours after transfection, at least >90% of our HEK293T cells were fluorescence-positive, selecting various titers for viral stock, investigating promoter regions and trying a variety of packaging methods. We did not explore inadequate transduction efficiency as a potential problem, because cells were fluorescent.

ii. *DNAzyme catalytic activity*

We have previously shown correlation between GDF15 levels and HER2-positivity using immunohistochemical analysis of a tumor tissue array (96). In collaboration with Dr. Khalid Salaita and his laboratory in the Emory University Department of Chemistry, we evaluated the utility of gold nanoparticle catalytic deoxyribozyme (GDF15 DNAzyme) conjugates. Conceptually, the DNAzyme hydrolyzes GDF15 mRNA. To improve target selectivity, we conjugated a HER2-targeting aptamer to the complex to enhance tumor (HER2-positive) selectivity**.**

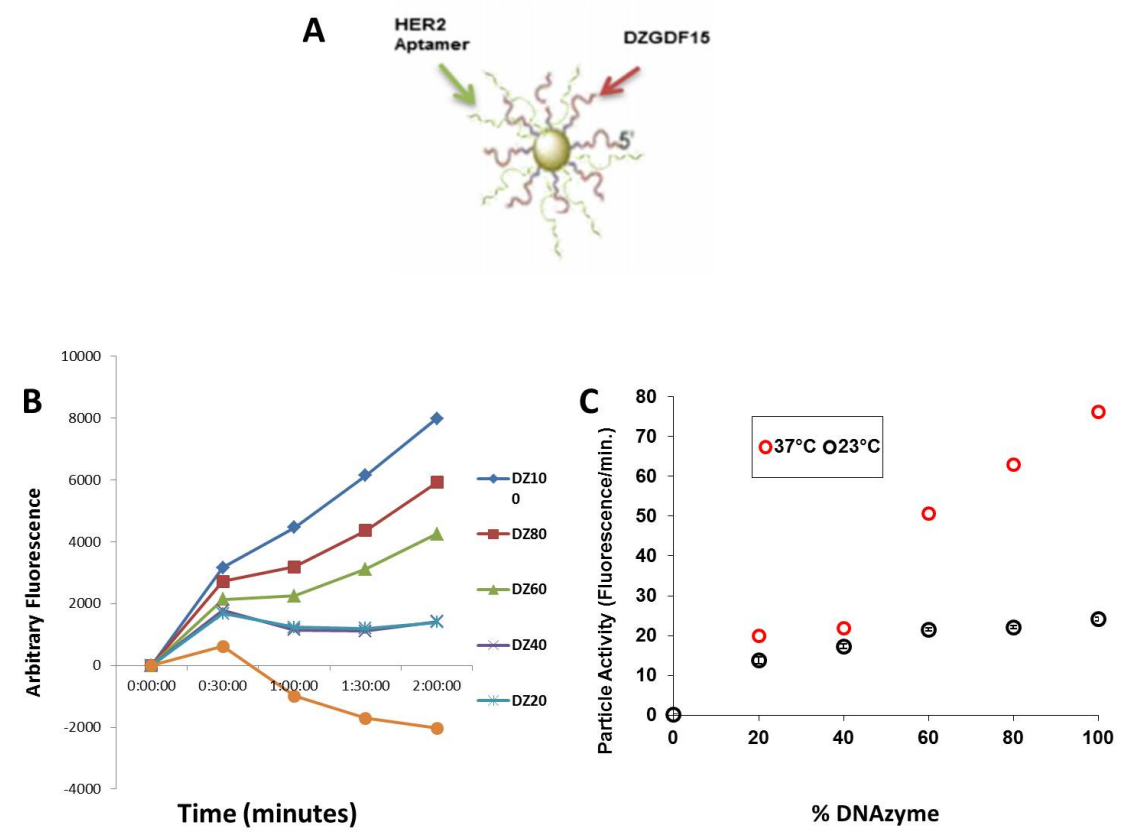

Modified (116)

Figure 6-2 Measurement of DzNP Catalytic Activity. (A) Schematic showing representative image of GDF15 (HER2 aptamer) DNAzyme. **(B)** A kinetic plot showing rate of catalysis for GDF15 DNAzyme density on particle surface in ratio to HER2. **(C)** A kinetic plot showing the DNAzyme surface density (%DNAzyme) as determined in ratio to HER2 aptamer. Open circles represent oligonucleotide fluorescence at 23°C. Red circles represent oligonucleotide fluorescence at 37°C. Error bars represents the standard deviation of three measurements.

The effects of GDF15 DNAzyme density on particle surface in ratio to HER2 on catalysis was determined by measuring the fluorescence intensity as a function of time (Figure 6-2B).

The HER2 aptamer was cofunctionalized to the GDF15 gold nanoparticles (Dz $_{GDF15}$NPs) conjugate in the following ratios, 0/100, 20/80, 40/60, 60/40, 80/20 and 100/0. Fluorescence intensity was used as an indicator of rate of hydrolysis of DNA/RNA chimera substrate that was functionalized with a 5'6-fluorescein (FAM6) and 3' Black Hole Quencher ™ (BHQ). Thus, if DNAzyme is catalytically active, the FAM-Quencher-tagged GDF15 substrate (GDF15 mRNA target sequence) will be cleaved and emit a fluorescent signal. Particles with 100% (Figure 6-2B) GDF15 DNAzyme (no aptamer) demonstrated highest catalytic activity. Moreover, as GDF15 DNAzyme concentration decreased, so did fluorescent signal. Next, we controlled the DNA density on particle surface in ratio to the HER2 aptamer, and assessed dependence of cleavage on temperature. Particle activity was tested at 37°C and 27°C respectively (Figure 6-2C). From these findings we were able to determine a 3-fold decrease in particle activity when 80% HER2 aptamer was present. However, the HER2 aptamer did not completely inhibit DNAzyme activity.

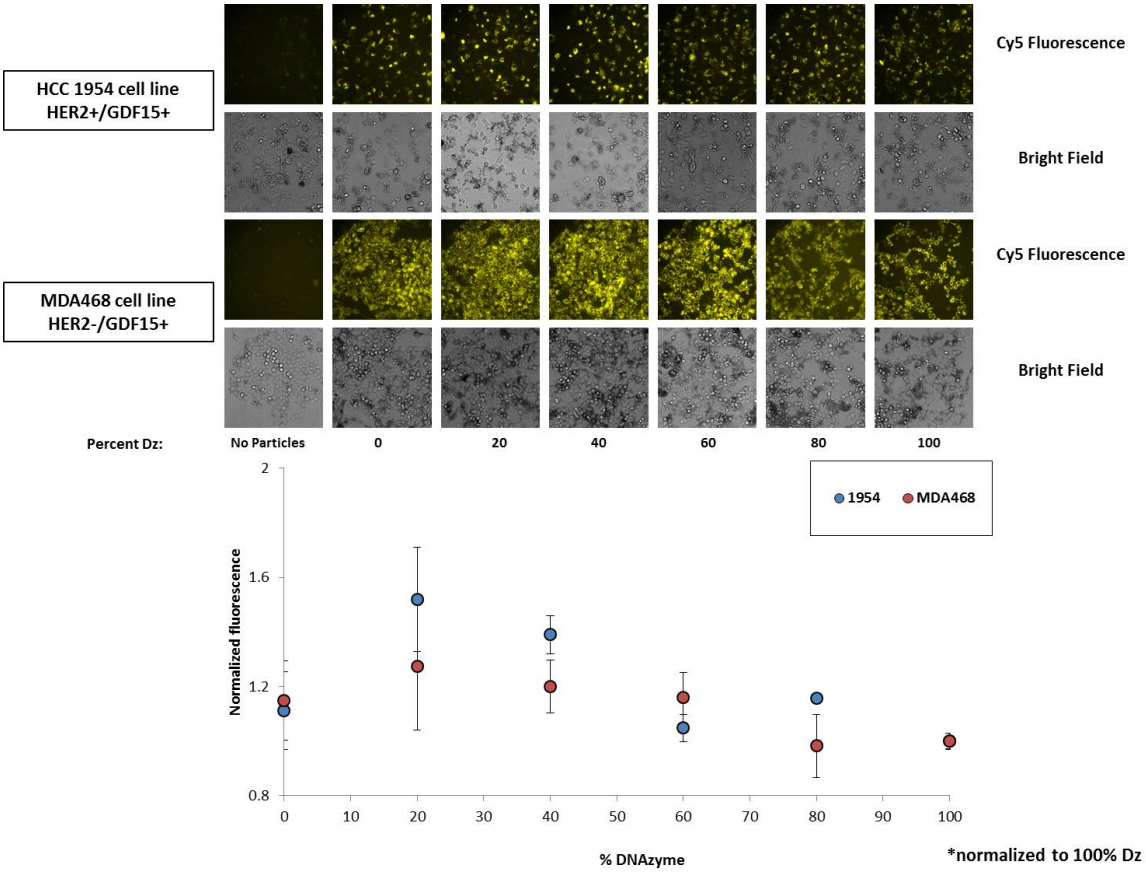
HCC 1954 cell line
HER2+/GDF15+
Cy5 Fluorescence
Bright Field
MDA468 cell line
HER2-/GDF15+
Cy5 Fluorescence
Bright Field
Percent Dz:
No Particles
0
20
40
60
80
100
1954
MDA468
Normalized fluorescence
% DNAzyme
*normalized to 100% Dz

Figure 6-3. Cellular uptake of GDF15 DNAzyme^{cy5}-loaded HER2 AUNP.

Fluorescent microscope images of HCC1954 and MDA468 breast cancer cells treated with GDF15 DNAzyme^{cy5}-loaded HER2 AUNP at ratios of 0/100, 20/80, 40/60, 60/40, 80/20 and 100/0. Fluorescence images were collected at 6 hours.

iii. GDF15 DNAzyme-HER2 aptamer cellular uptake

To determine the cellular uptake and gene regulation of particles in mammalian cells, we coupled the HER2/GDF15 functionalized DNAzymes to Cyanine 5 (Cy5). For this experiment, we chose HER2-positive HCC1954 as our experimental group and HER2-negative MDA468 as our control group. Both breast cancer cells were seeded at the same density and treated with equal amounts of each GDF15/HER2 ratio. After 6 hours, cells were viewed by microscopy, and uptake was measured (Figure 6-3).

To demonstrate HER2 selectivity, we would expect increased Cy5 fluorescence as HER2 aptamer ratio increases in HCC1954 HER2-positive cells). Our data demonstrated 1.6-fold increase in selective uptake at 80% HER2: aptamer. However, our negative control, MDA468, also showed increased cellular uptake at 80% HER2: aptamer. These findings suggest the need for further studies and optimization of cellular uptake and targeting. Other questions that remain unanswered include the potential limitations of steric hindrance, as well as the optimization of seeding density in accordance with proliferation rates for breast cancer cells.

iv. Dz $_{GDF15}$NP regulation of gene expression

After confirming cellular uptake, a dose response was performed using HCC1954 breast cancer cells. Cells were treated with control (untreated), 5 nM, 10 nM, and 20 nM Dz $_{GDF15}$NPs for 48 h. We then analyzed GDF15 mRNA expression using real-time PCR relative to housekeeping gene RPLPO (a component of the 60S ribosomal subunit). We observed a dose-dependent knockdown using the catalytically active Dz $_{GDF15}$NP (Figure

6-4A). However, our control, a nonspecific catalytic DNAzyme, showed a dose-dependent increase in GDF15 expression. To assess dose toxicity, viable cells were counted by trypan blue exclusion. The 5 nM dose was selected for further studies, as 20 nM was associated with significantly reduced viability, suggesting toxicity (Figure 6-4B).

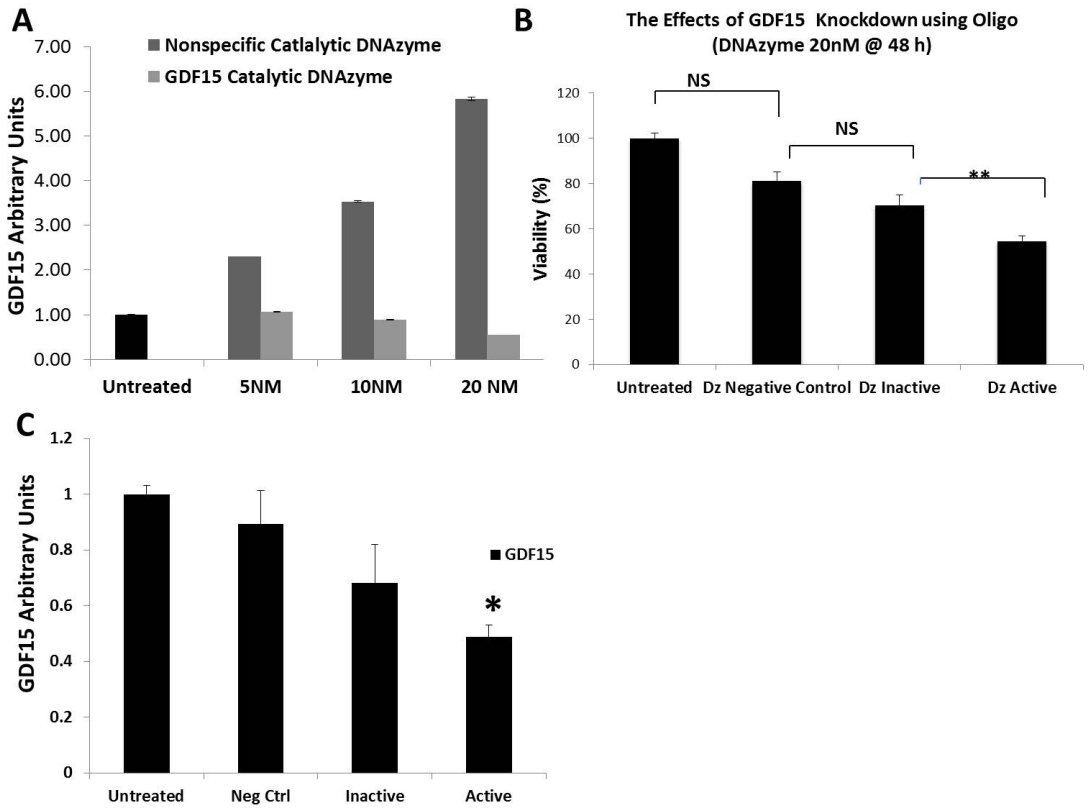
A
Nonspecific Catlalytic DNAzyme
GDF15 Catalytic DNAzyme
GDF15 Arbitrary Units
7.00
6.00
5.00
4.00
3.00
2.00
1.00
0.00
Untreated
5NM
10NM
20 NM
B
The Effects of GDF15 Knockdown using Oligo
(DNAzyme 20nM @ 48 h)
Viability (%)
120
100
80
60
40
20
0
NS
NS
**
Untreated
Dz Negative Control
Dz Inactive
Dz Active
C
GDF15 Arbitrary Units
1.2
1
0.8
0.6
0.4
0.2
0
GDF15
*
Untreated
Neg Ctrl
Inactive
Active

Figure 6-4. Inhibition of GDF15 using Dz $_{GDF15}$NP.

(A) Real-time PCR analysis of GDF15 mRNA expression of HCC1954 cells, untreated or treated with 5 nM, 10 nM or 20 nM of catalytic Dz $_{GDF15}$NPs for 48 h. **(B)** After 48 h, viable cells were counted by trypan blue exclusion. Viability is presented as a percentage of untreated cells vs DZNP negative control, Dz $_{GDF15}$NP inactive or Dz $_{GDF15}$NP active. Data reflect the average of 3 replicates per treatment group. Error bars represent standard deviation between replicates. P-values were determined by t-test. **(C)** Real-time PCR analysis of GDF15 mRNA expression of HCC1954 cells. Cells were either untreated (control), treated with in non-catalytic (i-Dz$_{GDF15}$NP) and nonspecific catalytic (Dz$_{NC}$NP) DzNPs and catalytic (Dz$_{GDF15}$NP) at concentration of 5 nM for 48 h. The catalytic particles down regulated GDF15 mRNA by approximately 45% relative to nonspecific particles (p<0.005).

These studies provide preliminary data related to the design and optimization of target-specific DNAzyme-conjugated nanoparticles. Moreover, this study suggests that Dz NPs may effectively inhibit gene expression.

3. Conclusion

In this study, we investigated different methods of inhibiting GDF15 gene expression. GDF15 siRNA transfection demonstrated robust knockdown of GDF15. Although effective this method is transient and does not allow investigation of effects associated with stable knockdown of GDF15. Next, we tried lentiviral shRNA infection; however, our efforts to knockdown GDF15 were unsuccessful. According to Fellman and colleagues, in addition to off-target effects, it is difficult to identify potent shRNA given the immense possibility of options. As a result many shRNA predictions can oftentimes be inefficient, and lead to false results in functional screens (217). Moreover, the major challenges using RNAi have been overcoming instability *in vivo* and undesirable off-target effects. Fortunately, within the past decade major advancements have been made in the optimization of RNAi (218). In 2012, Hamasaki and colleagues discovered a novel class of RNAi agents (nkRNA®, PnKRNA™) that are resistant to degradation and effectively suppress TGF-β mRNA with no off-target side effects in models of lung disease. (219). One challenge with members of the TGF-β family has been identifying tissue-specific profiles and the potential for variable expression of isoforms.

Our data demonstrate successful synthesis and optimization of gold nanoparticle Dz_{GDF15}NPs *in vitro*. Our oligonucleotide sequence successfully cleaved the GDF15 target gene and resulted in decreased expression. This data is supported by previous studies that demonstrated the ability of Dz_{GDF15}NPs to effectively enter cells and regulate GDF15 gene expression (116). Previous studies using optimized lentiviral shRNA knockdown of GDF15 reported approximately a 50% reduction in GDF15 expression (96), a reduction comparable to that observed with 5 nM Dz_{GDF15}NPs (116). These data indicate the importance of further studies using Dz_{GDF15}NPs in targeted therapy and breast cancer.

Chapter 7

Conclusions

i. Summary & conclusions

My research describes investigation of the mechanisms that drive metastatic breast cancer. Here, I provide evidence for the regulation and function of GDF15 in breast cancer. Overexpression of GDF15 correlates with poor prognosis in multiple pathologies. Moreover, GDF15 serum levels serve as a prognostic marker for cardiovascular disease, colorectal cancer, prostate cancer and cancer-associated anorexia/cachexia. My findings demonstrate that GDF15 promotes activation of critical pathways that drive resistance, proliferation, invasion and EMT in breast cancer. Further investigation into these signaling pathways revealed that IGF-1R, TGFβR, and FoxM1 are key players in promoting metastatic potential in the presence of GDF15 overexpression. Importantly, the data presented here identifies GDF15 overexpression as a mediator of invasion and EMT.

Chapter 1 provided a detailed overview on breast cancer and summarized subtypes, focusing on HER2-positive breast cancer treatment approaches and mechanisms of resistance. The proliferation associated transcription factor FoxM1 is increased in HER2-postive breast cancer and mediates trastuzumab resistance. Inhibition of Raf/MEK/ERK signaling prevents FoxM1-medited chemoresistance. While activation of FoxM1 sustains TGF-β signaling Smad3/Smad4 nuclear translocation and subsequent activation of EMT transcription factors SLUG and SNAIL. Results from preceding chapters suggest that the TGF-β superfamily cytokine GDF15 is a major inducer of FoxM1 expression via IGF-1R activation.

Chapter 3 provides evidence for the *in vitro* characterization of GDF15 in breast cancer. First, I provide a detailed overview of GDF15 expression, regulation and

function. Importantly, I elaborate on the genomic and proteomic processing of GDF15. Located on chromosome 19p12-13.1; GDF15 has a number of regulatory sites, including p53, Egr-1 and sites that recruit transcription factors that drive differentiation and mitogenesis. Moreover the MAPK signaling pathway has been implicated in partial regulation of GDF15. Additionally GDF15 enhances p38-MAPK in HER2-positive breast cancer cells and promotes invasion. Fascinatingly, the MAPK-MEK/ERK has been shown to phosphorylate FoxM1 and promote nuclear translocation. Pharmacologic inhibition of FoxM1 using DIM has been shown to downregulate AKT and increase trastuzumab efficacy in breast cancer. The GDF15 promoter has an AKT response element and AKT/TGF-β signaling crosstalk has been shown to play a major role in regulation of cell response. Given the influence of GDF15 on multiple signaling pathways, we sought to determine the effects of stable GDF15 overexpression *in vitro.*

Our data demonstrated that transfection of constituently active GDF15 drives upregulation of ERK, TGF-βR, Foxm1 and IGF-1R signaling. Knockdown of Foxm1 using transient siRNA transfection reduced GDF15 transcript levels. In vitro studies, examining co-localization of GDF15 stable transfectants revealed significant overlap with TGF-βRII. These findings cannot conclusively determine that GDF15 is binding to the TGF-βRII; however they do suggest that GDF15 is in exceptionally close proximity to TGF-βRII. Pharmacologic inhibition of TGF-βR partially blocked IGF-1R phosphorylation and FoxM1 expression. However, inhibition of TGF-βR did not reduce expression of mesenchymal markers, suggesting that GDF15-mediated EMT is independent of TGF-β signaling.

In chapter 4, we proceeded to investigate a potential relationship between GDF15 and clinical characteristics of patients having breast cancer. Patient data revealed a high correlation between GDF15 expression and reduced survival among patients having HER2-positive/ER-negative breast cancer. Next, I further investigated the mechanistic influence of these findings *in vitro* using the HER2-postive/ER-negative HCC1954 breast cancer cells. Our data indicates that GDF15 transcript and serum levels are significantly increased in HCC1954 breast cancer cells. This observation is of interest because our stable transfectants display no observable increase in GDF15serum levels. However, in both stable GDF15 transfectants and HCC1954 cells we observed increased invasive potential. We went on to show that GDF15 colocalization with TGF-βRII is significantly less in HCC1954 compared to stable clones. Lastly, pharmacologic inhibition of secreted GDF15 using a neutralizing monoclonal antibody shows no change in expression of GDF15-mediated activation of downstream signaling proteins or transcription factors. Our data suggest that GDF15 can be differentially regulated as a result of how it is expressed. These finding support further studies into the individual roles of GDF15 precursors and mature proteins.

Chapter 5 presents my studies investigating the process by which GDF15 promotes EMT and invasion in breast cancer. Our data indicates that GDF15 overexpression drives proliferation and acquisition of mesenchymal markers in breast cancer. Moreover we observe changes in cell morphology and migratory potential *in vitro*. Exogenous stimulation with recombinant GDF15 promotes activation of IGF-1R and upregulation of FoxM1, both key players in activation of EMT and proliferation. In addition GDF15 drives upregulation of matrix metalloproteinases MMP2 and MMP9.

While pharmacological and inhibition of MMP2 and MMP9 attenuates invasion in the presence of GDF15 overexpression. Genetic inhibition of FoxM1 inhibits MMP2 and MMP9 as well as invasive potential. These findings suggest that GDF15 overexpression drives IGF-1R/FoxM1 signaling and subsequent activation of MMP2 and MMP9 to drive invasion and EMT in breast cancer (Figure 7-1).

We went on to show that genetic knockdown of GDF15 inhibits invasion in breast cancer. We also explored using shGDF15 for stable knockdown of GDF15 in stable GDF15 clones and HCC954 cells, but our infection was unsuccessful. These findings sparked our interest in alternative methods of gene knockdown. Our goal was to optimize deoxyribozymes for knockdown of GDF15. We optimized studies using a catalytic deoxyribozyme targeting GDF15 functionalized to a HER2 aptamer for target specificity. Our data demonstrated successful catalytic activity and cellular uptake of our DNAzyme. Interestingly, conjugation to the HER2 aptamer did not significantly increase efficiency of cellular uptake. Finally, we performed a dose response *in vitro* and determined the effective non-toxic dose was 5 nM of particles. These preliminary findings also revealed inhibition of GDF15 expression with 5nM particle treatment. Our data suggest that DNAzyme treatment is an alternative to RNAi and demonstrate the potential of optimizing DNAzymes for targeted therapy in GDF15 overexpressing breast cancer.

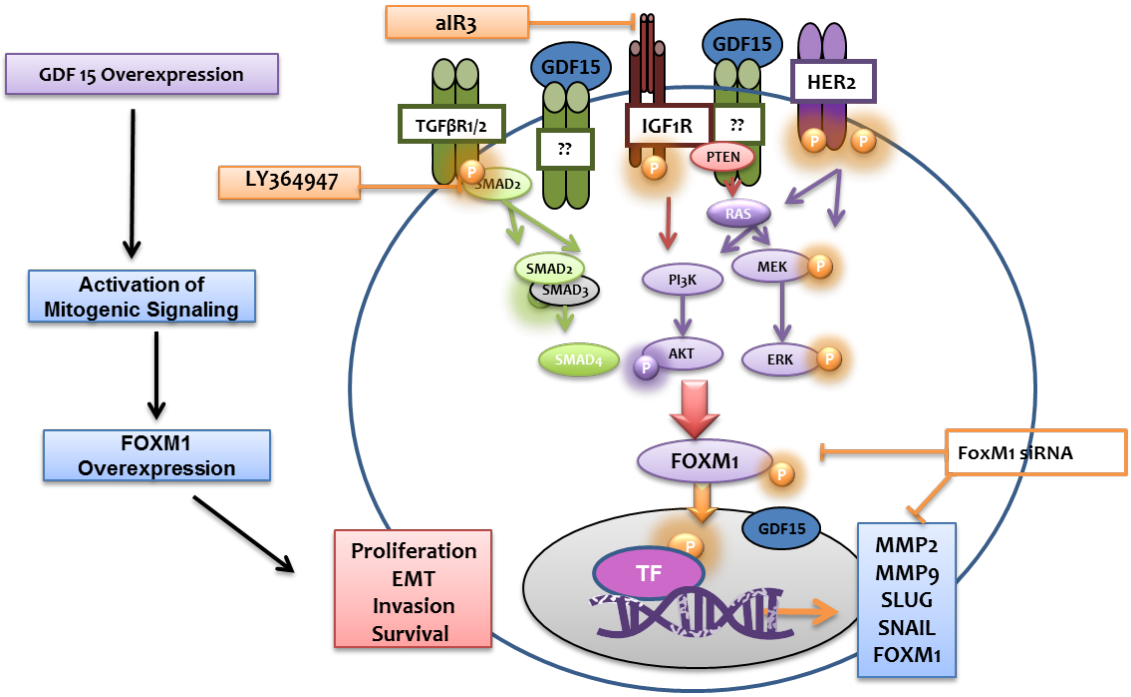
GDF 15 Overexpression
Activation of Mitogenic Signaling
FOXM1 Overexpression
Proliferation
EMT
Invasion
Survival
alR3
LY364947
GDF15
TGFβR1/2
??
IGF1R
??
GDF15
HER2
PTEN
RAS
SMAD2
SMAD2
SMAD3
SMAD4
PI3K
MEK
AKT
ERK
FOXM1
FoxM1 siRNA
GDF15
TF
MMP2
MMP9
SLUG
SNAIL
FOXM1

Figure 7-1 Summary of Key Results. We propose that GDF15 overexpression drives activation of key mitogenic signaling pathways (HER2, IGF-1R and TGF-βR) and activates signaling cascades (MEK/ERK, PI3K, and Smad) that drive tumor progression. GDF15 appears to activate IGF-1R and has been previously linked to the activation of HER2 (joshi et al., 2011). GDF15 also activates TGF-βR, as measured by phosphorylation of the TGF-β substrate Smad2. Our findings suggest some unknown mechanism of crosstalk between IGF-1R and TGF- β. Previous studies have indicated that GDF15 activates Src in a TGF- β dependent manner, promoting cross talk amongst other receptor tyrosine kinases. Inhibition of TGF-βR partially inhibits GDF15 – mediated activation of IGF-1R, but does not prevent EMT or invasive potential. Furthermore inhibition of IGF-1R signaling and the proliferation associated transcription factor FOXM1 abrogates invasive potential and restores epithelial marker E-cadherin. These findings suggest that GDF15-mediated activation of IGF-1R and TGF-βR, may be due to intracellular crosstalk that drives a variety of downstream signaling pathways that promote cancer progression.

ii. Clinical implications

Elevated circulating levels of GDF-15 have been used as an indicator of poor prognosis and progression of colorectal cancer, prostate cancer, ovarian cancer diabetes, cardiovascular disease and metabolic disorders (147; 156; 220). A pancreatic ductal adenocarcinoma (PDAC) study having over 1,400 participants reported that serum GDF15 was dramatically elevated in tissue and serum samples. Moreover, increased circulating GDF15 levels were determined to be a predictive marker of early-stage PDAC and relapse (221). A blinded colorectal cancer study evaluating 987 serum samples revealed that GDF15 circulating levels are significantly increased in patients with tumor recurrence and liver metastasis (222). A recent study evaluated a group of patients with prostate, breast, lung and colorectal cancer for correlation and determined that increased circulating levels of GDF15 were associated with bone metastasis. These *in vivo* findings suggest that assessment of circulating GDF15 levels can potentially serve as a prognostic indicator for metastatic progression.

Currently, limitations exist in elucidating the full role of GDF15, because the receptor remains to be identified. It is assumed that GDF15 regulates cellular response through TGF-β receptor signaling. However, further studies are necessary to fully confirm a direct link between GDF15 and the TGF-β receptor complex (223). Interestingly, studies investigating the autocrine/paracrine signaling of GDF15 have shown that GDF15, but not TGFβ, is able to induce its own expression (192). Additionally, GDF15 is suggested to maintain cancer stem-like cells in breast cancer and

induce tumor growth (192). Thus, studies targeting GDF15 expression may lead to inhibition of tumor formation. However, similar to other members of the TGF-β superfamily, GDF15 has been shown to have opposite (anti-tumorigenic) effects, thus controversial data exists. Murine models of TRAMP prostate cancer with deletion of the MIC-1/GDF15 gene ($TRAMP^{MIC-/-}$) displayed a significant increase in tumor size and decreased survival as compared to wild type. Moreover, the expression of GDF15 in transgenic murine models was shown to promote a p53-dependent cell cycle arrest, and GDF15 inhibits apoptosis (224) in wild-type p53 MCF-7 breast cancer cells. However, given that p53 is a significant regulator of GDF15 expression, it is likely that cancers having mutated p53 may be differentially regulated. Additionally studies have suggested that p53-dependent regulation of GDF15 is influenced by the environment (i.e. age, oxidative stress), rather than genetic influence (225). Further studies in bladder cancer show that the p53 overexpression induces GDF15 expression; however, knockdown of GDF15 demonstrated that p53 was not a downstream target of GDF15 (226). These findings suggest that regulation of GDF15 is multifaceted, having tissue- and cell-specific functions.

Interestingly, studies involving models of *p53* mutation show a pro-tumorigenic function for GDF15 as compared to the p53-dependent regulation. For example, studies using the p53 mutant LM2 mouse breast cancer cells suggest that GDF15 plays a role in promoting cell survival and preventing radiation-induced cell death (227). Studies in glioma and myeloma cells demonstrate that GDF15 overexpression contributes to tumor growth and survival (148; 162). In prostate cancer cell lines DU145 and PC3 (both having *p53* mutations), stimulation with recombinant GDF15 resulted in chemoresistance

(228). It is suggested that GD15 promotes pro-tumorigenic signaling via activation of mitogenic signaling pathways, such as ERK, AKT and ErbB family members. Previous studies in HER2-positive breast cancer show that both exogenous and endogenous GDF15 overexpression drive trastuzumab resistance (96). HER2 tyrosine kinase inhibition blocked GDF15-mediated trastuzumab sensitivity (96). Moreover, stimulation of SK-BR-3 cells with GDF15 was shown to increase the activation of Src kinase and promote invasiveness. Pharmacologic inhibition of Src activity prevents GDF15-mediated phosphorylation of EGFR signaling and MMP-9 in SK-BR-3 breast cancer cells (104). Thus, in order to adequately target GDF15 we must further investigate the mechanisms, genetic conditions and cancer subtypes that drive differential regulation of GDF15. More importantly, we should identify the transcription factors that are regulated under multiple conditions via DNA binding assays. For example, chromatin immunoprecipitation (chIP) assays could be performed to investigate direct interaction of transcription factor candidates with the *GDF15* promoter.

Our findings together with those previously reported suggest that GDF15 is elevated in a majority of breast cancers. However, few studies have been published about the role of GDF15 in breast cancer. Future studies will examine a larger set of patient tissues to determine whether the relationship between GDF15 expression, tumor grade, survival or response to treatment correlates with subtypes of breast cancer other than HER2-positive and ER-negative, which was discussed here. Studies in prostate cancer have shown that GDF15 plays a protective role in early primary tumor development; germ-line gene deletion caused an increase in local tumor growth and decreased survival (223). Whereas in advanced disease; GDF15 overexpression induced local invasion and

metastatic spread. There is a need for further patient analysis of GDF15 expression in intrinsic vs. acquired resistance in the setting of HER2-positive breast cancer. Here, we show that stable overexpression of GDF15 in HER2-positive cells was sufficient to induce a change in proliferation, invasion, morphology and expression of mesenchymal markers. We observed restoration of the epithelial marker E-cadherin and attenuation of invasive potential in the presence of IGF-1R inhibition. The results presented here support a potential for co-targeting IGF-1R/ TGF-βR/FoxM1 in HER2-positive breast cancer. Moreover, upregulation of compensatory signaling pathways is a known mechanism of trastuzumab resistance. Previous studies have shown that GDF15-mediates activation of TGFβR-Src-HER2 crosstalk (96), and that Src is essential for IGF-1R / HER2 crosstalk (87). Moreover, phosphoactivation of the serine/threonine kinase Akt, which is downstream of IGF1-R, has been shown to promote corsstalk with the TGF-β signaling pathway. In addition, both TGF-βR and IGF-1R have been implicated as key signaling pathways involved in the induction of epithelial-to-mesenchymal transition (EMT) (194; 229).

In conclusion, more studies are required to fully elucidate the pleiotropic role of GDF15 in breast cancer. Further studies investigating tissue and cell specific regulation of GDF15 and the subsequent effects that GDF15 expression levels have on gene transcription will increase our knowledge of GDF15 as a molecular target in breast cancer.

iii. *Limitations and Future Directions*

In this dissertation, we investigate the role of GDF15 in breast cancer *in vitro* using methods of nanotechnology, pharmacologic inhibition, and genetic knockdown. We also present immunofluorescence and immunohistochemical analysis of human breast cancer cells and patient tissue samples, respectively. Whilst the methods utilized in this dissertation serve as useful tools, *in vitro* studies have limitations for the development of targeted therapeutics and drug delivery. Breast cancer is a heterogeneous disease having diverse histopathological characteristics that drive genetic diversity and determines prognosis. Thus, the *in vitro* models used in this study do not completely recapitulate the conditions in the cellular environment that would exist within the patient. Here we have shown that GDF15 mRNA levels and secreted levels can both drive cell invasion. However, we also show that GDF15 drives proliferation via cell cycle analysis. It is possible that these invasive cancer cells are proliferating, but may not be proliferating while actively moving; for example halting migration while proliferating for a transient time period then switching back to migration post-proliferation. The best way to asses this process occurring *in vitro* would be to investigate invasive potential and proliferation during certain time points. These future experiments would allow us to determine if GDF15 is driving invasion, proliferation or both processes uncoupled within the same cell.

Interestingly, the HCC 1954 cell line is HER2-positive and ER-negative, while the BT474 GDF15 stable clones are HER2-positive and ER-positive. These results

confirm the pleiotropic role of GDF15 signaling and suggest a need to further investigate how GDF15 precursors impact intracellular signaling. Neutralizing antibody successfully inhibited secreted levels of GDF15, but had no influence on phenotypic changes or mRNA levels of GDF15. These findings suggest an unknown mechanism that may be regulating GDF15 transcription and proteolytic cleavage in the HCC1954 cell line. Future studies should investigate GDF15 expression in all breast cancer subtypes to further understand the mechanisms driving differential signaling.

Moreover, studies have shown that metastasis and invasion of breast cancer into the surrounding stroma microenvironment promotes crosstalk and interaction between paracrine signaling and biochemical cues (230). Thus, failure to incorporate these complexities into our studies may cause future difficulties in accurately determining cell response to targeted therapy in the presence of GDF15 overexpression. Future *in vitro* studies could investigate the complex interrelation between the tumor and the microenvironment, by using *in vitro* co-culture models. Current transwell systems allow for the simultaneous culture of two different cell types sharing the same culture medium but without direct contact.

Another limitation is the minimal consideration of the immunomodulatory effects of GDF15 on tumor response. Increased secretion of GDF15 has been shown to suppress immune cell function and simultaneously enhance cancer cell growth via autocrine signaling (231; 232) . Moreover, endogenous GDF15 expression has been shown to induce immune escape and promote tumorigenecity of glioma cells (148). In summary, there is a need to further investigate GDF15-mediated effects on the tumor stroma

microenvironment and immune function. Within the last decade, advancements in immunotherapies have demonstrated the importance of the immune system and heterogeneity of the tumor environment (233). Patient-derived tumor xenograft (PDX) models are an emerging platform for translational cancer research. PDX models are advantageous in the prediction of clinical outcomes, drug evaluation and biomarker identification (234). Moreover, recent studies have proposed the use of PDX models to investigate the role of immunity-cancer interactions, by using human hemato-lymphoid chimeric mice or human immune system models (235). Future studies should utilize HER2-positive trastuzumab resistant PDX models to investigate the role of GDF15 overexpression *in* vivo. We propose treatment with optimized $DN_{GDF15}ZPs$ conjugated to pharmacologic inhibitors of IGF-1R and/or TGF-β. These studies will provide preclinical evidence for GDF15-targeted therapy and future drug development in breast cancer.

\

Chapter 8

References

1. Steel CM, Smyth E. 1999. Molecular pathology of breast cancer and its impact on clinical practice. *Schweiz Med Wochenschr* 129:1749-57
2. Olah E, Kokeny S, Papp J, Bozsik A, Keszei M. 2006. Modulation of cancer pathways by inhibitors of guanylate metabolism. *Adv Enzyme Regul* 46:176-90
3. Kenemans P, Verstraeten RA, Verheijen RH. 2004. Oncogenic pathways in hereditary and sporadic breast cancer. *Maturitas* 49:34-43
4. Edler L, Kopp-Schneider A. 2005. Origins of the mutational origin of cancer. *Int J Epidemiol* 34:1168-70
5. Schulz WA, Hatina J. 2006. Epigenetics of prostate cancer: beyond DNA methylation. *J Cell Mol Med* 10:100-25
6. Wang M, Gartel AL. 2011. The suppression of FOXM1 and its targets in breast cancer xenograft tumors by siRNA. *Oncotarget* 2:1218-26
7. Wu Y, Sarkissyan M, Vadgama JV. 2016. Epithelial-Mesenchymal Transition and Breast Cancer. *J Clin Med* 5
8. Smid M, Wang Y, Zhang Y, Sieuwerts AM, Yu J, et al. 2008. Subtypes of breast cancer show preferential site of relapse. *Cancer Res* 68:3108-14
9. Chaffer CL, Weinberg RA. 2011. A perspective on cancer cell metastasis. *Science* 331:1559-64
10. Howlader N, Altekruse SF, Li CI, Chen VW, Clarke CA, et al. 2014. US incidence of breast cancer subtypes defined by joint hormone receptor and HER2 status. *J Natl Cancer Inst* 106
11. Parsa Y, Mirmalek SA, Kani FE, Aidun A, Salimi-Tabatabaee SA, et al. 2016. A Review of the Clinical Implications of Breast Cancer Biology. *Electron Physician* 8:2416-24
12. Connolly CK, Van Schil PE, Milroy R, Braendli O, Prescott RJ. 2003. The approach to the surgical management of cancer in four European countries. *Eur Respir J* 22:838-44
13. Whitman GJ, Sheppard DG, Phelps MJ, Gonzales BN. 2006. Breast cancer staging. *Semin Roentgenol* 41:91-104
14. Dawood S, Broglio K, Esteva FJ, Ibrahim NK, Kau SW, et al. 2008. Defining prognosis for women with breast cancer and CNS metastases by HER2 status. *Ann Oncol* 19:1242-8
15. Moulder SL, Craft BS, Hortobagyi GN. 2008. Inhibition of receptor tyrosine kinases in combination with chemotherapy for the treatment of breast cancer. *Anticancer Agents Med Chem* 8:481-7
16. Cardoso F, Senkus-Konefka E, Fallowfield L, Costa A, Castiglione M, Group EGW. 2010. Locally recurrent or metastatic breast cancer: ESMO Clinical Practice Guidelines for diagnosis, treatment and follow-up. *Ann Oncol* 21 Suppl 5:v15-9
17. Cheng YC, Ueno NT. 2012. Improvement of survival and prospect of cure in patients with metastatic breast cancer. *Breast Cancer* 19:191-9
18. Perou CM, Sorlie T, Eisen MB, van de Rijn M, Jeffrey SS, et al. 2000. Molecular portraits of human breast tumours. *Nature* 406:747-52

19. Nielsen JS, Jakobsen E, Holund B, Bertelsen K, Jakobsen A. 2004. Prognostic significance of p53, Her-2, and EGFR overexpression in borderline and epithelial ovarian cancer. *Int J Gynecol Cancer* 14:1086-96
20. Neven P, Pochet N, Drijkoningen M, Amant F, De Smet F, et al. 2006. Progesterone receptor in estrogen receptor-positive breast cancer: the association between HER-2 and lymph node involvement is age related. *J Clin Oncol* 24:2595; author reply -7
21. Shipitsin M, Campbell LL, Argani P, Weremowicz S, Bloushtain-Qimron N, et al. 2007. Molecular definition of breast tumor heterogeneity. *Cancer Cell* 11:259-73
22. Prat A, Ellis MJ, Perou CM. 2011. Practical implications of gene-expression-based assays for breast oncologists. *Nat Rev Clin Oncol* 9:48-57
23. Yoshida T, Ozawa Y, Kimura T, Sato Y, Kuznetsov G, et al. 2014. Eribulin mesilate suppresses experimental metastasis of breast cancer cells by reversing phenotype from epithelial-mesenchymal transition (EMT) to mesenchymal-epithelial transition (MET) states. *British journal of cancer*
24. Harrell JC, Prat A, Parker JS, Fan C, He X, et al. 2012. Genomic analysis identifies unique signatures predictive of brain, lung, and liver relapse. *Breast Cancer Res Treat* 132:523-35
25. Sorlie T, Tibshirani R, Parker J, Hastie T, Marron JS, et al. 2003. Repeated observation of breast tumor subtypes in independent gene expression data sets. *Proc Natl Acad Sci U S A* 100:8418-23
26. O'Brien KM, Cole SR, Tse CK, Perou CM, Carey LA, et al. 2010. Intrinsic breast tumor subtypes, race, and long-term survival in the Carolina Breast Cancer Study. *Clin Cancer Res* 16:6100-10
27. Dai X, Shi X, Wang Y, Qiao Y. 2012. Solubilization of saikosaponin a by ginsenoside Ro biosurfactant in aqueous solution: mesoscopic simulation. *Journal of colloid and interface science* 384:73-80
28. Badve S, Dabbs DJ, Schnitt SJ, Baehner FL, Decker T, et al. 2011. Basal-like and triple-negative breast cancers: a critical review with an emphasis on the implications for pathologists and oncologists. *Mod Pathol* 24:157-67
29. Bertucci F, Finetti P, Cervera N, Birnbaum D. 2008. [Prognostic classification of breast cancer and gene expression profiling]. *Med Sci (Paris)* 24:599-606
30. de Ronde J, Wessels L, Wesseling J. 2010. Molecular subtyping of breast cancer: ready to use? *Lancet Oncol* 11:306-7
31. Doane AS, Danso M, Lal P, Donaton M, Zhang L, et al. 2006. An estrogen receptor-negative breast cancer subset characterized by a hormonally regulated transcriptional program and response to androgen. *Oncogene* 25:3994-4008
32. Farmer P, Bonnefoi H, Becette V, Tubiana-Hulin M, Fumoleau P, et al. 2005. Identification of molecular apocrine breast tumours by microarray analysis. *Oncogene* 24:4660-71
33. Hennessy BT, Gonzalez-Angulo AM, Carey MS, Mills GB. 2009. A systems approach to analysis of molecular complexity in breast cancer. *Clin Cancer Res* 15:417-9
34. Bultman SJ, Herschkowitz JI, Godfrey V, Gebuhr TC, Yaniv M, et al. 2008. Characterization of mammary tumors from Brg1 heterozygous mice. *Oncogene* 27:460-8

35. Rugo HS, O'Shaughnessy JA, Perez EA. 2011. Clinical roundtable monograph. Current treatment options for metastatic breast cancer: what now? *Clin Adv Hematol Oncol* 9:1-16
36. Berrada N, Delaloge S, Andre F. 2010. Treatment of triple-negative metastatic breast cancer: toward individualized targeted treatments or chemosensitization? *Ann Oncol* 21 Suppl 7:vii30-5
37. Shih C, Padhy LC, Murray M, Weinberg RA. 1981. Transforming genes of carcinomas and neuroblastomas introduced into mouse fibroblasts. *Nature* 290:261-4
38. Margolis GJ, Goodman RL, Rubin A, Pajac TF. 1989. Psychological factors in the choice of treatment for breast cancer. *Psychosomatics* 30:192-7
39. Graus-Porta D, Beerli RR, Daly JM, Hynes NE. 1997. ErbB-2, the preferred heterodimerization partner of all ErbB receptors, is a mediator of lateral signaling. *EMBO J* 16:1647-55
40. Kaufman B, Trudeau M, Awada A, Blackwell K, Bachelot T, et al. 2009. Lapatinib monotherapy in patients with HER2-overexpressing relapsed or refractory inflammatory breast cancer: final results and survival of the expanded HER2+ cohort in EGF103009, a phase II study. *Lancet Oncol* 10:581-8
41. Tzahar E, Waterman H, Chen X, Levkowitz G, Karunagaran D, et al. 1996. A hierarchical network of interreceptor interactions determines signal transduction by Neu differentiation factor/neuregulin and epidermal growth factor. *Mol Cell Biol* 16:5276-87
42. Moasser MM. 2007. Targeting the function of the HER2 oncogene in human cancer therapeutics. *Oncogene* 26:6577-92
43. Melenhorst WB, Mulder GM, Xi Q, Hoenderop JG, Kimura K, et al. 2008. Epidermal growth factor receptor signaling in the kidney: key roles in physiology and disease. *Hypertension* 52:987-93
44. Schulze WX, Deng L, Mann M. 2005. Phosphotyrosine interactome of the ErbB-receptor kinase family. *Mol Syst Biol* 1:2005 0008
45. Finigan JH, Faress JA, Wilkinson E, Mishra RS, Nethery DE, et al. 2011. Neuregulin-1-human epidermal receptor-2 signaling is a central regulator of pulmonary epithelial permeability and acute lung injury. *J Biol Chem* 286:10660-70
46. Hazan R, Margolis B, Dombalagian M, Ullrich A, Zilberstein A, Schlessinger J. 1990. Identification of autophosphorylation sites of HER2/neu. *Cell Growth Differ* 1:3-7
47. Qian X, LeVea CM, Freeman JK, Dougall WC, Greene MI. 1994. Heterodimerization of epidermal growth factor receptor and wild-type or kinase-deficient Neu: a mechanism of interreceptor kinase activation and transphosphorylation. *Proc Natl Acad Sci U S A* 91:1500-4
48. Griner SE, Joshi JP, Nahta R. 2013. Growth differentiation factor 15 stimulates rapamycin-sensitive ovarian cancer cell growth and invasion. *Biochemical pharmacology* 85:46-58
49. Garrett TP, McKern NM, Lou M, Elleman TC, Adams TE, et al. 2003. The crystal structure of a truncated ErbB2 ectodomain reveals an active conformation, poised to interact with other ErbB receptors. *Mol Cell* 11:495-505

50. Cho HS, Mason K, Ramyar KX, Stanley AM, Gabelli SB, et al. 2003. Structure of the extracellular region of HER2 alone and in complex with the Herceptin Fab. *Nature* 421:756-60
51. Penuel E, Akita RW, Sliwkowski MX. 2002. Identification of a region within the ErbB2/HER2 intracellular domain that is necessary for ligand-independent association. *J Biol Chem* 277:28468-73
52. Yaziji H, Gown AM. 2004. Accuracy and precision in HER2/neu testing in breast cancer: are we there yet? *Human pathology* 35:143-6
53. Owens MA, Horten BC, Da Silva MM. 2004. HER2 amplification ratios by fluorescence in situ hybridization and correlation with immunohistochemistry in a cohort of 6556 breast cancer tissues. *Clinical breast cancer* 5:63-9
54. Kallioniemi OP, Kallioniemi A, Kurisu W, Thor A, Chen LC, et al. 1992. ERBB2 amplification in breast cancer analyzed by fluorescence in situ hybridization. *Proc Natl Acad Sci U S A* 89:5321-5
55. Jones KL, Buzdar AU. 2009. Evolving novel anti-HER2 strategies. *Lancet Oncol* 10:1179-87
56. Carter WB, Niu G, Ward MD, Small G, Hahn JE, Muffly BJ. 2007. Mechanisms of HER2-induced endothelial cell retraction. *Annals of surgical oncology* 14:2971-8
57. Wolff AC, Hammond ME, Schwartz JN, Hagerty KL, Allred DC, et al. 2007. American Society of Clinical Oncology/College of American Pathologists guideline recommendations for human epidermal growth factor receptor 2 testing in breast cancer. *J Clin Oncol* 25:118-45
58. Wang SC, Hung MC. 2001. HER2 overexpression and cancer targeting. *Seminars in oncology* 28:115-24
59. Carter P, Presta L, Gorman CM, Ridgway JB, Henner D, et al. 1992. Humanization of an anti-p185HER2 antibody for human cancer therapy. *Proc Natl Acad Sci U S A* 89:4285-9
60. Ocana A, Cruz JJ, Pandiella A. 2006. Trastuzumab and antiestrogen therapy: focus on mechanisms of action and resistance. *Am J Clin Oncol* 29:90-5
61. Yakes FM, Chinratanalab W, Ritter CA, King W, Seelig S, Arteaga CL. 2002. Herceptin-induced inhibition of phosphatidylinositol-3 kinase and Akt Is required for antibody-mediated effects on p27, cyclin D1, and antitumor action. *Cancer Res* 62:4132-41
62. Albanell J, Codony J, Rovira A, Mellado B, Gascon P. 2003. Mechanism of action of anti-HER2 monoclonal antibodies: scientific update on trastuzumab and 2C4. *Advances in experimental medicine and biology* 532:253-68
63. du Manoir JM, Francia G, Man S, Mossoba M, Medin JA, et al. 2006. Strategies for delaying or treating in vivo acquired resistance to trastuzumab in human breast cancer xenografts. *Clin Cancer Res* 12:904-16
64. Izumi Y, Xu L, di Tomaso E, Fukumura D, Jain RK. 2002. Tumour biology: herceptin acts as an anti-angiogenic cocktail. *Nature* 416:279-80
65. Clynes RA, Towers TL, Presta LG, Ravetch JV. 2000. Inhibitory Fc receptors modulate in vivo cytotoxicity against tumor targets. *Nat Med* 6:443-6
66. Petricevic B, Laengle J, Singer J, Sachet M, Fazekas J, et al. 2013. Trastuzumab mediates antibody-dependent cell-mediated cytotoxicity and phagocytosis to the

same extent in both adjuvant and metastatic HER2/neu breast cancer patients. *Journal of translational medicine* 11:307

67. Kaplan MA, Ertugrul H, Firat U, Kucukoner M, Inal A, et al. 2014. Brain metastases in HER2-positive metastatic breast cancer patients who received chemotherapy with or without trastuzumab. *Breast Cancer*
68. Lazaro G, Smith C, Goddard L, Jordan N, McClelland R, et al. 2013. Targeting focal adhesion kinase in ER+/HER2+ breast cancer improves trastuzumab response. *Endocrine-related cancer* 20:691-704
69. Korkaya H, Kim GI, Davis A, Malik F, Henry NL, et al. 2012. Activation of an IL6 inflammatory loop mediates trastuzumab resistance in HER2+ breast cancer by expanding the cancer stem cell population. *Mol Cell* 47:570-84
70. Ferguson YO, Eng E, Bentley M, Sandelowski M, Steckler A, et al. 2009. Evaluating nurses' implementation of an infant-feeding counseling protocol for HIV-infected mothers: The Ban Study in Lilongwe, Malawi. *AIDS Educ Prev* 21:141-55
71. Nahta R, Esteva FJ. 2004. In vitro effects of trastuzumab and vinorelbine in trastuzumab-resistant breast cancer cells. *Cancer Chemother Pharmacol* 53:186-90
72. Wood RY, Della-Monica NR. 2015. Breast cancer threat appraisal: design and psychometric analysis of a new scale for older women. *Int J Older People Nurs* 10:94-104
73. Hurvitz SA, Kakkar R. 2012. Role of lapatinib alone or in combination in the treatment of HER2-positive breast cancer. *Breast Cancer (Dove Med Press)* 4:35-51
74. Johnston SR, Leary A. 2006. Lapatinib: a novel EGFR/HER2 tyrosine kinase inhibitor for cancer. *Drugs of today* 42:441-53
75. Nahta R, Yuan LX, Du Y, Esteva FJ. 2007. Lapatinib induces apoptosis in trastuzumab-resistant breast cancer cells: effects on insulin-like growth factor I signaling. *Molecular cancer therapeutics* 6:667-74
76. Yardley DA, Hart L, Bosserman L, Salleh MN, Waterhouse DM, et al. 2013. Phase II study evaluating lapatinib in combination with nab-paclitaxel in HER2-overexpressing metastatic breast cancer patients who have received no more than one prior chemotherapeutic regimen. *Breast Cancer Res Treat* 137:457-64
77. Verma S, Miles D, Gianni L, Krop IE, Welslau M, et al. 2012. Trastuzumab emtansine for HER2-positive advanced breast cancer. *The New England journal of medicine* 367:1783-91
78. Franklin MC, Carey KD, Vajdos FF, Leahy DJ, de Vos AM, Sliwkowski MX. 2004. Insights into ErbB signaling from the structure of the ErbB2-pertuzumab complex. *Cancer Cell* 5:317-28
79. Keating GM. 2012. Pertuzumab: in the first-line treatment of HER2-positive metastatic breast cancer. *Drugs* 72:353-60
80. Li X, Lewis MT, Huang J, Gutierrez C, Osborne CK, et al. 2008. Intrinsic resistance of tumorigenic breast cancer cells to chemotherapy. *J Natl Cancer Inst* 100:672-9

81. Fiszman GL, Jasnis MA. 2011. Molecular Mechanisms of Trastuzumab Resistance in HER2 Overexpressing Breast Cancer. *Int J Breast Cancer* 2011:352182
82. Price-Schiavi SA, Jepson S, Li P, Arango M, Rudland PS, et al. 2002. Rat Muc4 (sialomucin complex) reduces binding of anti-ErbB2 antibodies to tumor cell surfaces, a potential mechanism for herceptin resistance. *Int J Cancer* 99:783-91
83. Nahta R, Yuan LX, Zhang B, Kobayashi R, Esteva FJ. 2005. Insulin-like growth factor-I receptor/human epidermal growth factor receptor 2 heterodimerization contributes to trastuzumab resistance of breast cancer cells. *Cancer Res* 65:11118-28
84. Huang X, Gao L, Wang S, McManaman JL, Thor AD, et al. 2010. Heterotrimerization of the growth factor receptors erbB2, erbB3, and insulin-like growth factor-i receptor in breast cancer cells resistant to herceptin. *Cancer Res* 70:1204-14
85. Shattuck DL, Miller JK, Carraway KL, 3rd, Sweeney C. 2008. Met receptor contributes to trastuzumab resistance of Her2-overexpressing breast cancer cells. *Cancer Res* 68:1471-7
86. Chakraborty AK, Liang K, DiGiovanna MP. 2008. Co-targeting insulin-like growth factor I receptor and HER2: dramatic effects of HER2 inhibitors on nonoverexpressing breast cancer. *Cancer Res* 68:1538-45
87. Sanabria-Figueroa E, Donnelly SM, Foy KC, Buss MC, Castellino RC, et al. 2015. Insulin-like growth factor-1 receptor signaling increases the invasive potential of human epidermal growth factor receptor 2-overexpressing breast cancer cells via Src-focal adhesion kinase and forkhead box protein M1. *Molecular pharmacology* 87:150-61
88. Donnelly SM, Paplomata E, Peake BM, Sanabria E, Chen Z, Nahta R. 2014. P38 MAPK contributes to resistance and invasiveness of HER2- overexpressing breast cancer. *Curr Med Chem* 21:501-10
89. Huang HJ, Lee KJ, Yu HW, Chen CY, Hsu CH, et al. 2010. Structure-based and ligand-based drug design for HER 2 receptor. *J Biomol Struct Dyn* 28:23-37
90. Lu Y, Zi X, Zhao Y, Mascarenhas D, Pollak M. 2001. Insulin-like growth factor-I receptor signaling and resistance to trastuzumab (Herceptin). *J Natl Cancer Inst* 93:1852-7
91. Nagata Y, Lan KH, Zhou X, Tan M, Esteva FJ, et al. 2004. PTEN activation contributes to tumor inhibition by trastuzumab, and loss of PTEN predicts trastuzumab resistance in patients. *Cancer Cell* 6:117-27
92. Berns K, Horlings HM, Hennessy BT, Madiredjo M, Hijmans EM, et al. 2007. A functional genetic approach identifies the PI3K pathway as a major determinant of trastuzumab resistance in breast cancer. *Cancer Cell* 12:395-402
93. Kute T, Lack CM, Willingham M, Bishwokama B, Williams H, et al. 2004. Development of Herceptin resistance in breast cancer cells. *Cytometry A* 57:86-93
94. Crawford A, Nahta R. 2011. Targeting Bcl-2 in Herceptin-Resistant Breast Cancer Cell Lines. *Curr Pharmacogenomics Person Med* 9:184-90
95. Ritter CA, Perez-Torres M, Rinehart C, Guix M, Dugger T, et al. 2007. Human breast cancer cells selected for resistance to trastuzumab in vivo overexpress

epidermal growth factor receptor and ErbB ligands and remain dependent on the ErbB receptor network. *Clin Cancer Res* 13:4909-19

96. Joshi JP, Brown NE, Griner SE, Nahta R. 2011. Growth differentiation factor 15 (GDF15)-mediated HER2 phosphorylation reduces trastuzumab sensitivity of HER2-overexpressing breast cancer cells. *Biochemical pharmacology* 82:1090-9
97. Koo CY, Muir KW, Lam EW. 2012. FOXM1: From cancer initiation to progression and treatment. *Biochimica et biophysica acta* 1819:28-37
98. Wierstra I. 2013. The transcription factor FOXM1 (Forkhead box M1): proliferation-specific expression, transcription factor function, target genes, mouse models, and normal biological roles. *Advances in cancer research* 118:97-398
99. Bektas N, Haaf A, Veeck J, Wild PJ, Luscher-Firzlaff J, et al. 2008. Tight correlation between expression of the Forkhead transcription factor FOXM1 and HER2 in human breast cancer. *BMC cancer* 8:42
100. Park YY, Jung SY, Jennings NB, Rodriguez-Aguayo C, Peng G, et al. 2012. FOXM1 mediates Dox resistance in breast cancer by enhancing DNA repair. *Carcinogenesis* 33:1843-53
101. Kwok JM, Myatt SS, Marson CM, Coombes RC, Constantinidou D, Lam EW. 2008. Thiostrepton selectively targets breast cancer cells through inhibition of forkhead box M1 expression. *Molecular cancer therapeutics* 7:2022-32
102. Millour J, Constantinidou D, Stavropoulou AV, Wilson MS, Myatt SS, et al. 2010. FOXM1 is a transcriptional target of ERalpha and has a critical role in breast cancer endocrine sensitivity and resistance. *Oncogene* 29:2983-95
103. Sanders DA, Ross-Innes CS, Beraldi D, Carroll JS, Balasubramanian S. 2013. Genome-wide mapping of FOXM1 binding reveals co-binding with estrogen receptor alpha in breast cancer cells. *Genome biology* 14:R6
104. Carr JR, Park HJ, Wang Z, Kiefer MM, Raychaudhuri P. 2010. FoxM1 mediates resistance to herceptin and paclitaxel. *Cancer Res* 70:5054-63
105. Francis RE, Myatt SS, Krol J, Hartman J, Peck B, et al. 2009. FoxM1 is a downstream target and marker of HER2 overexpression in breast cancer. *International journal of oncology* 35:57-68
106. Gayle SS, Castellino RC, Buss MC, Nahta R. 2013. MEK inhibition increases lapatinib sensitivity via modulation of FOXM1. *Curr Med Chem* 20:2486-99
107. Baselga J, Cortes J, Kim SB, Im SA, Hegg R, et al. 2012. Pertuzumab plus trastuzumab plus docetaxel for metastatic breast cancer. *The New England journal of medicine* 366:109-19
108. McGovern UB, Francis RE, Peck B, Guest SK, Wang J, et al. 2009. Gefitinib (Iressa) represses FOXM1 expression via FOXO3a in breast cancer. *Molecular cancer therapeutics* 8:582-91
109. Zhao F, Lam EW. 2012. Role of the forkhead transcription factor FOXO-FOXM1 axis in cancer and drug resistance. *Frontiers of medicine* 6:376-80
110. Xue J, Lin X, Chiu WT, Chen YH, Yu G, et al. 2014. Sustained activation of SMAD3/SMAD4 by FOXM1 promotes TGF-beta-dependent cancer metastasis. *The Journal of clinical investigation* 124:564-79

111. Yang C, Chen H, Yu L, Shan L, Xie L, et al. 2013. Inhibition of FOXM1 transcription factor suppresses cell proliferation and tumor growth of breast cancer. *Cancer gene therapy* 20:117-24
112. Raychaudhuri P, Park HJ. 2011. FoxM1: a master regulator of tumor metastasis. *Cancer Res* 71:4329-33
113. Liu XQ, Xiong MH, Shu XT, Tang RZ, Wang J. 2012. Therapeutic delivery of siRNA silencing HIF-1 alpha with micellar nanoparticles inhibits hypoxic tumor growth. *Molecular pharmaceutics* 9:2863-74
114. Ahmad A, Ali S, Ahmed A, Ali AS, Raz A, et al. 2013. 3, 3'-Diindolylmethane enhances the effectiveness of herceptin against HER-2/neu-expressing breast cancer cells. *PloS one* 8:e54657
115. Ahmad A, Sakr WA, Rahman KM. 2012. Novel targets for detection of cancer and their modulation by chemopreventive natural compounds. *Frontiers in bioscience* 4:410-25
116. Yehl K, Joshi JP, Greene BL, Dyer RB, Nahta R, Salaita K. 2012. Catalytic deoxyribozyme-modified nanoparticles for RNAi-independent gene regulation. *ACS Nano* 6:9150-7
117. Bootcov MR, Bauskin AR, Valenzuela SM, Moore AG, Bansal M, et al. 1997. MIC-1, a novel macrophage inhibitory cytokine, is a divergent member of the TGF-beta superfamily. *Proc Natl Acad Sci U S A* 94:11514-9
118. Bauskin AR, Jiang L, Luo XW, Wu L, Brown DA, Breit SN. 2010. The TGF-beta superfamily cytokine MIC-1/GDF15: secretory mechanisms facilitate creation of latent stromal stores. *J Interferon Cytokine Res* 30:389-97
119. Santibanez JF, Quintanilla M, Bernabeu C. 2011. TGF-beta/TGF-beta receptor system and its role in physiological and pathological conditions. *Clin Sci (Lond)* 121:233-51
120. Weiss A, Attisano L. 2013. The TGFbeta superfamily signaling pathway. *Wiley Interdiscip Rev Dev Biol* 2:47-63
121. Derynck R, Zhang YE. 2003. Smad-dependent and Smad-independent pathways in TGF-beta family signalling. *Nature* 425:577-84
122. Yan X, Liu Z, Chen Y. 2009. Regulation of TGF-beta signaling by Smad7. *Acta Biochim Biophys Sin (Shanghai)* 41:263-72
123. Sakurai H, Suzuki S, Kawasaki N, Nakano H, Okazaki T, et al. 2003. Tumor necrosis factor-alpha-induced IKK phosphorylation of NF-kappaB p65 on serine 536 is mediated through the TRAF2, TRAF5, and TAK1 signaling pathway. *J Biol Chem* 278:36916-23
124. Masaki T, Miwa S, Sawamura T, Ninomiya H, Okamoto Y. 1999. Subcellular mechanisms of endothelin action in vascular system. *Eur J Pharmacol* 375:133-8
125. Irie T, Muta T, Takeshige K. 2000. TAK1 mediates an activation signal from toll-like receptor(s) to nuclear factor-kappaB in lipopolysaccharide-stimulated macrophages. *FEBS Lett* 467:160-4
126. Ying Z, Yue P, Xu X, Zhong M, Sun Q, et al. 2009. Air pollution and cardiac remodeling: a role for RhoA/Rho-kinase. *Am J Physiol Heart Circ Physiol* 296:H1540-50

127. Min KW, Liggett JL, Silva G, Wu WW, Wang R, et al. 2016. NAG-1/GDF15 accumulates in the nucleus and modulates transcriptional regulation of the Smad pathway. *Oncogene* 35:377-88
128. Kim KK, Lee JJ, Yang Y, You KH, Lee JH. 2008. Macrophage inhibitory cytokine-1 activates AKT and ERK-1/2 via the transactivation of ErbB2 in human breast and gastric cancer cells. *Carcinogenesis* 29:704-12
129. Park YJ, Lee H, Lee JH. 2010. Macrophage inhibitory cytokine-1 transactivates ErbB family receptors via the activation of Src in SK-BR-3 human breast cancer cells. *BMB Rep* 43:91-6
130. Xu J, Kimball TR, Lorenz JN, Brown DA, Bauskin AR, et al. 2006. GDF15/MIC-1 functions as a protective and antihypertrophic factor released from the myocardium in association with SMAD protein activation. *Circ Res* 98:342-50
131. Bottner M, Suter-Crazzolara C, Schober A, Unsicker K. 1999. Expression of a novel member of the TGF-beta superfamily, growth/differentiation factor-15/macrophage-inhibiting cytokine-1 (GDF-15/MIC-1) in adult rat tissues. *Cell Tissue Res* 297:103-10
132. Corre J, Hebraud B, Bourin P. 2013. Concise review: growth differentiation factor 15 in pathology: a clinical role? *Stem Cells Transl Med* 2:946-52
133. Wollmann W, Goodman ML, Bhat-Nakshatri P, Kishimoto H, Goulet RJ, Jr., et al. 2005. The macrophage inhibitory cytokine integrates AKT/PKB and MAP kinase signaling pathways in breast cancer cells. *Carcinogenesis* 26:900-7
134. Osada M, Park HL, Park MJ, Liu JW, Wu G, et al. 2007. A p53-type response element in the GDF15 promoter confers high specificity for p53 activation. *Biochem Biophys Res Commun* 354:913-8
135. Baek SJ, Kim JS, Moore SM, Lee SH, Martinez J, Eling TE. 2005. Cyclooxygenase inhibitors induce the expression of the tumor suppressor gene EGR-1, which results in the up-regulation of NAG-1, an antitumorigenic protein. *Molecular pharmacology* 67:356-64
136. Eling TE, Baek SJ, Shim M, Lee CH. 2006. NSAID activated gene (NAG-1), a modulator of tumorigenesis. *J Biochem Mol Biol* 39:649-55
137. Bauskin AR, Zhang HP, Fairlie WD, He XY, Russell PK, et al. 2000. The propeptide of macrophage inhibitory cytokine (MIC-1), a TGF-beta superfamily member, acts as a quality control determinant for correctly folded MIC-1. *EMBO J* 19:2212-20
138. Fairlie WD, Zhang H, Brown PK, Russell PK, Bauskin AR, Breit SN. 2000. Expression of a TGF-beta superfamily protein, macrophage inhibitory cytokine-1, in the yeast Pichia pastoris. *Gene* 254:67-76
139. Bauskin AR, Brown DA, Junankar S, Rasiah KK, Eggleton S, et al. 2005. The propeptide mediates formation of stromal stores of PROMIC-1: role in determining prostate cancer outcome. *Cancer Res* 65:2330-6
140. Kingsley DM. 1994. The TGF-beta superfamily: new members, new receptors, and new genetic tests of function in different organisms. *Genes Dev* 8:133-46
141. Hayes VM, Severi G, Southey MC, Padilla EJ, English DR, et al. 2006. Macrophage inhibitory cytokine-1 H6D polymorphism, prostate cancer risk, and survival. *Cancer Epidemiol Biomarkers Prev* 15:1223-5

142. Hromas R, Hufford M, Sutton J, Xu D, Li Y, Lu L. 1997. PLAB, a novel placental bone morphogenetic protein. *Biochimica et biophysica acta* 1354:40-4
143. Moore AG, Brown DA, Fairlie WD, Bauskin AR, Brown PK, et al. 2000. The transforming growth factor-ss superfamily cytokine macrophage inhibitory cytokine-1 is present in high concentrations in the serum of pregnant women. *J Clin Endocrinol Metab* 85:4781-8
144. Tong S, Marjono B, Brown DA, Mulvey S, Breit SN, et al. 2004. Serum concentrations of macrophage inhibitory cytokine 1 (MIC 1) as a predictor of miscarriage. *Lancet* 363:129-30
145. Wang X, Baek SJ, Eling TE. 2013. The diverse roles of nonsteroidal anti-inflammatory drug activated gene (NAG-1/GDF15) in cancer. *Biochemical pharmacology* 85:597-606
146. Brown DA, Ward RL, Buckhaults P, Liu T, Romans KE, et al. 2003. MIC-1 serum level and genotype: associations with progress and prognosis of colorectal carcinoma. *Clin Cancer Res* 9:2642-50
147. Mimeault M, Batra SK. 2010. Divergent molecular mechanisms underlying the pleiotropic functions of macrophage inhibitory cytokine-1 in cancer. *J Cell Physiol* 224:626-35
148. Roth P, Junker M, Tritschler I, Mittelbronn M, Dombrowski Y, et al. 2010. GDF-15 contributes to proliferation and immune escape of malignant gliomas. *Clin Cancer Res* 16:3851-9
149. Staff AC, Bock AJ, Becker C, Kempf T, Wollert KC, Davidson B. 2010. Growth differentiation factor-15 as a prognostic biomarker in ovarian cancer. *Gynecol Oncol* 118:237-43
150. Welsh JB, Sapinoso LM, Kern SG, Brown DA, Liu T, et al. 2003. Large-scale delineation of secreted protein biomarkers overexpressed in cancer tissue and serum. *Proc Natl Acad Sci U S A* 100:3410-5
151. Albertoni M, Shaw PH, Nozaki M, Godard S, Tenan M, et al. 2002. Anoxia induces macrophage inhibitory cytokine-1 (MIC-1) in glioblastoma cells independently of p53 and HIF-1. *Oncogene* 21:4212-9
152. Heger J, Schiegnitz E, von Waldthausen D, Anwar MM, Piper HM, Euler G. 2010. Growth differentiation factor 15 acts anti-apoptotic and pro-hypertrophic in adult cardiomyocytes. *J Cell Physiol* 224:120-6
153. Feng K, Wang S, Ma H, Chen Y. 2013. Chirality plays critical roles in enhancing the aqueous solubility of nocathiacin I by block copolymer micelles. *The Journal of pharmacy and pharmacology* 65:64-71
154. Fairlie WD, Moore AG, Bauskin AR, Russell PK, Zhang HP, Breit SN. 1999. MIC-1 is a novel TGF-beta superfamily cytokine associated with macrophage activation. *J Leukoc Biol* 65:2-5
155. Buckhaults P, Rago C, St Croix B, Romans KE, Saha S, et al. 2001. Secreted and cell surface genes expressed in benign and malignant colorectal tumors. *Cancer Res* 61:6996-7001
156. Welsh JB, Sapinoso LM, Su AI, Kern SG, Wang-Rodriguez J, et al. 2001. Analysis of gene expression identifies candidate markers and pharmacological targets in prostate cancer. *Cancer Res* 61:5974-8

157. Koniaris LG. 2003. Induction of MIC-1/growth differentiation factor-15 following bile duct injury. *J Gastrointest Surg* 7:901-5
158. Liu T, Bauskin AR, Zaunders J, Brown DA, Pankhurst S, et al. 2003. Macrophage inhibitory cytokine 1 reduces cell adhesion and induces apoptosis in prostate cancer cells. *Cancer Res* 63:5034-40
159. Baek SJ, Horowitz JM, Eling TE. 2001. Molecular cloning and characterization of human nonsteroidal anti-inflammatory drug-activated gene promoter. Basal transcription is mediated by Sp1 and Sp3. *J Biol Chem* 276:33384-92
160. Zhang L, Yang X, Pan HY, Zhou XJ, Li J, et al. 2009. Expression of growth differentiation factor 15 is positively correlated with histopathological malignant grade and in vitro cell proliferation in oral squamous cell carcinoma. *Oral Oncol* 45:627-32
161. Yang CZ, Ma J, Zhu DW, Liu Y, Montgomery B, et al. 2014. GDF15 is a potential predictive biomarker for TPF induction chemotherapy and promotes tumorigenesis and progression in oral squamous cell carcinoma. *Ann Oncol* 25:1215-22
162. Corre J, Labat E, Espagnolle N, Hebraud B, Avet-Loiseau H, et al. 2012. Bioactivity and prognostic significance of growth differentiation factor GDF15 secreted by bone marrow mesenchymal stem cells in multiple myeloma. *Cancer Res* 72:1395-406
163. Vivanco I. 2014. Targeting molecular addictions in cancer. *British journal of cancer* 111:2033-8
164. Rodriguez-Berriguete G, Fraile B, Martinez-Onsurbe P, Olmedilla G, Paniagua R, Royuela M. 2012. MAP Kinases and Prostate Cancer. *J Signal Transduct* 2012:169170
165. Cuadrado A, Nebreda AR. 2010. Mechanisms and functions of p38 MAPK signalling. *Biochem J* 429:403-17
166. Chen L, Mayer JA, Krisko TI, Speers CW, Wang T, et al. 2009. Inhibition of the p38 kinase suppresses the proliferation of human ER-negative breast cancer cells. *Cancer Res* 69:8853-61
167. Tanizaki J, Okamoto I, Sakai K, Nakagawa K. 2011. Differential roles of trans-phosphorylated EGFR, HER2, HER3, and RET as heterodimerisation partners of MET in lung cancer with MET amplification. *British journal of cancer* 105:807-13
168. Amin AR, Karpowicz PA, Carey TE, Arbiser J, Nahta R, et al. 2015. Evasion of anti-growth signaling: A key step in tumorigenesis and potential target for treatment and prophylaxis by natural compounds. *Semin Cancer Biol* 35 Suppl:S55-77
169. Zhang Z, Wu L, Wang J, Li G, Feng D, et al. 2014. Opposing effects of PI3K/Akt and Smad-dependent signaling pathways in NAG-1-induced glioblastoma cell apoptosis. *PloS one* 9:e96283
170. Adela R, Banerjee SK. 2015. GDF-15 as a Target and Biomarker for Diabetes and Cardiovascular Diseases: A Translational Prospective. *J Diabetes Res* 2015:490842
171. Peake BF, Nahta R. 2014. Resistance to HER2-targeted therapies: a potential role for FOXM1. *Breast Cancer Manag* 3:423-31

172. Lee JJ, Loh K, Yap YS. 2015. PI3K/Akt/mTOR inhibitors in breast cancer. *Cancer Biol Med* 12:342-54
173. Porta C, Paglino C, Mosca A. 2014. Targeting PI3K/Akt/mTOR Signaling in Cancer. *Front Oncol* 4:64
174. Zhang L, Zhou F, ten Dijke P. 2013. Signaling interplay between transforming growth factor-beta receptor and PI3K/AKT pathways in cancer. *Trends Biochem Sci* 38:612-20
175. Lok GT, Chan DW, Liu VW, Hui WW, Leung TH, et al. 2011. Aberrant activation of ERK/FOXM1 signaling cascade triggers the cell migration/invasion in ovarian cancer cells. *PloS one* 6:e23790
176. Jin YJ, Lee JH, Kim YM, Oh GT, Lee H. 2012. Macrophage inhibitory cytokine-1 stimulates proliferation of human umbilical vein endothelial cells by up-regulating cyclins D1 and E through the PI3K/Akt-, ERK-, and JNK-dependent AP-1 and E2F activation signaling pathways. *Cellular signalling* 24:1485-95
177. Urakawa N, Utsunomiya S, Nishio M, Shigeoka M, Takase N, et al. 2015. GDF15 derived from both tumor-associated macrophages and esophageal squamous cell carcinomas contributes to tumor progression via Akt and Erk pathways. *Laboratory investigation; a journal of technical methods and pathology* 95:491-503
178. Kulkarni AB, Thyagarajan T, Letterio JJ. 2002. Function of cytokines within the TGF-beta superfamily as determined from transgenic and gene knockout studies in mice. *Current molecular medicine* 2:303-27
179. Carrillo-Garcia C, Prochnow S, Simeonova IK, Strelau J, Holzl-Wenig G, et al. 2014. Growth/differentiation factor 15 promotes EGFR signalling, and regulates proliferation and migration in the hippocampus of neonatal and young adult mice. *Development* 141:773-83
180. Danielpour D, Song K. 2006. Cross-talk between IGF-I and TGF-beta signaling pathways. *Cytokine & growth factor reviews* 17:59-74
181. He SY, Shen HW, Xu L, Zhao XH, Yuan L, et al. 2012. FOXM1 promotes tumor cell invasion and correlates with poor prognosis in early-stage cervical cancer. *Gynecol Oncol* 127:601-10
182. Wen N, Wang Y, Wen L, Zhao SH, Ai ZH, et al. 2014. Overexpression of FOXM1 predicts poor prognosis and promotes cancer cell proliferation, migration and invasion in epithelial ovarian cancer. *Journal of translational medicine* 12:134
183. Spector NL, Blackwell KL. 2009. Understanding the mechanisms behind trastuzumab therapy for human epidermal growth factor receptor 2-positive breast cancer. *J Clin Oncol* 27:5838-47
184. Kong FF, Zhu YL, Yuan HH, Wang JY, Zhao M, et al. 2014. FOXM1 regulated by ERK pathway mediates TGF-beta1-induced EMT in NSCLC. *Oncology research* 22:29-37
185. Wiklund FE, Bennet AM, Magnusson PK, Eriksson UK, Lindmark F, et al. 2010. Macrophage inhibitory cytokine-1 (MIC-1/GDF15): a new marker of all-cause mortality. *Aging Cell* 9:1057-64

186. Kempf T, Eden M, Strelau J, Naguib M, Willenbockel C, et al. 2006. The transforming growth factor-beta superfamily member growth-differentiation factor-15 protects the heart from ischemia/reperfusion injury. *Circ Res* 98:351-60
187. Kehl DW, Iqbal N, Fard A, Kipper BA, De La Parra Landa A, Maisel AS. 2012. Biomarkers in acute myocardial injury. *Transl Res* 159:252-64
188. Kempf T, Zarbock A, Widera C, Butz S, Stadtmann A, et al. 2011. GDF-15 is an inhibitor of leukocyte integrin activation required for survival after myocardial infarction in mice. *Nat Med* 17:581-8
189. Bonaterra GA, Zugel S, Thogersen J, Walter SA, Haberkorn U, et al. 2012. Growth differentiation factor-15 deficiency inhibits atherosclerosis progression by regulating interleukin-6-dependent inflammatory response to vascular injury. *J Am Heart Assoc* 1:e002550
190. Selander KS, Brown DA, Sequeiros GB, Hunter M, Desmond R, et al. 2007. Serum macrophage inhibitory cytokine-1 concentrations correlate with the presence of prostate cancer bone metastases. *Cancer Epidemiol Biomarkers Prev* 16:532-7
191. Johnen H, Kuffner T, Brown DA, Wu BJ, Stocker R, Breit SN. 2012. Increased expression of the TGF-b superfamily cytokine MIC-1/GDF15 protects ApoE(-/-) mice from the development of atherosclerosis. *Cardiovasc Pathol* 21:499-505
192. Sasahara A, Tominaga K, Nishimura T, Yano M, Kiyokawa E, et al. 2017. An autocrine/paracrine circuit of growth differentiation factor (GDF) 15 has a role for maintenance of breast cancer stem-like cells. *Oncotarget*
193. Barbera MJ, Puig I, Dominguez D, Julien-Grille S, Guaita-Esteruelas S, et al. 2004. Regulation of Snail transcription during epithelial to mesenchymal transition of tumor cells. *Oncogene* 23:7345-54
194. Derynck R, Akhurst RJ. 2007. Differentiation plasticity regulated by TGF-beta family proteins in development and disease. *Nature cell biology* 9:1000-4
195. Xu J, Lamouille S, Derynck R. 2009. TGF-beta-induced epithelial to mesenchymal transition. *Cell Res* 19:156-72
196. Llorens A, Rodrigo I, Lopez-Barcons L, Gonzalez-Garrigues M, Lozano E, et al. 1998. Down-regulation of E-cadherin in mouse skin carcinoma cells enhances a migratory and invasive phenotype linked to matrix metalloproteinase-9 gelatinase expression. *Laboratory investigation; a journal of technical methods and pathology* 78:1131-42
197. Li C, Wang J, Kong J, Tang J, Wu Y, et al. 2016. GDF15 promotes EMT and metastasis in colorectal cancer. *Oncotarget* 7:860-72
198. Jiang J, Wen W, Brown DA, Crawford J, Thalamuthu A, et al. 2015. The relationship of serum macrophage inhibitory cytokine-1 levels with gray matter volumes in community-dwelling older individuals. *PloS one* 10:e0123399
199. Jiang R, Li Y, Xu Y, Zhou Y, Pang Y, et al. 2013. EMT and CSC-like properties mediated by the IKKbeta/IkappaBalpha/RelA signal pathway via the transcriptional regulator, Snail, are involved in the arsenite-induced neoplastic transformation of human keratinocytes. *Archives of toxicology* 87:991-1000
200. Wang CY, Huang AQ, Zhou MH, Mei YA. 2014. GDF15 regulates Kv2.1-mediated outward K+ current through the Akt/mTOR signalling pathway in rat cerebellar granule cells. *Biochem J* 460:35-47

201. Li YL, Chang JT, Lee LY, Fan KH, Lu YC, et al. 2017. GDF15 contributes to radioresistance and cancer stemness of head and neck cancer by regulating cellular reactive oxygen species via a SMAD-associated signaling pathway. *Oncotarget* 8:1508-28
202. Taliaferro-Smith L, Oberlick E, Liu T, McGlothen T, Alcaide T, et al. 2015. FAK activation is required for IGF1R-mediated regulation of EMT, migration, and invasion in mesenchymal triple negative breast cancer cells. *Oncotarget* 6:4757-72
203. Harner-Foreman N, Vadakekolathu J, Laversin SA, Mathieu MG, Reeder S, et al. 2017. A novel spontaneous model of epithelial-mesenchymal transition (EMT) using a primary prostate cancer derived cell line demonstrating distinct stem-like characteristics. *Sci Rep* 7:40633
204. Lazennec G, Lam PY. 2016. Recent discoveries concerning the tumor - mesenchymal stem cell interactions. *Biochimica et biophysica acta* 1866:290-9
205. Aref AR, Huang RY, Yu W, Chua KN, Sun W, et al. 2013. Screening therapeutic EMT blocking agents in a three-dimensional microenvironment. *Integrative biology : quantitative biosciences from nano to macro* 5:381-9
206. Senapati S, Rachagani S, Chaudhary K, Johansson SL, Singh RK, Batra SK. 2010. Overexpression of macrophage inhibitory cytokine-1 induces metastasis of human prostate cancer cells through the FAK-RhoA signaling pathway. *Oncogene* 29:1293-302
207. Rao DD, Senzer N, Cleary MA, Nemunaitis J. 2009. Comparative assessment of siRNA and shRNA off target effects: what is slowing clinical development. *Cancer gene therapy* 16:807-9
208. Burnett JC, Rossi JJ, Tiemann K. 2011. Current progress of siRNA/shRNA therapeutics in clinical trials. *Biotechnol J* 6:1130-46
209. Davis AR, Znosko BM. 2010. Positional and neighboring base pair effects on the thermodynamic stability of RNA single mismatches. *Biochemistry* 49:8669-79
210. Dassie JP, Liu XY, Thomas GS, Whitaker RM, Thiel KW, et al. 2009. Systemic administration of optimized aptamer-siRNA chimeras promotes regression of PSMA-expressing tumors. *Nat Biotechnol* 27:839-49
211. Watts JK, Corey DR. 2012. Silencing disease genes in the laboratory and the clinic. *J Pathol* 226:365-79
212. Silverman SK. 2004. Deoxyribozymes: DNA catalysts for bioorganic chemistry. *Org Biomol Chem* 2:2701-6
213. Niewiarowska J, Sacewicz I, Wiktorska M, Wysocki T, Stasikowska O, et al. 2009. DNAzymes to mouse beta1 integrin mRNA in vivo: targeting the tumor vasculature and retarding cancer growth. *Cancer gene therapy* 16:713-22
214. Dass CR, Choong PF, Khachigian LM. 2008. DNAzyme technology and cancer therapy: cleave and let die. *Molecular cancer therapeutics* 7:243-51
215. Elahy M, Dass CR. 2011. Dz13: c-Jun downregulation and tumour cell death. *Chem Biol Drug Des* 78:909-12
216. Fahmy RG, Dass CR, Sun LQ, Chesterman CN, Khachigian LM. 2003. Transcription factor Egr-1 supports FGF-dependent angiogenesis during neovascularization and tumor growth. *Nat Med* 9:1026-32

217. Fellmann C, Zuber J, McJunkin K, Chang K, Malone CD, et al. 2011. Functional identification of optimized RNAi triggers using a massively parallel sensor assay. *Mol Cell* 41:733-46
218. Davidson BL, McCray PB, Jr. 2011. Current prospects for RNA interference-based therapies. *Nat Rev Genet* 12:329-40
219. Hamasaki T, Suzuki H, Shirohzu H, Matsumoto T, D'Alessandro-Gabazza CN, et al. 2012. Efficacy of a novel class of RNA interference therapeutic agents. *PloS one* 7:e42655
220. Zhai Y, Zhang J, Wang H, Lu W, Liu S, et al. 2016. Growth differentiation factor 15 contributes to cancer-associated fibroblasts-mediated chemo-protection of AML cells. *J Exp Clin Cancer Res* 35:147
221. Wang XB, Jiang XR, Yu XY, Wang L, He S, et al. 2014. Macrophage inhibitory factor 1 acts as a potential biomarker in patients with esophageal squamous cell carcinoma and is a target for antibody-based therapy. *Cancer Sci* 105:176-85
222. Wang X, Yang Z, Tian H, Li Y, Li M, et al. 2017. Circulating MIC-1/GDF15 is a complementary screening biomarker with CEA and correlates with liver metastasis and poor survival in colorectal cancer. *Oncotarget* 8:24892-901
223. Yasmin R, Siraj S, Hassan A, Khan AR, Abbasi R, Ahmad N. 2015. Epigenetic regulation of inflammatory cytokines and associated genes in human malignancies. *Mediators Inflamm* 2015:201703
224. Li PX, Wong J, Ayed A, Ngo D, Brade AM, et al. 2000. Placental transforming growth factor-beta is a downstream mediator of the growth arrest and apoptotic response of tumor cells to DNA damage and p53 overexpression. *J Biol Chem* 275:20127-35
225. Carrero JJ, Yilmaz MI, Lindholm B, Stenvinkel P. 2008. Cytokine dysregulation in chronic kidney disease: how can we treat it? *Blood Purif* 26:291-9
226. Tsui KH, Hsu SY, Chung LC, Lin YH, Feng TH, et al. 2015. Growth differentiation factor-15: a p53- and demethylation-upregulating gene represses cell proliferation, invasion, and tumorigenesis in bladder carcinoma cells. *Sci Rep* 5:12870
227. Schilling T, Miralles F, Eder C. 2014. TRPM7 regulates proliferation and polarisation of macrophages. *J Cell Sci* 127:4561-6
228. Huang X, Yang N, Ou X, Li D, Wang Z, et al. 2008. Sequential activation of protein kinase C delta and JNK is required for interferon-alpha-induced expression of IFIT4. *Cellular signalling* 20:112-9
229. Lamouille S, Derynck R. 2007. Cell size and invasion in TGF-beta-induced epithelial to mesenchymal transition is regulated by activation of the mTOR pathway. *J Cell Biol* 178:437-51
230. Truong D, Puleo J, Llave A, Mouneimne G, Kamm RD, Nikkhah M. 2016. Breast Cancer Cell Invasion into a Three Dimensional Tumor-Stroma Microenvironment. *Sci Rep* 6:34094
231. Vanhara P, Hampl A, Kozubik A, Soucek K. 2012. Growth/differentiation factor-15: prostate cancer suppressor or promoter? *Prostate Cancer Prostatic Dis* 15:320-8

232. Soucek K, Slabakova E, Ovesna P, Malenovska A, Kozubik A, Hampl A. 2010. Growth/differentiation factor-15 is an abundant cytokine in human seminal plasma. *Hum Reprod* 25:2962-71
233. Junttila MR, de Sauvage FJ. 2013. Influence of tumour micro-environment heterogeneity on therapeutic response. *Nature* 501:346-54
234. Hidalgo M, Amant F, Biankin AV, Budinska E, Byrne AT, et al. 2014. Patient-derived xenograft models: an emerging platform for translational cancer research. *Cancer Discov* 4:998-1013
235. Lai Y, Wei X, Lin S, Qin L, Cheng L, Li P. 2017. Current status and perspectives of patient-derived xenograft models in cancer research. *J Hematol Oncol* 10:106